

Genotype by Environment Interactions affecting Simulation of Rice Phenology

Master's thesis

Linda Groot Nibbelink

Matr. No. 861841

MSc. Double degree,
University of Hohenheim &
Universität für Bodenkultur Wien

Supervisor: **Prof. Dr. Folkard Asch**
Institute of Agricultural Sciences in
the Tropics,
*Management of Crop Water Stress in
the Tropics and Subtropics*

August 2022



Thesis prepared in fulfilment of the double degree

**Master of Science in
Organic Agriculture and Food Systems**
University of Hohenheim

and

**Master of Science in
Organic Agricultural Systems and Agroecology**
Universität für Bodenkultur, Vienna (BOKU)

Supervisor: Prof. Dr. Folkard Asch

Institute of Agricultural Sciences in the Tropics
Management of Crop Water Stress in the Tropics and Subtropics
University of Hohenheim

Co-supervisor: Prof. Dr. Hermann Bürstmayr

Institute of Biotechnology in Plant Production
Institute of Plant Breeding
Universität für Bodenkultur, Vienna (BOKU)

This work was conducted in collaboration with AfricaRice
and financially supported by ATSAF's Junior Scientist Program



UNIVERSITY OF
HOHENHEIM



AfricaRice

Acknowledgements

First of all, I would like to express my gratitude to all researchers and employees at AfricaRice who were involved with executing the rice garden trials and collecting the data. Their work forms the basis for this study. My work is building forth on analysis previously done on this dataset by Pepijn van Oort (generating missing weather data) and Elke Vandamme (quality control), for which I am grateful. Special thanks go to Saito Kazuki, for managing this project and for being my contact person at AfricaRice.

I thank ATSAF for their financial support.

My thanks and appreciation go above all to prof. Folkard Asch, for long and fruitful scientific discussions, for all the advice and suggestions he provided during our (nearly) weekly meetings and for encouraging me. Thanks to Sabine Stuerz for her expertise and being available to answer my questions.

I appreciate my colleagues at GZPK, for giving me extra time off, even during the busy harvest season, so I could finish this thesis in a good manner. Special thanks to Monika Bauman for proofreading this thesis.

I may have been far from my family throughout my studies, but my parents always made sure I knew they support and love me. Many thanks for their emotional support and their trust in my ability to successfully complete this master thesis. Special thanks go to Annika Syrén and Pieter Vlag for their suggestions regarding data analysis.

Last but not least, I would like to thank my partner, Oskar Syrén, for his unwavering love, for bearing with me through difficult and stressful times and for happily agreeing to move across Europe with me.

Abstract

Adapting rice production in Sub-Saharan Africa to future challenges such as climate change and maintaining food security requires functional crop models to evaluate the potential of a production environment in combination with selected rice varieties. The backbone of such models is accurately simulating phenology across a wide spectrum of environments. Rice garden experiments were conducted at five of AfricaRice's research locations with 25 sowing dates (SD): Cotonou, Benin, 2SD; Mbe, Ivory Coast, 5SD; Ambohibary, Madagascar, 5SD; Fanaye, Senegal, 7SD; Ruvu, Tanzania, 6SD. Days from sowing to flowering (f) were simulated for 80 varieties across all these environments using cardinal temperatures derived from three existing phenology models developed by Summerfield et al. (1992), Dingkuhn et al. (1995) and Stuerz et al. (2020). The data from this project showed that the relationship between development rate (DR) and mean temperature is not linear, as assumed in Summerfield's model, but rather stagnates as temperature increases. Therefore a new model was developed (Asch-Groot Nibbelink; AGN) where this relationship was captured by fitting a second order regression ($DR = a * \bar{T}^2 + b * \bar{T} + c$) and taking two tangents: one horizontal at the vertex and one sloped with tangency point where DR is half of DR at the vertex. Base temperature is where DR=0 while optimum temperature is where the two tangents intersect. Temperature sum is the inverse of the slope of the sloped tangent. When regressing residuals (simulated f - observed f) against other climatic factors such as photoperiod, radiation, vapour pressure deficit, and relative air humidity (RH), it was found that RH explained 38,4% of the residuals. Therefore, AGN was adjusted to include a genotype-specific RH-adjustment factor resulting in optimum temperatures increasing with increasing RH. With a slope of 0.937, an r^2 of 0.938 and RMSE of 12.3 days when regressing simulated f against observed f , AGN proofed to simulate genotype by environment effects on phenology better than the three tested rice phenology models. It is therefore suggested to include an RH-adjustment factor for optimum temperature into the phenology routine of existing rice growth models.

Keywords: *Oryza sativa*, phenology, crop duration, temperature, relative humidity

Table of Contents

Declaration.....	vi
Acknowledgements.....	v
Abstract	vi
List of Abbreviations	x
List of Figures	xiii
List of Tables.....	xvii
List of Equations	xviii
1 Introduction	1
2 Hypothesis and Research Objectives	3
3 Literature review.....	4
3.1 Rice Phenology	4
3.2 Genotype by Environment Interactions	5
3.3 Rice crop models	7
3.4 Phenology models.....	8
3.4.1 Summerfield	8
3.4.2 Dingkuhn	9
3.4.3 Stuerz.....	10
4 Materials and Methods.....	12
4.1 Environments.....	12
4.1.1 Locations.....	12
4.1.2 Sowing dates	12
4.1.3 Weather conditions	13
4.2 Genetic material.....	16
4.3 Experimental design and management	16
4.4 Data collection	18

4.4.1	Rice garden trials	18
4.4.2	Microclimate plots	19
4.4.3	Meteorological data	19
4.5	Data analysis	20
4.5.1	Data preparation	20
4.5.2	Analysing phenology models	21
5	Results	22
5.1	Crop duration	22
5.2	Panicle Initiation	22
5.3	Cardinal temperatures	27
5.3.1	Summerfield	27
5.3.2	Dingkuhn	30
5.3.3	Stuerz.....	32
5.3.4	Asch-Groot Nibbelink	34
5.3.5	Cardinal Temperature Estimates	38
5.4	Simulated Flowering Dates	39
5.4.1	Summerfield	39
5.4.2	Dingkuhn	42
5.4.3	Stuerz.....	44
5.4.4	Asch-Groot Nibbelink	46
5.5	Comparing phenology models.....	48
5.6	Analysing residuals.....	49
5.7	Improved Asch-Groot Nibbelink model	53
5.7.1	AGN Version 1	54
5.7.2	AGN Version 2.....	55
5.7.3	AGN Version 3.....	56

5.7.4	AGN Version 4.....	57
5.7.5	AGN Version 5.....	58
5.7.6	Comparing model versions.....	58
6	Discussion	62
6.1	Timing of Panicle Initiation	62
6.2	Model Limits	63
6.2.1	Summerfield	64
6.2.2	Dingkuhn	64
6.2.3	Stuerz.....	66
6.2.4	Asch-Groot Nibbelink	66
6.3	Influence of relative humidity on phenology	67
6.4	Improving rice crop models	67
6.5	Future research	69
7	Conclusion	70
	References	71
	Appendix I: Genetic material.....	75
	Appendix II: SAS code.....	80
	Appendix III: Crop duration.....	92
	Appendix IV: Cardinal temperatures.....	95

List of Abbreviations

AfricaRice	Africa Rice Centre
AGN	Asch-Groot Nibbelink
Asl	Above sea level
BVP	Basic Vegetative Phase
CPP	Slope constant for photoperiodism
CV	Coefficient of Variation
dd	Degree-days
DR	Development Rate
DS	Development stage
E	Environment
Eqn	Equation
<i>f</i>	Days from sowing to flowering
FL	Flowering
G	Genotype
G x E	Genotype by Environment
IL	Irrigated Lowland
LAI	Leaf Area Index
LS	Least squares
MC	Microclimate
P	Phenotype
PI	Panicle Initiation
PP	Photoperiod

\overline{PP}	Mean photoperiod during a specific growing period
PP _{PI}	Photoperiod at panicle initiation
PP _{TWI}	Photoperiod including twilight
PSP	Photoperiod Sensitive Phase
RGT	Rice Garden Trial
RH	Relative Humidity
\overline{RH}	Mean relative humidity during a specific growing period
RH _{ADJ}	Relative humidity adjustment factor
RH _{ADJ.BASE}	Relative humidity adjustment factor for base temperature
RH _{ADJ.OPT}	Relative humidity adjustment factor for optimum temperature
RH _{ADJ.SUM}	Relative humidity adjustment factor for temperature sum
RH _{AV}	Average relative humidity, daily
RMSE	Root Mean Square Error
RIP	Ripening Phase
RL	Rainfed Lowland
RP	Reproductive Phase
RU	Rainfed Upland
SSA	Sub-Saharan Africa
SD	Sowing date
\bar{T}	Mean air temperature during a specific growing period
T _{AV}	Average air temperature, daily
T _{BASE}	Base temperature
T _{BASE_0}	Base temperature at RH = 0%

T _{MAX}	Maximum temperature
T _{OPT}	Optimum temperature
T _{OPT_0}	Optimum temperature at RH = 0%
T _{PHYS}	Physiological temperature
T _{SUM}	Temperature sum
T _{SUM11}	Sum of heat units required until flowering at PP = 11h
T _{WATER}	Water temperature
V	Variety
V _{CODE}	Variety-specific code
VP	Vegetative Phase
VPD	Vapour Pressure Deficit

List of Figures

Figure 1: Rice crop life cycle divided in phenological phases.....	4
Figure 2: Genotype by Environment interactions affecting crop duration.	6
Figure 3: Brief historical overview of rice models.....	8
Figure 4: Rice Garden Trial Sites. Map source: Google Maps	12
Figure 5: Weather graphs of Cotonou, Benin (A); Mbe, Ivory Coast (B); Ambohibary, Madagascar (C); Fanaye, Senegal (D); and Ruvu, Tanzania (E). T	15
Figure 6: Example of a field layout for the Rice Garden plots with different sowing dates of different genotypes in an augmented design..	17
Figure 7: Rice Garden plot of 1.92 m ² plot with 48 hills of a genotype	18
Figure 8: Days from sowing to PI regressed against days from sowing to flowering across all genotypes and environments..	23
Figure 9: Days from sowing to PI versus days from sowing to flowering across all genotypes for the sowing dates in Fanaye where PI was recorded.....	24
Figure 10: Boxplot of days from PI to flowering per environment where PI date was recorded.	25
Figure 11: Estimated versus observed days from sowing to PI. PI date estimated as 30 days before flowering.....	26
Figure 12: Boxplot of degree-days from PI to flowering per environment where PI date was recorded.....	26
Figure 13: Development rate (1/f) of IR64 versus mean air temperature during this period at 24 environments (E9 missing) across 5 different sites.	28
Figure 14: Development rate (1/f) of K5 versus mean air temperature during this period at 24 environments (E9 missing) across 5 different sites.	28
Figure 15: Development rate (1/f) of Chhomrong versus mean air temperature during this period at 25 environments across 5 different sites.....	29
Figure 16: Degree-days from sowing to flowering of IR64 versus number of days from sowing to flowering at 24 environments (E9 missing) across 5 different sites.	30

Figure 17: Degree-days from sowing to flowering of K5 vs number of days from sowing to flowering in 24 environments (E9 missing) across 5 different sites.....	31
Figure 18: Degree-days from sowing to flowering of Chhomrong vs number of days from sowing to flowering in 25 environments across 5 different sites ...	31
Figure 20: Multiple linear regression of DR of K5 versus mean air temperature and mean RH from sowing to flowering in 24 environments (E9 missing) across 5 different sites.....	33
Figure 19: Multiple linear regression of DR of IR64 versus mean air temperature and mean RH from sowing to flowering in 24 environments (E9 missing) across 5 different sites.....	33
Figure 21: Multiple linear regression of DR of Chhomrong versus mean air temperature and mean RH from sowing to flowering in 25 environments across 5 different sites.....	34
Figure 22: Development rate of IR64 versus mean air temperature from sowing to flowering in 24 environments (E9 missing)	36
Figure 23: Development rate of K5 versus mean air temperature from sowing to flowering in 24 environments (E9 missing)	37
Figure 24: Development rate of Chhomrong versus mean air temperature from sowing to flowering in 25 environments.....	37
Figure 25: Observed versus simulated days to flowering following Summerfield-model across all environments and genotypes.....	40
Figure 26: Observed vs simulated days to flowering following Summerfield-model for sowing dates in Ambohibary, Madagascar (E8-E12) across all genotypes.	41
Figure 27: Observed vs simulated days to flowering following Summerfield-model for sowing dates in Fanaye, Senegal (E13-E19) across all genotypes	41
Figure 28: Observed versus simulated days to flowering following Dingkuhn-model across all environments and genotypes.	42
Figure 29: Observed vs simulated days to flowering following Dingkuhn for Ambohibary (E8-E12) across all genotypes.	43

Figure 30: Observed versus simulated days to flowering following Dingkuhn for all sowing dates in Fanaye, Senegal (E13-E19) across all genotypes.....	43
Figure 31: Observed versus simulated days to flowering following Stuerz-model across all environments and genotypes.	44
Figure 32: Observed versus simulated days to flowering following Stuerz-model for all sowing dates in Ambohibary, Madagascar (E8-E12) across all genotypes.....	45
Figure 33: Observed versus simulated days to flowering following Stuerz-model for all sowing dates in Fanaye, Senegal (E13-E19) across all genotypes....	45
Figure 34: Observed versus simulated days to flowering following simple AGN-model across all environments and genotypes.....	46
Figure 35: Observed versus simulated days to flowering following simple AGN-model for all sowing dates in Fanaye, Senegal (E13-E19) across all genotypes.....	47
Figure 36: Observed versus simulated days to flowering following simple AGN-model for all sowing dates in Ambohibary, Madagascar (E8-E12) across all genotypes.....	47
Figure 37: Boxplot of residuals (simulated f - observed f) for the four tested phenology models.....	48
Figure 38: Multiple regression of development rate (1/f) of IR64 versus mean air temperature and mean relative air humidity (RH) in 24 environments (E9 missing) across 5 different sites. AGN version 1.....	54
Figure 39: Multiple regression of DR of IR64 vs mean T and mean RH in 24 environments (E9 missing) across 5 different sites. AGN version 2.....	55
Figure 40: Multiple regression of DR of IR64 vs mean T and mean RH in 24 environments (E9 missing) across 5 different sites. AGN version 3.....	56
Figure 41: Multiple regression of development rate (1/f) of IR64 versus mean air temperature and mean relative air humidity (RH) in 24 environments (E9 missing) across 5 different sites. AGN version 4.....	57

Figure 42: Multiple regression of development rate (1/f) of IR64 versus mean air temperature and mean relative air humidity (RH) in 24 environments (E9 missing) across 5 different sites. AGN version 5..... 58

Figure 43: Simulated versus observed days to flowering for all five versions of the improved AGN-model 60

Figure 44: Boxplot of residuals of the five AGN versions 61

List of Tables

Table 1: Description of environments incl. general weather conditions during growth season.....	13
Table 2: Cardinal temperature estimates for IR64 (V2), K5 (V27) and Chhomrong (V30) using four different phenology models.....	38
Table 3: Results from regressing simulated versus observed time to flowering for Summerfield, Dingkuhn, Stuerz and AGN phenology models.....	49
Table 4: Results of simple linear regressions of the individual environmental variables (RH, VPD, Rad, PP and PP _{TWI}) against residuals (simulated f - observed f) for each phenology model.	50
Table 5: Multiple linear regression with forward selection of environmental factors on residuals of Summerfield-model.	51
Table 6: Multiple linear regression with forward selection of environmental factors on residuals of Dingkuhn-model.	51
Table 7: Multiple linear regression with forward selection of environmental factors on residuals of Stuerz-model.....	51
Table 8: Multiple linear regression with forward selection of environmental factors on residuals of AGN-model.....	52
Table 9: Cardinal temperature for IR64 as estimates based on the five versions of AGN-model	58
Table 10: Results from regressing simulated vs. observed time to flowering for the five versions of AGN-model.....	59
Table 11: Characteristics of the genetic material tested in the Rice Garden Trials.	75
Table 12: Crop duration from sowing to flowering in days.....	92
Table 13: Cardinal temperatures estimated using four phenology models: Summerfield, Dingkuhn, Stuerz and simple AGN	95
Table 14: Results of Summerfield and Dingkuhn regressions.....	97
Table 15: Results of Stuerz and simple AGN regressions.....	99
Table 16: Results final AGN-model: $DR = a * T^2 + b * T + c * RH + d$. Cardinal temperatures according to AGNv1.	101

List of Equations

Summerfield:

- (1) $DR = 1/f$
- (2) $DR = a * \bar{T} + b * \bar{P} + c$
- (3) $DR = a * \bar{T} + b$
- (4) $T_{base} = -b/a$
- (5) $T_{SUM} = 1/a$

Dingkuhn:

- (6) $DD = T_{base} * f + T_{SUM}$
- (7) $DR = \frac{T_{av} - T_{base}}{T_{SUM}}$
- (8) $DS = \sum DR$
- (9) $DR = \frac{T_{av} - T_{base}}{T_{SUM} * 11 * (1 + CPP * (PPpi - 11))}$

Stuerz:

- (10) $DR = a * \bar{T} + b * \overline{RH} + c$
- (11) $T_{base_0} = -\frac{c}{a}$
- (12) $RH_{adj} = -\frac{b}{a}$
- (13) $T_{base} = T_{base_0} + RH_{adj} * RH$

Simple Asch-Groot Nibbelink (without RH):

- (14) $DR = a * \bar{T}^2 + b * \bar{T} + c$
- (15) $h = -\frac{b}{2a}$

$$(16) \quad k = a * h^2 + b * h + c.$$

$$(17) \quad y_{tan} = 0.5 * k$$

$$(18) \quad x_{tan} = \frac{\sqrt{-b + (b^2 - (4a * (c - y_{tan})))}}{2a}.$$

$$(19) \quad DR = m * \bar{T} + c_{tan}$$

$$(20) \quad m = 2a * x_{tan} + b.$$

$$(21) \quad c_{tan} = y_{tan} - (m * x_{tan})$$

$$(22) \quad T_{base} = -\frac{c_{tan}}{m}$$

$$(23) \quad T_{opt} = \frac{k - c_{tan}}{m}$$

$$(24) \quad T_{SUM} = \frac{1}{m}$$

$$(25) \quad T_{phys} = \max(\min(T_{opt}, T_{av}) - (T_{base} + RH_{adj} * RH_{av}), 0)$$

Asch-Groot Nibbelink (including RH):

$$(26) \quad DR = a * \bar{T}^2 + b * \bar{T} + c * \overline{RH} + d$$

$$(27) \quad RH_{adj.opt} = \frac{T_{opt100} - T_{opt0}}{100}$$

$$(28) \quad T_{phys} = \max(\min((T_{opt} + RH_{adj.opt} * RH_{av}), T_{av}) - (T_{base} + RH_{adj.base} * RH_{av}), 0)$$

1 Introduction

Rice (*Oryza sativa*) is a major staple food crop in Sub-Saharan Africa (SSA). However, paddy rice production falls behind global levels and is insufficient to fulfil the current demand. In 2019 average global rice yield was 4,631 kg/ha, while average yield in SSA was only 2,124 kg/ha, with lowest yields in Middle Africa (970 kg/ha) (FAO, 2020). In 2018 60% of rice consumption in SSA was covered by regional production while 40% was imported, mainly from Asia (AfricaRice, 2018; Saito et al., 2019). Besides being a major money drain out of the continent (AfricaRice, 2018), it leaves the region vulnerable to food insecurity. As we are currently witnessing with the war between Russia and Ukraine, global food trade can be disrupted quickly with massive impacts on food prices and availability elsewhere. Increasing rice self-sufficiency would improve food security and aid economic development in SSA.

Rice demand is expected to increase over the coming decades due to population growth. Currently 1.1 billion people live in SSA. This is expected to double by 2050 and to rise to around 3 billion by 2075 (United Nations, 2022). Moreover, climate change will result in more extreme weather events and prolonged periods of drought, thus challenging food production even further.

Crop modelling has the potential to positively contribute to food and nutritional security worldwide (Reynolds et al., 2018). Adapting rice production in SSA to future challenges such as climate change and maintaining food security requires well-functioning rice growth models to evaluate the potential of a production environment in combination with selected rice varieties. The backbone of such crop growth models is accurately simulating phenology, i.e. the timing of periodic growth events such as emergence, flowering and maturity and how these are influenced by the environment. Climate change makes model predictions less accurate if the underlying environmental factors influencing phenology and genotype by environment (G x E) interactions are not well understood and incorporated into the models (Stuerz et al., 2020).

Rice development is mainly influenced by temperature and photoperiod (Dingkuhn et al., 1995; Summerfield et al., 1992). Crop duration can be simulated using

cardinal temperatures: a base temperature (T_{BASE}), below which there is no development; an optimum temperature (T_{OPT}), where development rate is highest; a maximum temperature (T_{MAX}), above which there is no development; and temperature sum (T_{SUM}), the number of accumulated heat units i.e. degree-days a plant requires to complete a phenological phase. These phenological parameters are assumed to be genetically fixed and thus should not change when grown under different environmental conditions (Dingkuhn et al., 1995). Accurate simulation of crop duration depends on the phenology model applied and on the environments in which the photothermal constants were determined. For better estimation of cardinal temperatures, a given genotype should be grown in a wide range of environments.

Cardinal temperatures are used in rice growth models (e.g. ORYZA, CERES-RICE) in combination with weather data to simulate crop duration. This can be used to create cropping calendars and advice on an optimum sowing window to increase production levels. This can be applied in e.g. decision-support tools. An example of such a decision-support tool is RiceAdvice, developed by the Africa Rice Center (AfricaRice). This smartphone app has been designed to provide location-specific advice to farmers and extension agents on nutrient management, cropping calendars and good agricultural practices (RiceAdvice, 2022). Being able to accurately model phenology over a wider range of environments, can be used to improve accuracy and applicability of such tools.

2 Hypothesis and Research Objectives

A project was conducted between 2013 and 2017 where 80 rice varieties with diverse genetic backgrounds and characteristics were grown in rice garden trials. These varieties were exposed to a wide range of photo-thermal environments by planting them at different seasons and at five locations across Sub-Saharan Africa, while management was the same in each of the 25 environments. This study is based on data collected during that project.

The hypothesis at the basis of this thesis is that photothermal responses to the environment are genetically fixed. Therefore, cardinal temperatures can be derived, and crop duration can be estimated using phenological models.

Adapting rice production in Sub-Saharan Africa to future challenges such as climate change and maintaining food security requires functional crop models to evaluate the potential of a production environment in combination with selected rice varieties. The backbone of such models is accurately simulating phenology across a wide spectrum of environments. Therefore, the research objectives are:

1. To analyse how genotype by environment interactions affect rice phenology
2. To estimate genotype-specific cardinal temperatures of 80 rice varieties
3. To suggest improvements for rice phenology models

3 Literature review

3.1 Rice Phenology

Phenology is the study of plant growth and development regarding the timing of the various developmental stages. The life cycle of a rice crop is illustrated in figure 1. A rice plant's development can be divided into three phenological phases (Vergara, 1991):

1. Vegetative phase (VP): From sowing to panicle initiation
2. Reproductive phase (RP): From panicle initiation to flowering
3. Ripening phase (RIP): From flowering to maturity

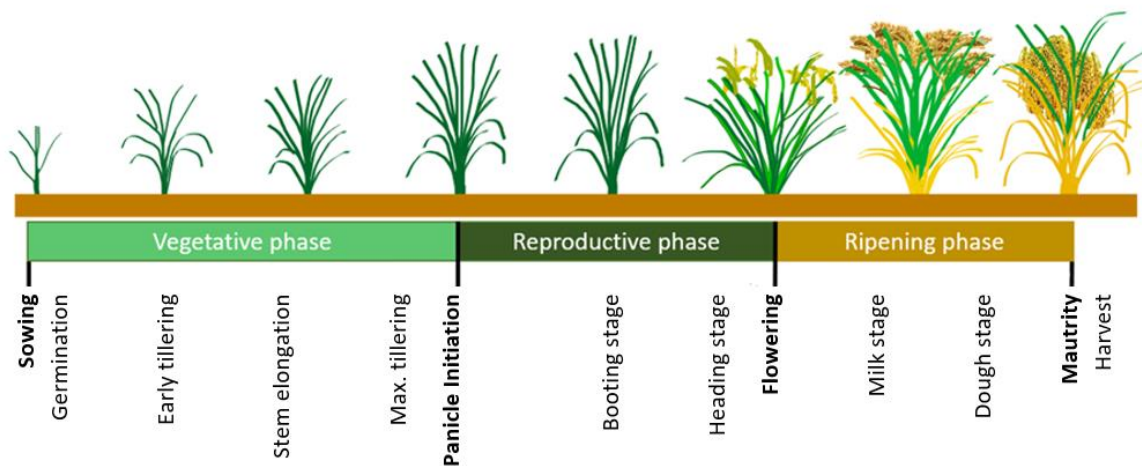


Figure 1: Rice crop life cycle divided in phenological phases. Adapted from (Aguilar, 2019).

The vegetative phase starts with sowing, followed by germination, leaf emergence, tillering, stem elongation, increase in biomass and ends with panicle initiation (PI). This phase is the main source of variation in crop duration. Duration of VP is mainly influenced by temperature experienced by the rice plant at the meristem and daylength i.e. photoperiod (PP) (Dingkuhn et al., 1995; Summerfield et al., 1992; Vergara, 1991). However, it has also been reported that relative air humidity (RH) is negatively correlated with crop duration (Stuerz et al., 2020).

VP consists of a basic vegetative phase (BVP) and a photoperiod sensitive phase (PSP). If during BVP a genotype-specific number of heat units (T_{SUM}) are accumulated and PP conditions are favourable, the rice plant will proceed to panicle initiation and

the reproductive phase. Rice is, like many tropical species, a short-day plant. That means that for PP-sensitive plants flowering is induced when PP falls below a certain threshold. During long days, PSP is extended and flowering is delayed. However, not all genotypes are sensitive to daylength.

The reproductive phase starts with PI, encompasses booting and heading stage and ends with flowering. This phase typically lasts 30 - 35 days (IRRI, n.d.; Vergara, 1991). During booting the plant is most sensitive to cold and heat spells, causing spikelet sterility and thereby reducing yields (Dingkuhn, 1995; Jagadish et al., 2007; Shrestha et al., 2013).

During the ripening phase grains increase in size and weight. Ripening starts with flowering, followed by the milky and doughy stage and ends with physiological maturity, when the seeds have become hard and dry and are ready to be harvested. RIP is reported to be relatively constant at about 30 days (IRRI, n.d.; Vergara, 1991). However, in temperate and high-altitude regions, RP and RIP may take twice as long to complete (Vergara, 1991).

3.2 Genotype by Environment Interactions

The phenotype of any plant is the result of the genotype, the environment and its interactions. Phenotypic value can thus be understood as the sum of genotypic value, the environmental influence and the interactions of these: $P = G + E + G * E$.

Environmental factors can be divided into a) fixed factors, which are defined by the location and experimental setup, such as location, altitude, soil, fertilization, weed and pest management; and b) random factors, such as weather conditions, drought, spontaneous pest outbreaks. The environment influences certain traits, one of them being crop duration. E.g. in one environment a rice plant may take 90 days to reach flowering, while in another environment it takes 110 days. The genotype influences crop duration as well: some genotypes are typical short-duration varieties, while others are typical long-duration varieties. On top of this, there are G x E interactions.

Without G x E interactions, the best genotype in one environment, would be the best in all environments and the difference between the genotypes would remain equal. However, in reality this is not the case. As illustrated in figure 2, crop duration of genotype A and B differs from one environment to the other.

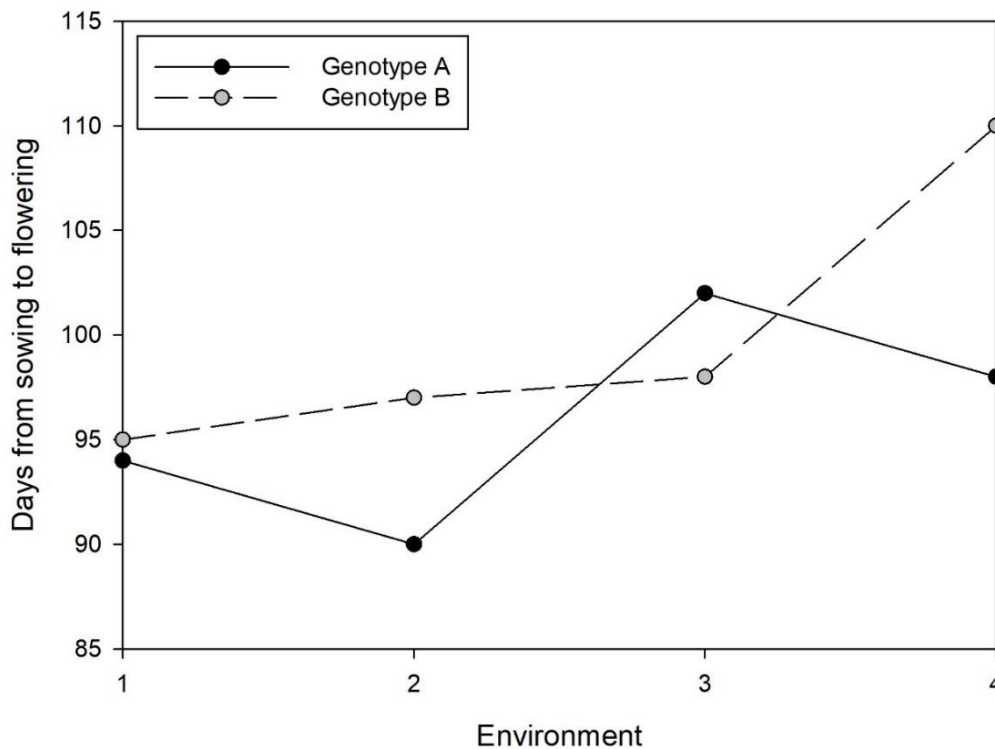


Figure 2: Genotype by Environment interactions affecting crop duration. Data from Rice Garden Trials. Genotype A is WITA 4 (V5), Genotype B is WAB 2101-WAC1-1-TGR5-WAT B6 (V38). Environments correspond to E1-E4.

The difference in crop duration between genotype A and B does not remain equal: at E1 the difference in crop duration is just 1 day, while at E2 the difference is 7 days and at E3 the ranking even changes. At E3 genotype A takes longer to reach flowering than genotype B. This is called a cross-over effect, or quantitative interaction (Bernardo, 2010). A specific environmental difference may have a greater effect on some genotypes than on others. The greater the effect, the more sensitive this genotype is to the environment (Bernardo, 2010). These interactions do not only complicate selection of superior genotypes for plant breeders, since it limits the association between phenotypic and genotypic values (Romagosa et al., 1993), but It also complicates phenological modelling.

The biological basis of G x E interactions is complex, as usually many genes are involved. A trait such as crop duration is the result of a series of biochemical

reactions and interactions within the plant initiated by genes, modified and controlled by other genes and by the external environment (Romagosa et al., 1993). Some researcher therefore try to link the genes to phenology through genome-wide association studies to find the QTL linked to phenological parameters (Dingkuhn et al., 2017).

When individuals of different genotypes are grown in specific environments, the G x E interaction can be studied in more detail. When environmental factors are known, the influence of these individual factors can be studied. In this study the meteorological data is known, which allows us to study the influence of these factors on crop duration.

3.3 Rice crop models

Rice crop models e.g. ORYZA, CERES-RICE and APSIM are complex models built on several subroutines. There are subroutines for e.g. yield, spikelet sterility, soil interactions, nitrogen limitation, water balance, and of course for phenology. RIDEV2 for example has a subroutine dedicated to calculating water temperature, as this is the temperature the rice plant experiences for the majority of time to flowering (Dingkuhn et al., 2017). This is used to calculate physiological temperature and subsequently to simulate crop duration.

Crop models have been combined and improved over the years creating new models, with subroutines tailored to different applications. A comprehensive overview of the history of rice crop models has been given by van Oort & Dingkuhn (2021), figure 3.

ORYZA is one of the major rice crop models. The original ORYZA1 model was developed by (Kropff et al., 1994) and written in the code language FORTRAN (Bouman et al., 2001). RIDEV1 and RIDEV2 are able to model rice development and spikelet sterility and are therefore suitable for creating cropping calendars, but not for modelling yield (Dingkuhn et al., 2014). ORYZA1 was further developed to ORYZA2000, which was then combined with RIDEV2 creating version ORYZAv2n14, which is able to model heat and cold-induced spikelet sterility (van Oort et al., 2015).

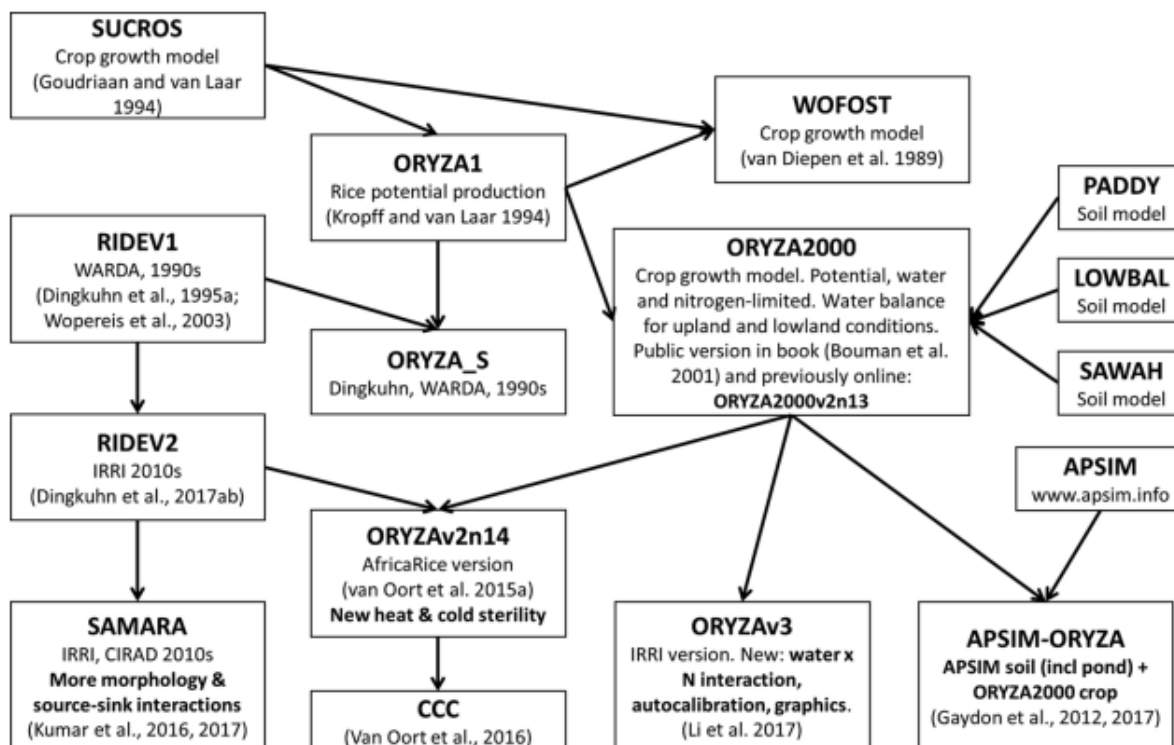


Figure 3: Brief historical overview of rice models. Source: van Oort & Dingkuhn, 2021

3.4 Phenology models

It is important to understand the difference between crop models, based on several subroutines, and the simpler phenology models, which are used to simulate timing of different phenological phases and crop duration and form the backbone of these crop models. In this thesis three readily available simple phenology models are compared (Dingkuhn et al., 1995; Stuerz et al., 2020; Summerfield et al., 1992).

3.4.1 Summerfield

Summerfield et al. (1992) conducted pot experiments with 16 diverse rice genotypes grown under 13 different photo-thermal regimes in controlled-environment growth chambers. They found that if rice was grown in 11.5h days and at sub-optimal temperatures the rate of development from sowing to flowering was a linear function of both temperature and photoperiod, without interaction between these two factors. The rate of progress, or development rate (DR) is the inverse of the time in days from sowing to flowering (f):

$$(1) \quad DR = 1/f$$

This resulted in the phenology model:

$$(2) \quad DR = a * \bar{T} + b * \overline{PP} + c$$

Where \bar{T} is the mean diurnal air temperature ($^{\circ}\text{C}$), \overline{PP} is the photoperiod (h d^{-1}) over the period from sowing to flowering and a , b , and c are genotype-specific constants. b typically has a negative value in short-day plants, such as rice.

In PP-insensitive plants, in environments where PP is maintained constant throughout the growing period and for PP-sensitive plants where daylength is maintained below the critical photoperiod, which is genotype-specific but generally around 11,5 h, the photoperiod term can be deleted from the equation, which results in the simplified phenology model:

$$(3) \quad DR = a * \bar{T} + b$$

This relationship is only linear if two conditions are met: a) the minimum daily temperature experienced by the plant is not below T_{BASE} ; and b) the warmest temperatures do not exceed T_{OPT} .

The base temperature is where $DR = 0$. Below this temperature, there is no development in the rice plant and no heat units are accumulated. When regressing mean temperature on the x-axis against DR on the y-axis, the base temperature is the intersect with the x-axis. This can be calculated as:

$$(4) \quad T_{\text{base}} = -b/a$$

The temperature sum (T_{SUM}) is the genotype-specific amount of heat units i.e. degree-days above T_{BASE} required for flowering to occur and is calculated as:

$$(5) \quad T_{\text{SUM}} = 1/a$$

3.4.2 Dingkuhn

Dingkuhn et al. (1995) developed a simple model for photothermal effects on flowering to explain variations in crop duration, based on air temperature.

Genotype-specific cardinal temperatures were quantified by linear regression of the sum of average daily air temperature against observed f across environments:

$$(6) \quad DD = T_{base} * f + T_{SUM}$$

Where DD is the sum of the average daily air temperature $> 0^{\circ}\text{C}$ from sowing to flowering, i.e. degree-days [$^{\circ}\text{Cd}$]. From this regression it follows that T_{BASE} is the slope of the regression line and T_{SUM} is the intercept. This equation only holds if temperatures reflect the temperatures experienced by the plant and if PP is either corrected for, or insignificant.

Development rate can be expressed as the number of heat units experienced during a day divided by the number of heat units required for flowering:

$$(7) \quad DR = \frac{T_{av} - T_{base}}{T_{SUM}}$$

The development stage (DS) ranges from 0 at sowing to 1 at flowering (Penning de Vries et al., 1989). Since DR is the inverse of f , it follows that summing the daily development rate steps will give $DS = 1$ when flowering is reached:

$$(8) \quad DS = \sum DR$$

The fit of the model calibration and thus of the cardinal temperatures was tested by dividing observed f by simulated f . Dingkuhn et al. (1995) found that prediction errors following from the simple model only based on thermal effects, could be partially explained by daylength at PI. Incorporating PP_{PI} into eqn 7 lead to:

$$(9) \quad DR = \frac{T_{av} - T_{base}}{T_{SUM11} * (1 + CPP * (PP_{PI} - 11))}$$

T_{SUM11} are the sum of heat units required until flowering at $PP = 11\text{h}$. CPP is the slope constant for photoperiodism. PP_{PI} is the photoperiod at PI, estimated as 30 days before heading.

3.4.3 Stuerz

Currently existing phenology models based on photoperiod and temperature often have reduced replicability beyond the environments they have been calibrated for (Stuerz et al., 2020). In order to increase applicability of phenology models to a wider

range of environments, Stuerz et al. (2020) looked at which environmental factors i.e. climatic determinants, could explain differences in crop duration between environments. They tested the international test variety IR 64 at eight sites at in total 87 sowing dates, covering the complete environmental range where rice is commonly produced.

Stuerz et al. (2020) first applied eqn 3 to their data and calculated crop duration as the inverse of DR. They subsequently regressed residuals (simulated f - observed f) against a range of climatic determinants. Stuerz et al. (2020) found that mean relative air humidity is negatively correlated with the residuals, indicating that low RH reduces DR and increases f . They corrected the crop duration for the effect of RH. Time to flowering was not simulated using cardinal temperatures.

4 Materials and Methods

4.1 Environments

4.1.1 Locations

This experiment was conducted at five of AfricaRice’s research locations across SSA: Fanaye in Senegal (16.54N, -15.19W, altitude 10m asl), Cotonou in Benin (6.42N, 2.33E, altitude 27m asl), Mbé in Ivory Coast (7.88N, -5.11W, altitude 273m asl), Ruvu in Tanzania (-6.72S, 38.67E, altitude 29m asl) and Ambohibary in Madagascar (-19.63S, 47.14E, altitude 1645m asl), see figure 4.

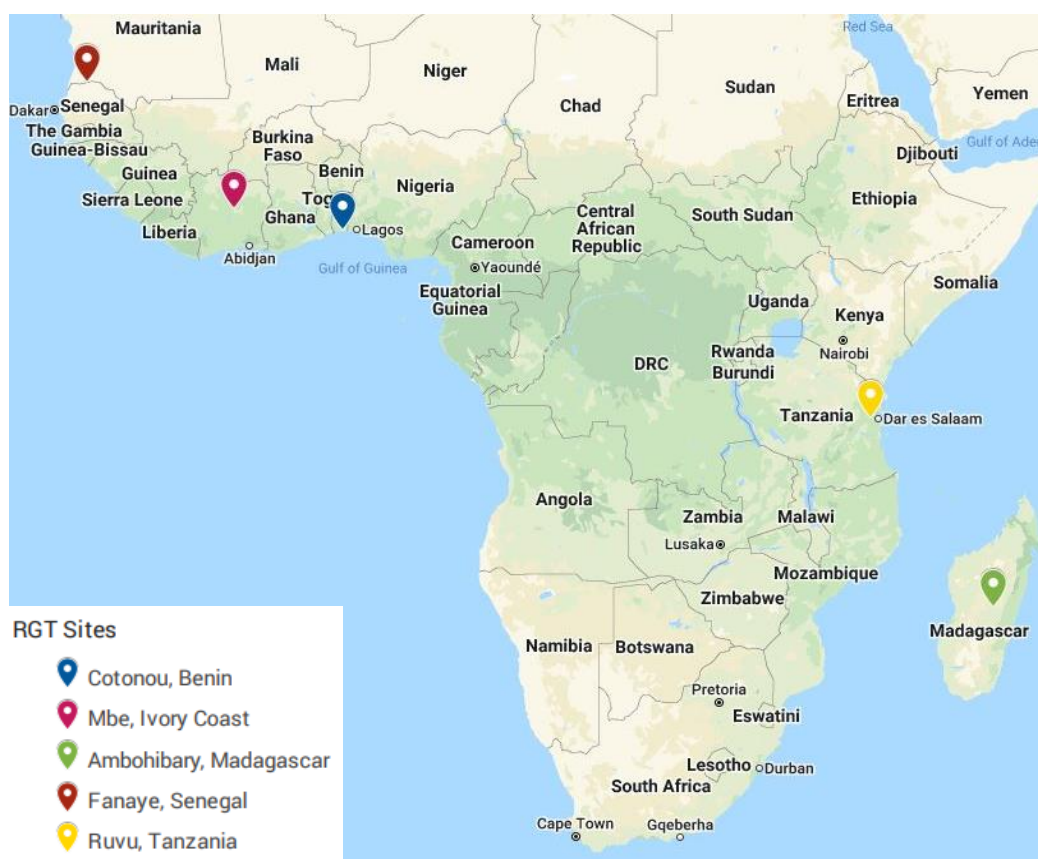


Figure 4: Rice Garden Trial Sites. Map source: Google Maps

4.1.2 Sowing dates

At each of the five locations the trial was repeated at different sowing dates (SD) between 2013 and 2017. In total there were 25 sowing dates: Cotonou, Benin, 2SD; Mbé, Ivory Coast, 5SD; Ambohibary, Madagascar, 5SD; Fanaye, Senegal, 7SD; Ruvu, Tanzania, 6SD.

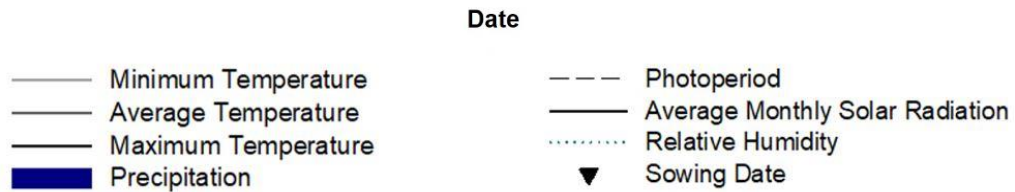
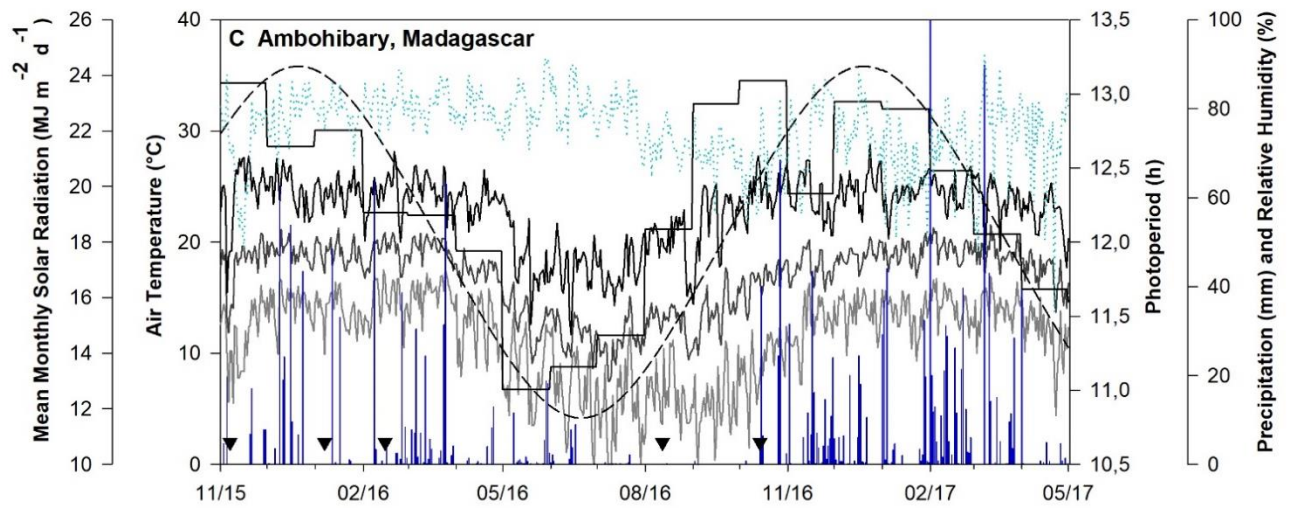
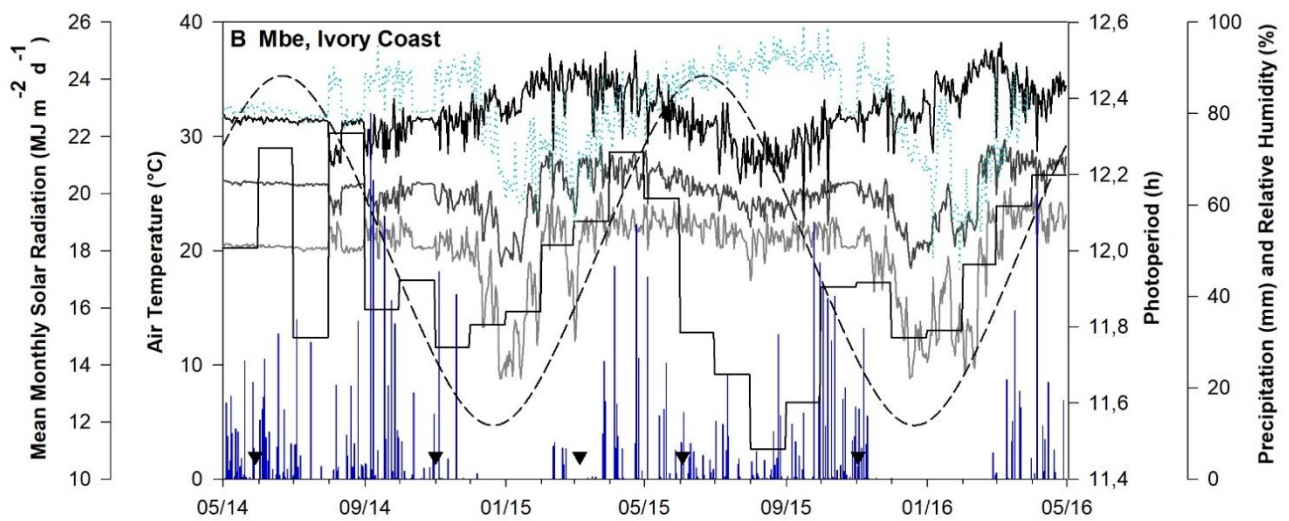
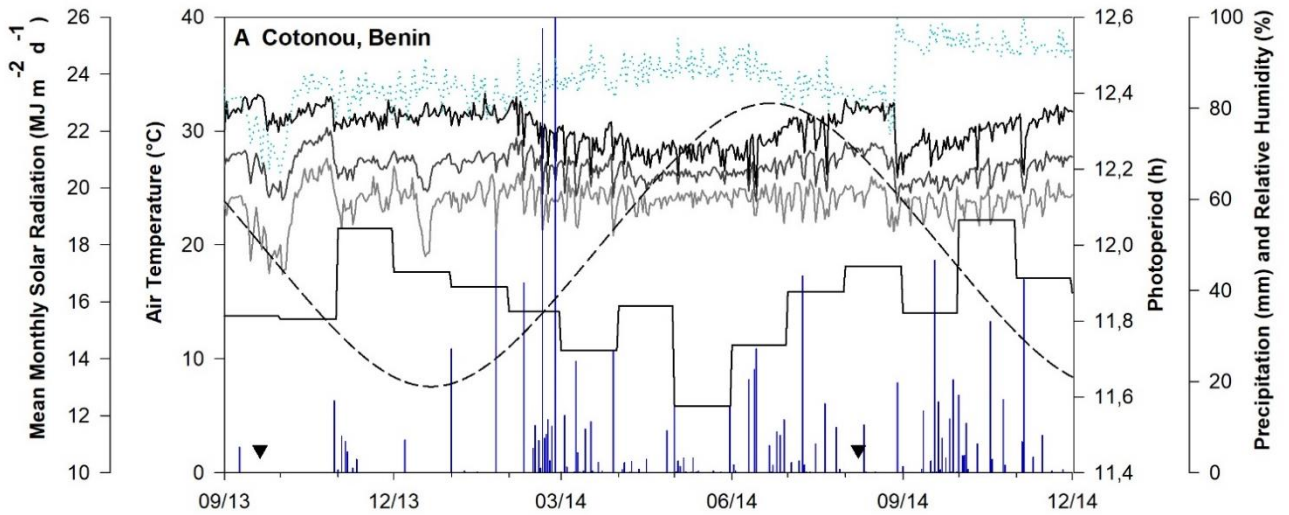
An environment is a general term that covers different spatial, temporal and management conditions under which a plant is grown (Romagosa et al., 1993), so each SD is a different environment. The environments were chosen to cover a wide range of environmental conditions (table 1).

Table 1: Description of environments incl. general weather conditions during growth season. Env. is environment. Lat is latitude; Long is longitude, both given in degrees; alt. is altitude in m asl.

Env	Country	Site	Lat	Long	Alt	Sowing date	Weather conditions
E1	Benin	Cotonou	6.42	2.33	27	20-9-2013	Warm, humid
E2	Benin	Cotonou	6.42	2.33	27	8-8-2014	Warm, wet
E3	Ivory Coast	Mbe	7.88	-5.11	273	29-5-2014	Warm, humid
E4	Ivory Coast	Mbe	7.88	-5.11	273	1-11-2014	Warm days, cool nights, humid to arid
E5	Ivory Coast	Mbe	7.88	-5.11	273	6-3-2015	Warm, humid
E6	Ivory Coast	Mbe	7.88	-5.11	273	3-6-2015	Warm, humid
E7	Ivory Coast	Mbe	7.88	-5.11	273	2-11-2015	Warm days, cool nights, humid to arid
E8	Madagascar	Ambohibary	-19.63	47.15	1645	7-11-2015	Cool, humid
E9	Madagascar	Ambohibary	-19.63	47.15	1645	7-1-2016	Cool, humid
E10	Madagascar	Ambohibary	-19.63	47.15	1645	15-2-2016	Cold, humid
E11	Madagascar	Ambohibary	-19.63	47.15	1645	12-8-2016	Cool, arid to humid
E12	Madagascar	Ambohibary	-19.63	47.15	1645	14-10-2016	Cool, humid
E13	Senegal	Fanaye	16.54	-15.19	10	13-3-2014	Very hot, very arid
E14	Senegal	Fanaye	16.54	-15.19	10	27-7-2014	Very hot, arid to humid
E15	Senegal	Fanaye	16.54	-15.19	10	28-10-2014	Hot days, cool nights, very arid
E16	Senegal	Fanaye	16.54	-15.19	10	26-1-2015	Hot, very arid
E17	Senegal	Fanaye	16.54	-15.19	10	27-2-2015	Very hot, very arid
E18	Senegal	Fanaye	16.54	-15.19	10	16-7-2015	Hot, humid
E19	Senegal	Fanaye	16.54	-15.19	10	16-10-2015	Hot days, cool nights, very arid
E20	Tanzania	Ruvu	-6.72	38.67	29	13-3-2014	Warm, wet
E21	Tanzania	Ruvu	-6.72	38.67	29	5-6-2014	Warm, arid
E22	Tanzania	Ruvu	-6.72	38.67	29	15-8-2014	Warm, arid
E23	Tanzania	Ruvu	-6.72	38.67	29	11-3-2015	Warm, wet
E24	Tanzania	Ruvu	-6.72	38.67	29	18-5-2015	Warm, humid to dry
E25	Tanzania	Ruvu	-6.72	38.67	29	22-10-2015	Warm, humid

4.1.3 Weather conditions

The weather graphs (figure 5) show the wide range in temperature, precipitation, RH, solar radiation and PP between the sites and sowing dates.



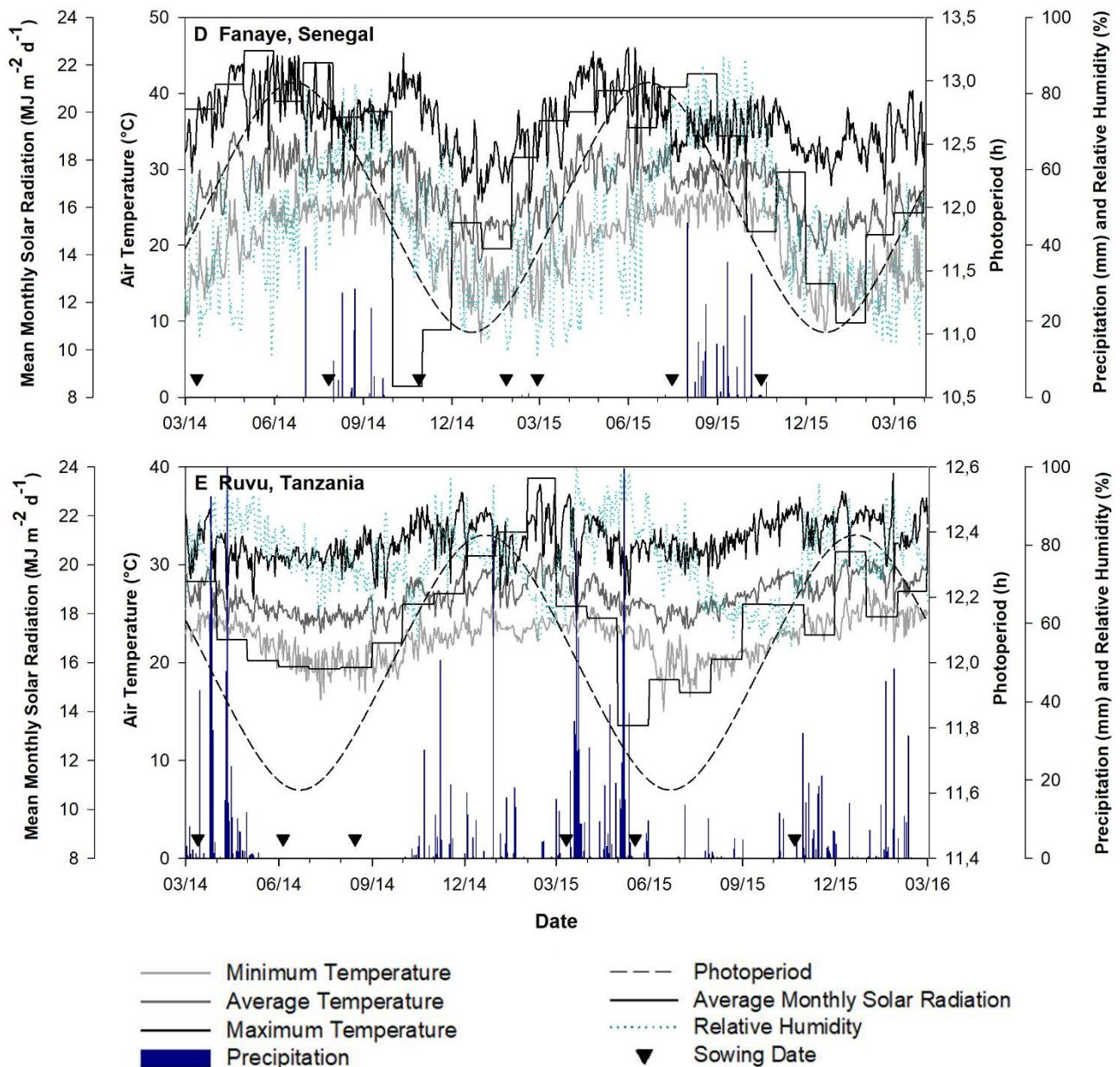


Figure 5: Weather graphs of Cotonou, Benin (A); Mbe, Ivory Coast (B); Ambohibary, Madagascar (C); Fanaye, Senegal (D); and Ruvu, Tanzania (E). The black, dark grey and medium grey lines visualise maximum, mean and minimum daily temperature [°C]. The solid black line that changes with monthly steps is the mean solar radiation [$\text{MJ}\cdot\text{m}^{-2}\cdot\text{d}^{-1}$]. The dashed black sinus-shaped line is photoperiod in hours. The dotted turquoise line represents daily mean relative air humidity [%]. Blue bars represent precipitation [mm]. For certain dates, rainfall exceeded 100mm: Cotonou 26/02/2014 122mm; Ambihibary 01/02/2017 109mm; Ruvu 11/04/2014 103mm. Black triangles at the bottom indicate sowing dates.

Ambohibary, with its high altitude and furthest distance to the equator, is cooler than other sites with occasional night frost during winter season and has greatest variation in daylength over the year. Fanaye has the most extreme hot temperatures with large variation between diurnal minimum and maximum temperatures. It is also the driest site with RH dropping regularly below 20% during the dry season.

4.2 Genetic material

Eighty rice genotypes were tested during this project. A table with the characteristics of the genetic material including variety code, variety name, breeding line, country of origin, parents, species, subspecies and the production system is given in appendix I. Some varieties are interspecific, which means they are a cross between Asian rice (*O. sativa*) and African rice (*O. glaberrima*). Some genotypes are not official varieties, but rather breeding lines that have not (yet) been approved as such. However, for simplicity all genotypes will be referred to as 'varieties' and have been given a variety code number (V_{CODE}).

Rice is commonly grown in three different production systems: Irrigated lowland (IL), rainfed lowland (RL) and rainfed upland (RU). IL is paddy rice, where rice is grown in bunded fields in a standing layer of water. RL is rainfed with small bunds i.e. dykes around the fields that capture and store rainwater in the field. RU is purely rainfed, the fields have no bunds to retain rainwater (Rao et al., 2017). The varieties have been bred for these different production systems but were all grown under IL conditions during this project.

In E7 (Ivory coast) and E19 (Senegal) V61 was omitted and 6 ARICA genotypes were added to the RGTs. In Madagascar 20 additional genotypes were tested, totalling 100 genotypes. The genotypes that were tested at few environments have been excluded from further analysis.

4.3 Experimental design and management

The 80 genotypes were grown in an augmented design with 5 check genotypes and 5 blocks. Each block within one environment consisted of 20 plots, i.e. 5 check genotypes and 15 test genotypes (Figure 6). At each sowing date the test and check genotypes were randomized within each block, except for E25, where the design had not been randomized.

Sowing 1																			
Block 1				Block 2				Block 3				Block 4				Block 5			
CV-1	TV-n	TV-n	TV-n	TV-n	CV-2	TV-n	TV-n	CV-1	TV-n	TV-n	TV-n	TV-n	TV-n	CV-2	TV-n	TV-n	CV-3	TV-n	TV-n
TV-n	TV-n	CV-3	TV-n	TV-n	TV-n	TV-n	TV-n	TV-n	TV-n	CV-4	TV-n	TV-n	TV-n	TV-n	TV-n	TV-n	TV-n	TV-n	CV-2
TV-n	TV-n	TV-n	CV-5	CV-3	TV-n	TV-n	CV-1	TV-n	CV-2	TV-n	TV-n	TV-n	CV-3	TV-n	TV-n	TV-n	TV-n	TV-n	TV-n
TV-n	CV-2	TV-n	TV-n	TV-n	TV-n	CV-5	TV-n	TV-n	TV-n	CV-3	TV-n	CV-5	TV-n	TV-n	CV-4	TV-n	CV-5	TV-n	TV-n
TV-n	TV-n	TV-n	CV-4	TV-n	CV-4	TV-n	TV-n	TV-n	TV-n	TV-n	CV-5	TV-n	TV-n	CV-1	TV-n	CV-1	TV-n	TV-n	CV-4

Sowing 2																			
Block 1				Block 2				Block 3				Block 4				Block 5			
TV-n	TV-n	CV-4	TV-n	CV-5	TV-n	TV-n	TV-n	TV-n	CV-3	TV-n	TV-n	TV-n	TV-n	TV-n	CV-5	TV-n	TV-n	CV-5	TV-n
CV-3	TV-n	TV-n	TV-n	TV-n	CV-1	TV-n	TV-n	CV-4	TV-n	TV-n	TV-n	CV-2	TV-n	TV-n	TV-n	TV-n	CV-2	TV-n	TV-n
TV-n	CV-1	TV-n	TV-n	TV-n	TV-n	TV-n	CV-2	TV-n	TV-n	TV-n	CV-2	TV-n	CV-4	TV-n	CV-3	TV-n	TV-n	TV-n	TV-n
TV-n	TV-n	TV-n	CV-2	TV-n	CV-3	TV-n	TV-n	TV-n	TV-n	CV-5	TV-n	TV-n	TV-n	CV-1	TV-n	TV-n	TV-n	CV-3	CV-4
CV-5	TV-n	TV-n	TV-n	TV-n	TV-n	TV-n	CV-4	TV-n	CV-1	TV-n	TV-n	TV-n	TV-n	TV-n	TV-n	CV-1	TV-n	TV-n	TV-n

Sowing 3																			
Block 1				Block 2				Block 3				Block 4				Block 5			
TV-n	TV-n	TV-n	CV-5	TV-n	TV-n	TV-n	CV-2	TV-n	TV-n	CV-2	TV-n	TV-n	TV-n	TV-n	CV-5	TV-n	TV-n	TV-n	TV-n
CV-2	TV-n	TV-n	TV-n	CV-4	TV-n	TV-n	TV-n	TV-n	TV-n	TV-n	TV-n	TV-n	TV-n	CV-1	TV-n	TV-n	CV-5	CV-2	TV-n
TV-n	TV-n	CV-1	TV-n	TV-n	TV-n	TV-n	TV-n	CV-3	TV-n	CV-1	TV-n	TV-n	CV-2	TV-n	TV-n	TV-n	TV-n	TV-n	CV-4
CV-4	TV-n	TV-n	TV-n	TV-n	CV-1	CV-5	TV-n	TV-n	TV-n	TV-n	TV-n	TV-n	TV-n	CV-4	TV-n	CV-1	TV-n	TV-n	TV-n
TV-n	TV-n	CV-3	TV-n	CV-3	TV-n	TV-n	TV-n	TV-n	CV-5	TV-n	CV-4	CV-3	TV-n	TV-n	TV-n	TV-n	CV-3	TV-n	TV-n

Figure 6: Example of a field layout for the Rice Garden plots with different sowing dates of different genotypes in an augmented design. Green colours indicate the different replicate blocks in each sowing block. TV-n = Test variety where n represents the number of the test variety; CV-n = Check variety where n represents the number of the check variety. Check varieties are planted in each replicate block (within sowing block), while test varieties are planted only once within each sowing block.

The trials were established by transplanting. Seeds were sown in nursery beds (after pre-germination in the trials in Mbé, Fanaye and Ambohibary) and transplanted at 2 plants per hill after two to three weeks in plots of 1.2 m × 1.6 m (1.92 m²) and a hill to hill spacing of 20 x 20 cm, thus totalling 48 rice plants per plot (Figure 7). Plot to plot spacing was 40cm. Urea, Triple Super Phosphate and KCl were applied at transplanting at rates of 50 kg N ha⁻¹, 30 kg P ha⁻¹ and 50 kg K ha⁻¹. At 20 days after transplanting, urea was top-dressed at 75 kg N ha⁻¹. 50 days after transplanting another top-dress of urea and KCl was applied at rates of 75 kg N ha⁻¹ and 50 kg K ha⁻¹.

Plots were flooded with the water table adapted to seedling size at transplanting and later on maintained at 5 - 10 cm. Weeds were controlled by regular manual weeding. Pesticides were applied where necessary and fields were protected by nets against birds. Off-types were removed.

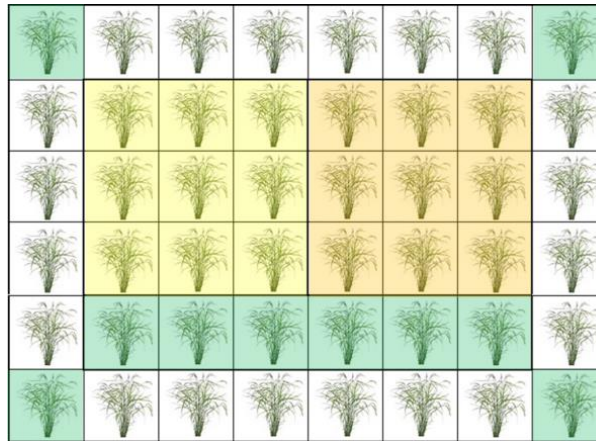


Figure 7: Rice Garden plot of 1.92 m² plot with 48 hills of a genotype (24 hills in the border lines and 24 hills in the middle of the plot for observations (2 squares of 9 hills for harvest and post-harvest observations and 1 line of 6 hills for destructive observations and 1 line of 6 hills for destructive observations on panicle initiation).

4.4 Data collection

4.4.1 Rice garden trials

Field technicians visited the trials on a daily basis and recorded dates of sowing, 50% emergence, transplanting, 50% panicle initiation of the main stems (PI), 50% heading of all stems, 50% flowering of all stems, 85% maturity and harvest. The date of panicle initiation was monitored through destructive observation in six plants of each plot. Since the panicle is only visible a number of days after actual PI, five to seven days were deducted from the date when PI was first observed. The date of 50% flowering was recorded as the date at which 50% of the stems in a plot were flowering. Dates of 85% maturity and harvest were recorded as well, except for Madagascar, where 50% maturity date was recorded. Besides phenological data, spikelet sterility and grain separation data were recorded, but not further used for this thesis.

In roughly a quarter of the cases (563 out of 2000) 50% emergence date was not registered. Since sowing date was always registered, this was used in further phenology analysis. For roughly a quarter (499 out of 2000) PI data was missing. At E1, E8, E9, E10, E16, E17 no PI data was collected, at other environments PI data was missing for some genotypes. 92 times the flowering date was not observed, either because the plots had been damaged or because the variety never reached flowering. The latter was the case in the majority of genotypes in E9, where 62

flowering dates were missing. The 18 observed flowering dates were all from short-duration varieties.

Besides phenological data, agronomic data on plant height, number of panicles, grain yield, straw weight per area and per hill and spikelet sterility was collected. Percentage of partially filled grains and weight of empty, partially and completely filled grains were recorded as well. This data has not been analysed further in this thesis, but it forms an interesting source for further analysis.

At E1 and E14 there was rat damage, which influenced grain separation data, but not phenology data. At E6 there was wind damage and diseased plants, which resulted in stunted plant growth. At E20 there was flooding resulting in complete submergence which lasted for five days in mid-April, about two weeks after transplanting. At E22 there was a bird attack which caused some missing phenology and harvest data.

4.4.2 Microclimate plots

At three of the research locations (Cotonou, Ruvu and Fanaye) microclimate (MC) data was collected. At the MC plots, phenological stages were recorded as in the rice garden trials, plus leaf area index was recorded. Additionally, the time of flowering for the start, peak and end of flowering were visually inspected and recorded every day during the period of panicle emergence (i.e. heading) in Fanaye and Cotonou. Inside- and above-canopy temperature and humidity were monitored using MINCER devices (Cotonou and Fanaye). Tinytag data loggers were used to record water temperature and inside- and above-canopy temperature and humidity in Cotonou, Fanaye and Ruvu. However, MC data was often incomplete and of low quality due to dysfunctional measurement devices. E.g. for only two environments water temperature data was complete. Missing data could not be estimated. Thus, MC data was found to be insufficient and not further considered during analysis.

4.4.3 Meteorological data

Data on minimum, mean and maximum air temperature; minimum, mean and maximum relative air humidity; wind direction and speed; solar radiation and precipitation were collected on daily basis from meteorological stations nearby the

trial sites. Furthermore, daylength including and excluding twilight and minimum and maximum vapor pressure deficit were calculated. Missing data was estimated by P. van Oort based on the global yield gap project. Missing T_{AV} was calculated as the average of minimum and maximum recorded temperature of that day. Estimated data was checked against additional weather data from nearby stations in Madagascar and Ivory Coast and was found to be reliable. Since there was missing data for all five locations and not for all locations additional weather data from nearby weather stations was available, estimated data was kept to be consistent.

4.5 Data analysis

4.5.1 Data preparation

The dataset was prepared for analysis using Microsoft Excel. Data on phenology, spikelet sterility and grain yield were collected per trial and merged into one overview table. Data on check varieties was averaged, resulting in one data point per check variety per environment. Block effect was not taken into account, as this was complicated to estimate from the augmented design, would have considerably complicated further analysis and is negligible in comparison to differences between locations and sowing dates. Variation due to environment is larger than block effects, thus including a block effect was not expected to considerably change the outcome of the analysis.

Quality control of the phenology data was performed manually. Data that seemed unrealistic or doubtful was marked. Marked data was usually explained during further analysis; data that could only be explained as measurement or data entry error was omitted (155 PI dates for E13 and E15, explained why in chapter 5.2). Based on the phenological data in combination with the meteorological data, new variables were calculated per genotype/environment combination, e.g duration, DR, dd, mean air temperature, cumulative radiation, mean VPD, mean RH and PP of different phenological phases.

4.5.2 Analysing phenology models

Three rice phenology models described in chapter 3.4 were applied to estimate the genotype-specific cardinal temperatures and a new phenology model was developed. Stuerz' model was adapted so it could be used to estimate cardinal temperatures and include an RH-adjustment factor. f was simulated using the cardinal temperatures estimated for the different models and simulated f was regressed against observed f . Residuals (sim. f - obs. f) were regressed against several environmental factors. The outcome of this regression was used to improve the newly developed phenology model. All statistical tests (i.e. regressions, ANOVAs) and simulation of flowering dates were performed with SAS software, version 9.4 for windows. Significance level was set at $\alpha=.05$. Complete SAS code is given in Appendix II. Data was visualised using SigmaPlot version 12.5. Excel was used for data preparation, to compile input data for both SAS and SigmaPlot and to compile output tables.

5 Results

5.1 Crop duration

There is large variation in crop duration between environments and genotypes. Chhomrong (V30) had the shortest average crop duration at 81 days, followed shortly by V79 (FOFIFA 172) at 83 days. Shortest crop duration was recorded for Chhomrong sown September 2013 at Cotonou (E1), where it took only 53 days to reach flowering. V38 (WAB 2101-WAC1-1-TGR5-WAT B6) was the genotype with longest average crop duration at 129 days. The longest crop duration measured during this project was for V27 (K5) sown February 2015 at Ambohibary (E10). E10 was also the environment with the longest average crop duration at 313 days. Long crop durations in this environment can be explained by the fact that rice was sown at the start of the cold season with shortening days. This was considerably longer than the second longest duration environment: E11 (sown August 2016, Ambohibary) with 211 days. Rice sown March 2015 in Mbe had an average crop duration of 83 days, followed shortly by E23 (sown March 2015, Ruvu) with an average duration of 85 days. All observed crop durations from sowing to flowering for the 80 varieties in the 25 environments are presented in Appendix III.

5.2 Panicle Initiation

Since PI is difficult to observe, PI data was checked for possible errors. For the 1501 genotype-environment combinations where both PI and flowering date were recorded, days from sowing to PI were regressed against days from sowing to flowering, grouped per location (figure 8). In reality, the locations consist of several sowing dates, making up different environments. This explains why data from one location may appear as several groups of data points.

If time from PI to flowering would be constant at 30 days, as assumed by Dingkuhn et al. (1995), the regression equation would have been $y = x - 30$, while a regression equation of $y = 0.726x - 5.52$ with $r^2 = .818$ was found based on our data. There are clear differences between locations. Ambohibary has the longest crop duration, due to the low temperatures at this high-altitude location. However, with a

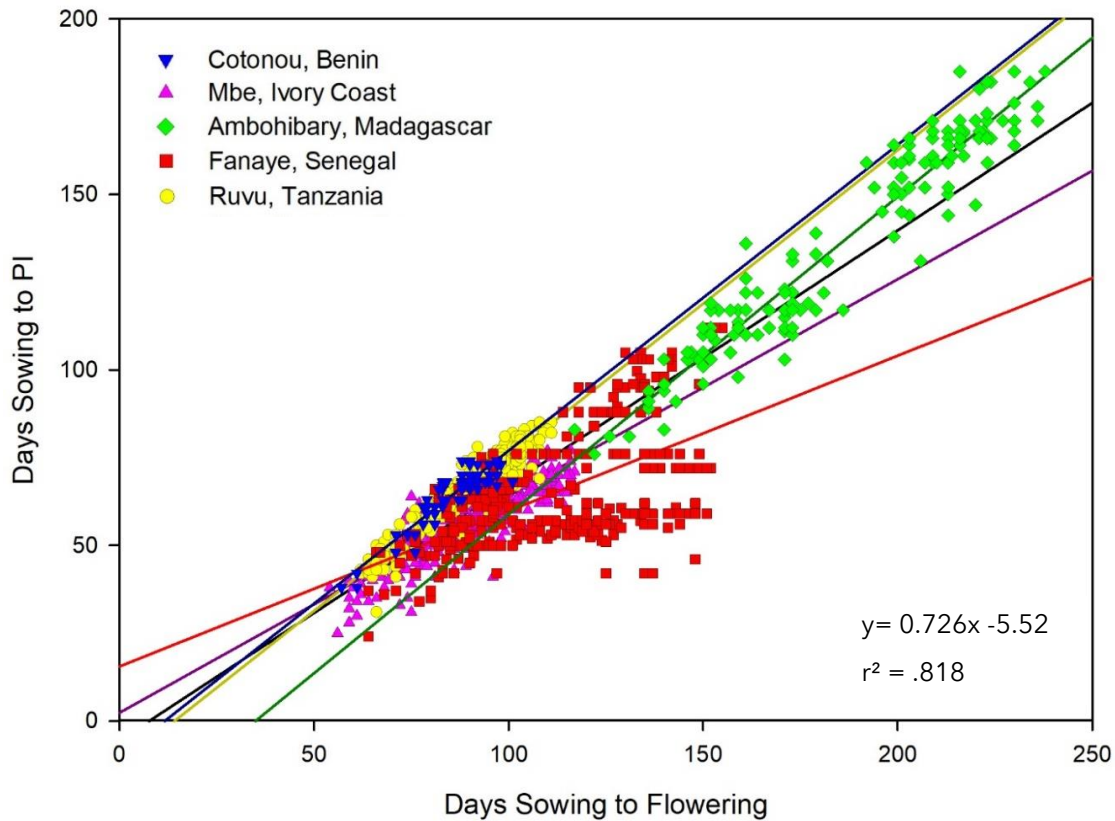


Figure 8: Days from sowing to PI regressed against days from sowing to flowering across all genotypes and environments. Environments are grouped per location.

regression equation of $y = 0.905x - 31.6$ and an r^2 of .920, it is actually closest to the expected outcome of all locations. PI data at some Senegalese environments behaves strangely. These were further investigated by separating the regression into individual sowing dates for Fanaye (figure 9).

At E13 the regression line ($y = -2.12 + 55.64x$) has a slightly negative slope. For E13 all PI dates were recorded between 51 and 57 days after sowing, whereas the observed flowering dates range from 77 to 134 days. This can only be explained in two ways: I) at E13 the length of VP is relatively stable, while RP varies; or II) measurement error. The first option is not in line with data observed at other environments nor with literature. Since the second option is more likely, PI data of E13 was discarded.

At E15 and to a lesser extent at E14 and E18 PI dates do not follow a normal distribution, but rather a stratified pattern. This indicates that PI data was not recorded daily, but instead only at certain dates. At E24 for 36 out of 80 genotypes

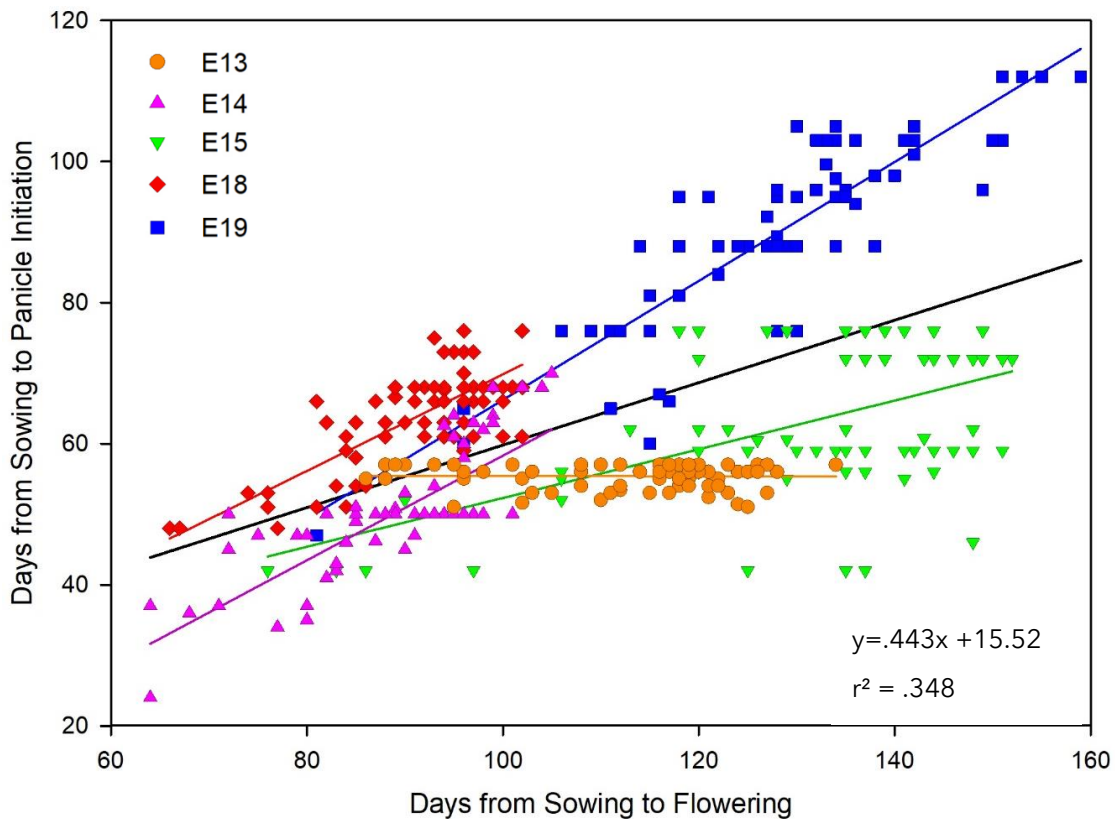


Figure 9: Days from sowing to PI regressed against days from sowing to flowering across all genotypes for the sowing dates in Fanaye where PI was recorded (E13, E14, E15, E18, E19).

PI date was recorded at 50 days after sowing. At E18 22 PI dates were recorded at 68 days after sowing. These are strong deviations from a normal distribution. However, despite this being likely due to measurement error, it cannot be ruled out with 100% certainty that there was a peak in PI on those dates. The PI data for E14, E18 and 19 is more or less in line with PI data observed at other locations and was therefore kept. PI data from E15 was omitted. After exclusion of the obviously erroneous PI data 1346 PI dates remained in total. A boxplot was made for the observed number of days from PI to flowering per environment for all locations (figure 10).

Pooled over genotypes and environments, average time from PI to flowering was 31.33 ± 0.28 days with a standard deviation of 10.37 days. Duration of RP in Ruvu (E20-E25) has less variation than at the other locations. Average duration of RP in Cotonou (E2) and at E5 in Mbe was similar to observations made in Ruvu. The short average durations in Ruvu and Cotonou could be environmentally caused, or it

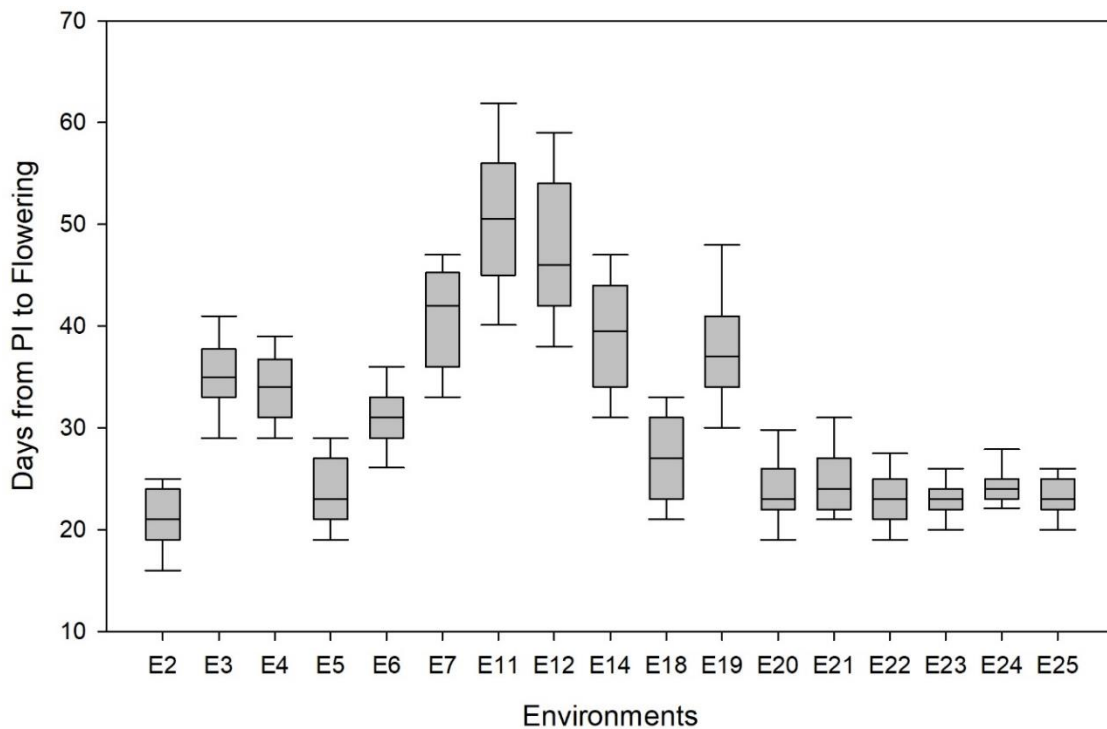


Figure 10: Boxplot of days from panicle initiation to flowering per environment where PI date was recorded.

could be a biased observation, e.g. the observers always observed PI late. In Ambohibary (E11 and E12) RP takes longer than at other sites.

Next, PI was estimated as 30 days before flowering. Estimated PI date was plotted against observed PI date (figure 11). If the simulation would have been accurate, data points should approximately fall on a 1:1 line with intercept close to 0 and slope close to 1. However, the intercept is -13.92 days and slope is 16.2% off. The coefficient of determination is high ($r^2=.921$), suggesting that the correlations between the observations are strong and therefore the model assumption might be incorrect. The result of estimating PI date as fixed at 30 days before flowering, independent of genotype and environment, was therefore found unsatisfactory.

Next, the amount of heat units accumulated from PI to flowering was calculated to check whether RP was fixed in amount of heat units required to complete this phase rather than days (figure 12).

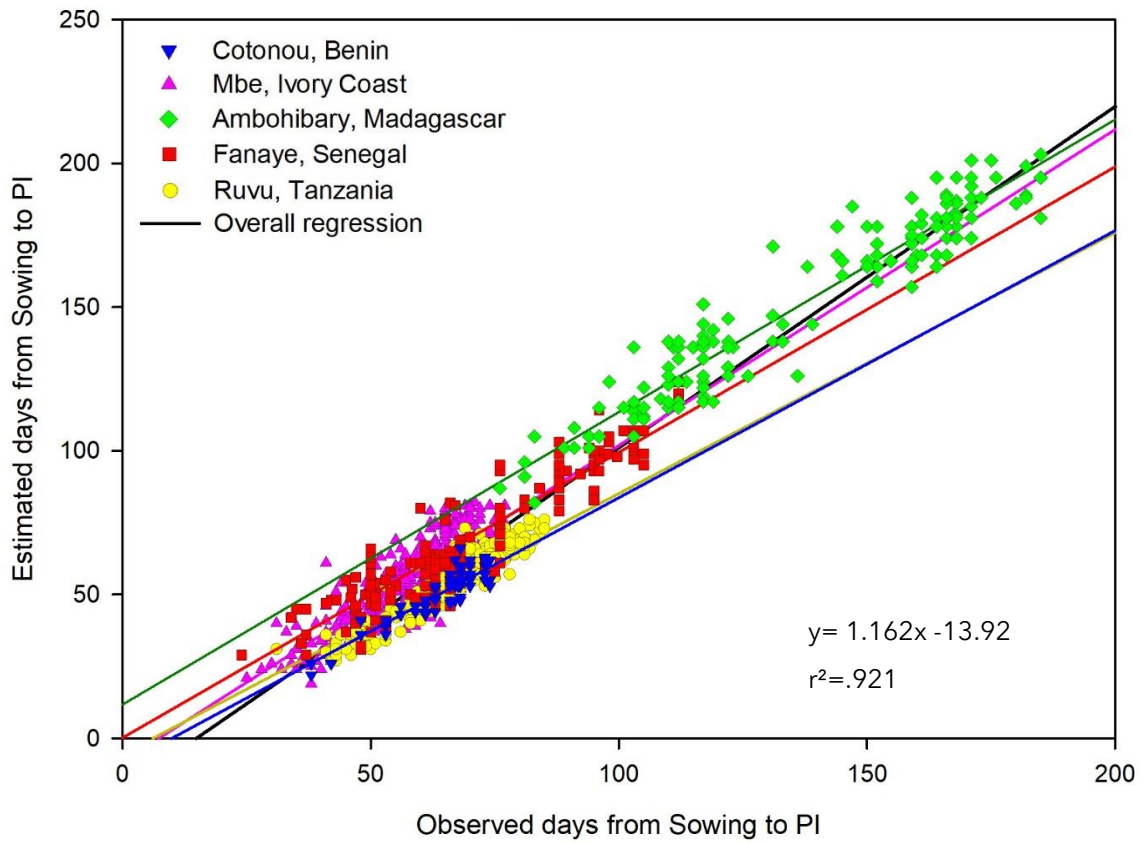


Figure 11: Estimated versus observed days from sowing to PI. PI date estimated as 30 days before flowering.

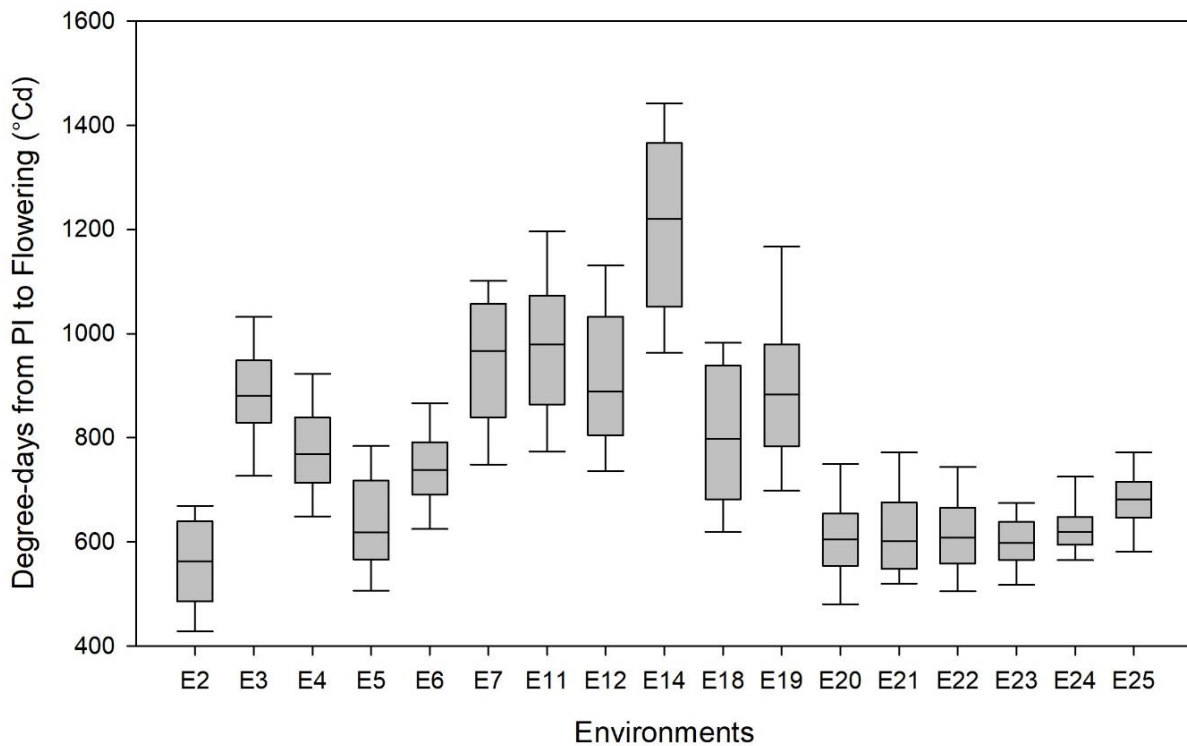


Figure 12: Boxplot of degree-days from PI to flowering per environment where PI date was recorded.

The mean amount of dd required to complete RP was 771.8 ± 11.4 °Cd with a standard deviation of 212.6 °Cd. Expressing duration of RP in thermal time instead of in days, brought duration for E11 and E12 in line with other environments. They have a similar duration to E7 and shorter duration than E14 when measured in dd. Thus RP lasts longer in cool environments in absolute time (days), but not when measured in thermal time. E14 sticks out with a significantly higher amount of dd required to reach PI than other environments at this location (E18 and E19). This is likely the result of measurement error. As discussed before, observed PI dates for E14 were doubtful. Variation in duration of RP in Mbe (E3-E7) remains. Duration of RP in Ruvu (E20-E25) remains lowest and most stable of all locations. Thus estimating PI based on number of degree-days improves results for the cool environments of Ambohibary, but not for the other locations.

Because observation of 50% flowering date is more reliable than observation of 50% PI, because there were more observed flowering dates than PI dates ($n=1908$ versus $n=1346$) and because missing PI dates could not be accurately estimated, it was decided to proceed analysis based on f and to leave PI out of further phenology modelling.

5.3 Cardinal temperatures

In this chapter cardinal temperature estimates for three out of 80 varieties are presented: 1) IR64 (V2), the international test variety and a medium-duration variety; 2) K5 (V27), a long-duration variety; and 3) Chhomrong (V30), a short-duration variety. Cardinal temperatures with accompanying regression equations including r^2 and CV for the other 77 varieties are provided in appendix IV.

5.3.1 Summerfield

Daylength only influences a rice plant's DR during PSP. Since PI dates were often missing or of doubtful quality and could not be accurately estimated, timing of PSP could not be established. Therefore the simple Summerfield-model based only on temperature (eqn 3) was applied to estimate T_{BASE} as the intersect with the x-axis (eqn 4) and T_{SUM} as the inverse of regression slope (eqn 5) (figures 13-15).

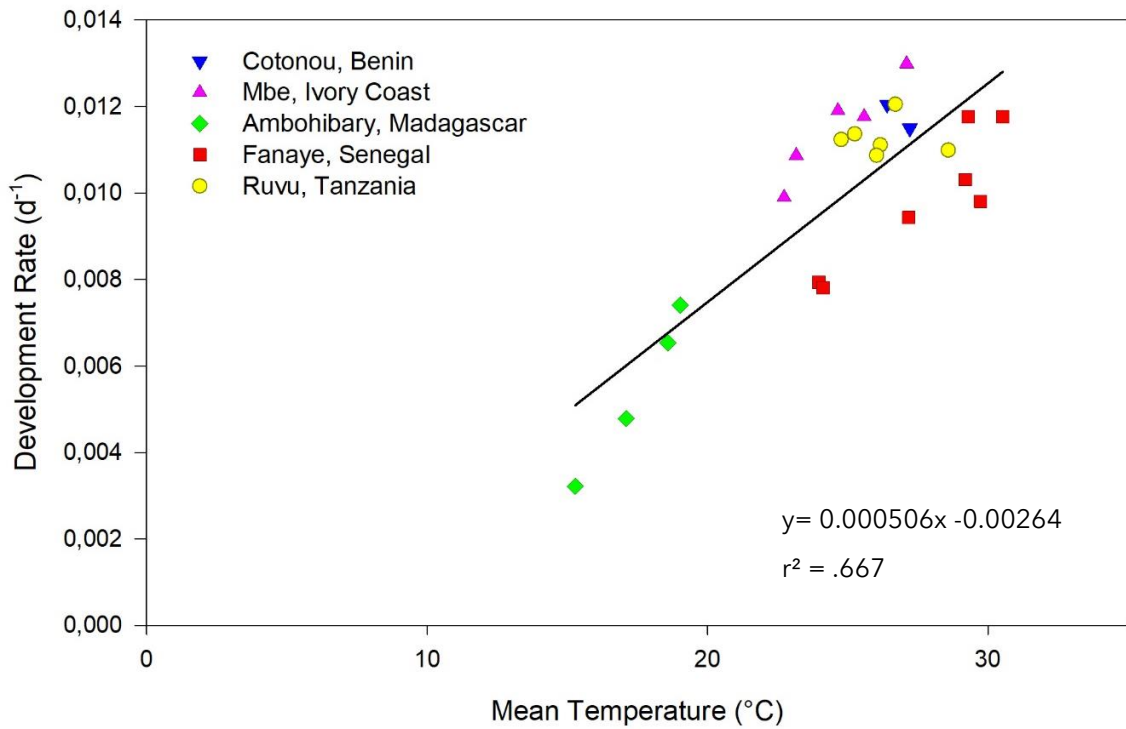


Figure 13: Development rate ($1/f$) of IR64 versus mean air temperature during this period at 24 environments (E9 missing) across 5 different sites.

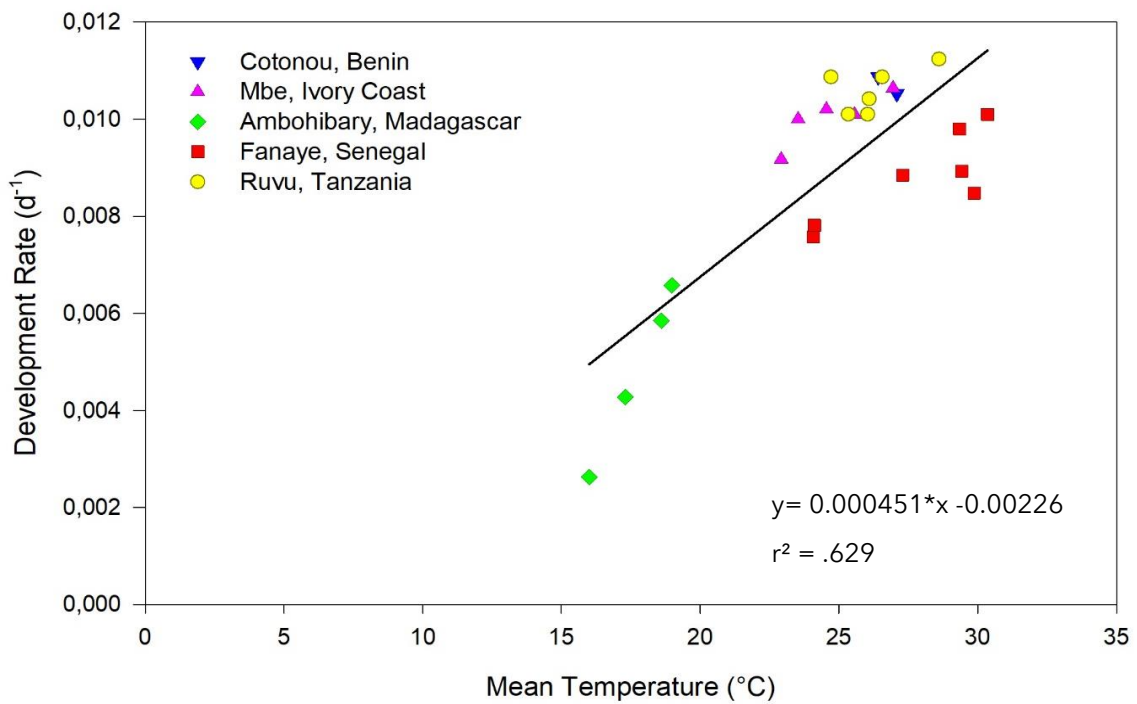


Figure 14: Development rate ($1/f$) of K5 versus mean air temperature during this period at 24 environments (E9 missing) across 5 different sites.

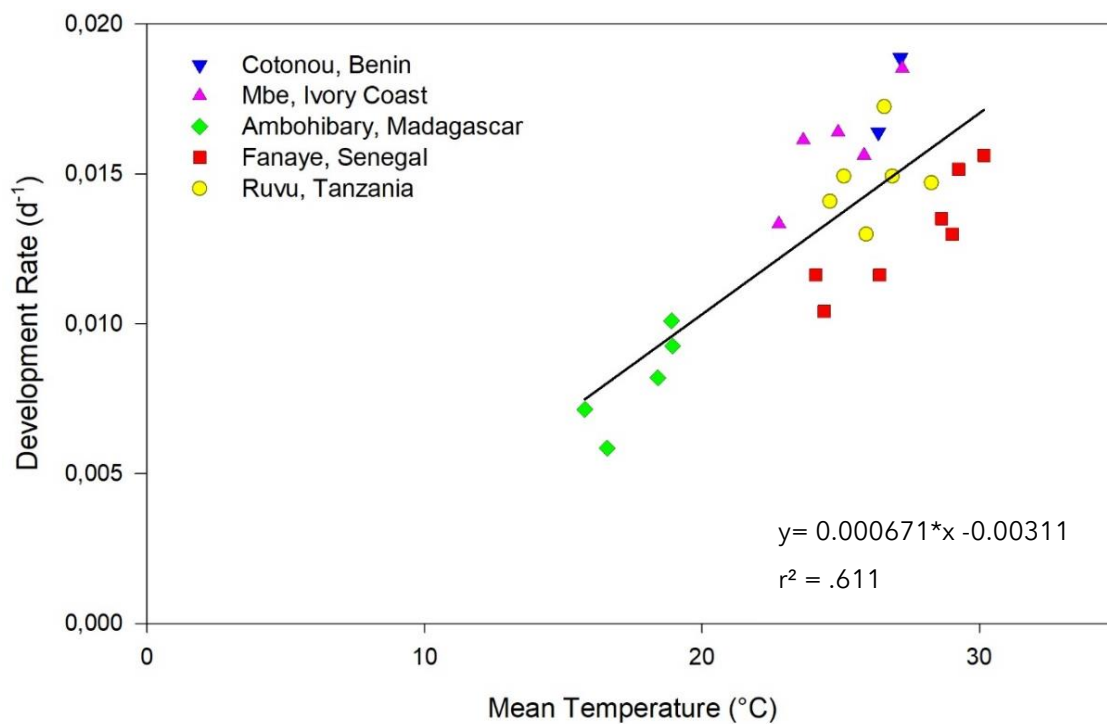


Figure 15: Development rate (1/f) of Chhomrong versus mean air temperature during this period at 25 environments across 5 different sites.

Chhomrong reaches higher DR and has lower T_{SUM} (1489°Cd) and T_{BASE} (4.64°C) compared to IR64 ($T_{SUM} = 1976°Cd$; $T_{BASE} = 5.22°C$) and K5 ($T_{SUM} = 2219°Cd$; $T_{BASE} = 5.01°C$). Development of Chhomrong starts at lower temperatures and requires less degree-days to reach flowering, resulting in shorter crop duration. When looking at all 80 varieties, r^2 ranges from .447 (V22) to .737 (V34), with average r^2 across all genotypes of .594, this indicates that the regression is not a very good fit to the data. Estimated T_{BASE} is low, for some genotypes unrealistically low. For three genotypes (V4, V28 and V77) T_{BASE} drops below the freezing point, while highest T_{BASE} was 7.92°C.

DR and mean temperature are lower at Ambohibary than at any other location, for every variety. A regression only through the four (IR64 & K5) or five (Chhomrong) datapoints at this site would result in a much steeper slope, thus a higher T_{BASE} and lower T_{SUM} . DR in Fanaye is consistently lower than at other locations with similar mean temperatures. This suggests that Summerfield's model is not applicable to this wide range of environments, including cool to hot and humid to arid conditions.

5.3.2 Dingkuhn

Since PI date could not be accurately simulated, eqn 6 was applied to estimate T_{SUM} as the intersect with the y-axis and T_{BASE} as the slope of this regression (figures 16-18). Ambohibary, with its long crop duration both in time (days) and thermal time (dd) disproportionately influences the regression. creates a leverage point: the effect of this single data point with its extreme x-value strongly influences the complete regression. E.g. for IR64 including E10 regression line is $y = 10.62x + 1439$; $r^2 = .848$, while without E10 the regression changes to $y = 10.51x + 1450$ with $r^2 = .640$.

Nevertheless, this phenology model, has a better overall fit than Summerfield with an average r^2 across all genotypes of .772, ranging from .486 (V4) to .921 (V21). At Fanaye consistently more dd were required to reach flowering than at other locations with similar crop durations. T_{BASE} ranges from 8.90°C (V42) to 10.96°C (V18). T_{SUM} has a wide range from 976°Cd in the short-duration variety V79 to 1825°Cd in V70. In V70 high T_{SUM} is combined with a low T_{BASE} (8.98°C), this explains why a variety that ranked 56th in crop duration can still have the highest T_{SUM} , because with a low T_{BASE} and without T_{OPT} it is possible to accumulate more dd per day.

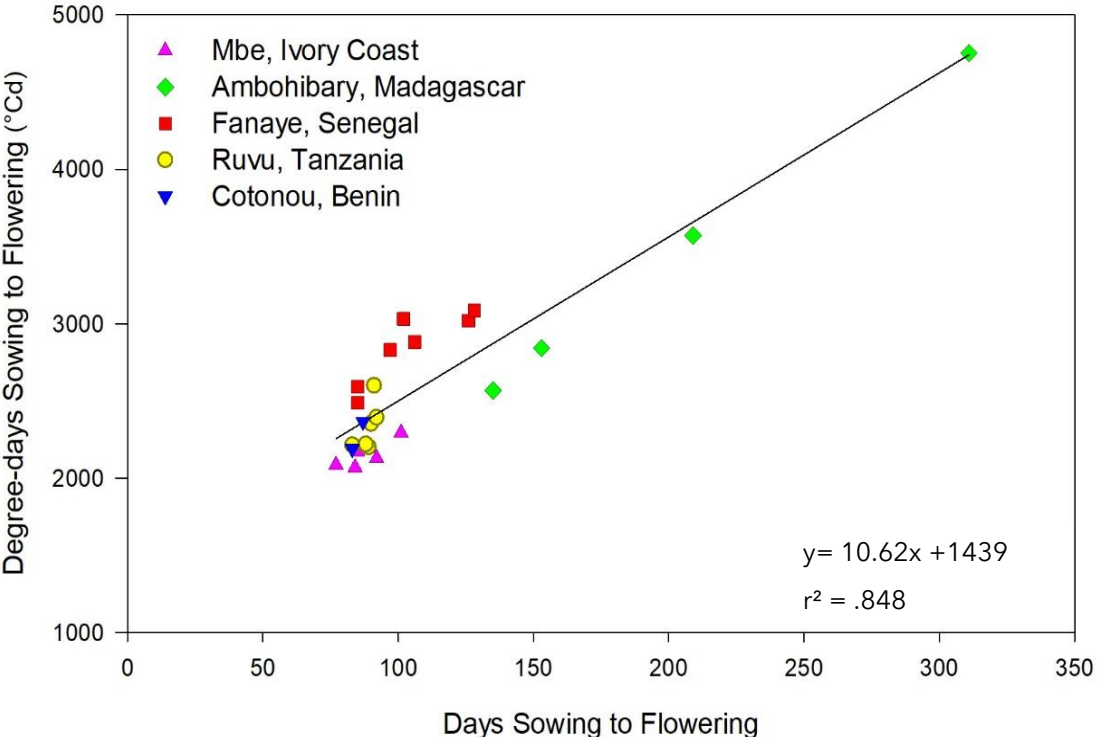


Figure 16: Degree-days from sowing to flowering of IR64 versus number of days from sowing to flowering at 24 environments (E9 missing) across 5 different sites.

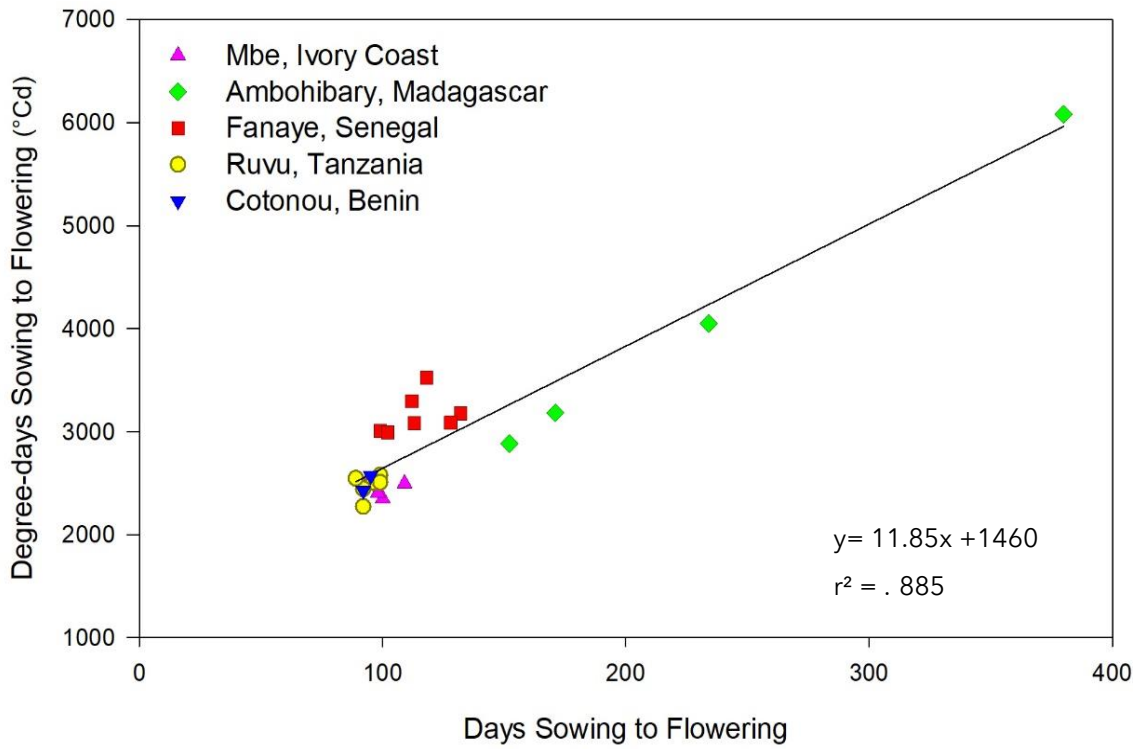


Figure 17: Degree-days from sowing to flowering of K5 versus number of days from sowing to flowering in 24 environments (E9 missing) across 5 different sites.

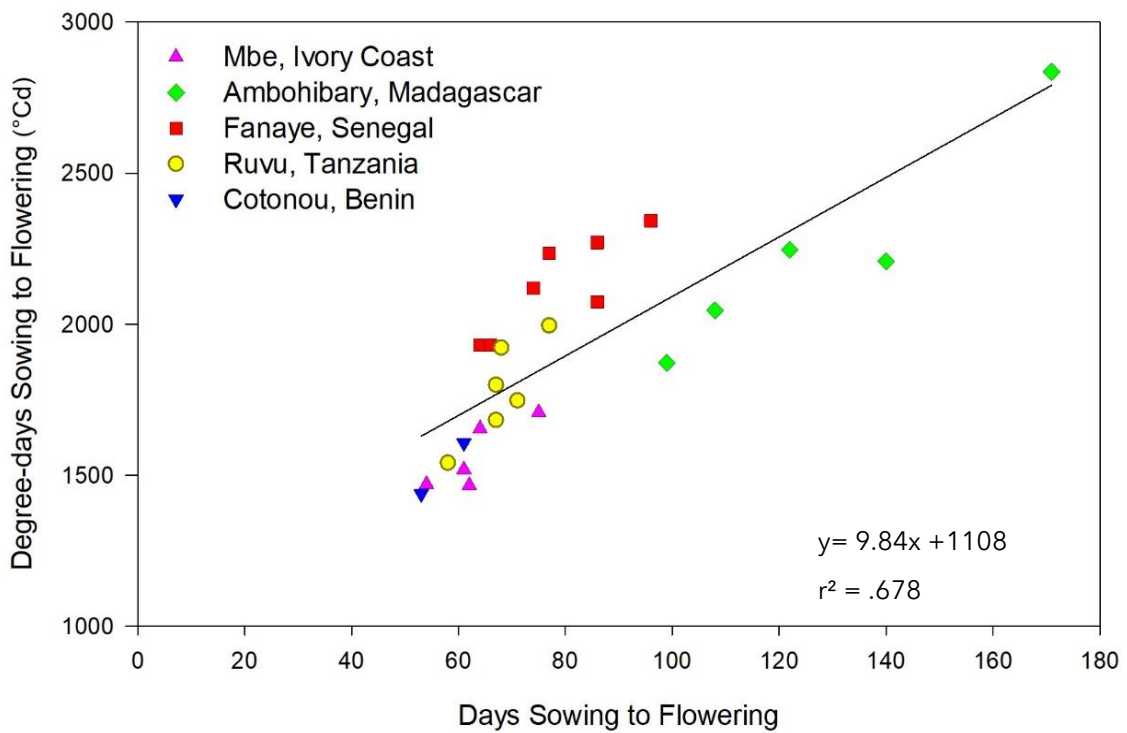


Figure 18: Degree-days from sowing to flowering of Chhomrong versus number of days from sowing to flowering in 25 environments across 5 different sites.

5.3.3 Stuerz

In this thesis Stuerz' model was applied in a different way than they did in their paper. Nevertheless, since my interpretation of this model is based on their publication and the main difference with other phenology models is the inclusion of RH when simulating crop duration, it will still be referred to as the Stuerz-model. Whereas they corrected the residuals for the effect of RH, here a multiple linear regression (eqn 10) was applied to get the regression parameters (a, b, and c) instead:

$$(10) \quad DR = a * \bar{T} + b * \overline{RH} + c$$

These regression parameters were used to calculate genotype-specific phenological parameters: T_{SUM} , T_{BASE_0} (base temperature at the theoretical value RH=0%) and an RH-adjustment factor (RH_{ADJ}). T_{SUM} is calculated as in Summerfield, so it remains unaffected by RH. T_{BASE_0} is calculated as:

$$(11) \quad T_{base_0} = -\frac{c}{a}$$

T_{BASE} is negatively correlated with RH, i.e. in a more humid environment development starts at a lower base temperature. This is captured by a genotype-specific RH-adjustment factor for T_{BASE} :

$$(12) \quad RH_{adj} = -\frac{b}{a}$$

Equations 11 and 12 were used in combination with average RH to calculate T_{BASE} :

$$(13) \quad T_{base} = T_{base_0} + RH_{adj} * RH_{av}$$

T_{BASE} depends on genotype-specific T_{BASE_0} , RH_{ADJ} and the measured daily RH_{AV} and therefore differs from day to day. Figures 19-21 show the resulting regression plane of eqn 10 for varieties IR64, K5 and Chhomrong. T_{BASE} decreases with increasing RH. According to this model, a rice plant starts developing at lower temperatures in humid environments.

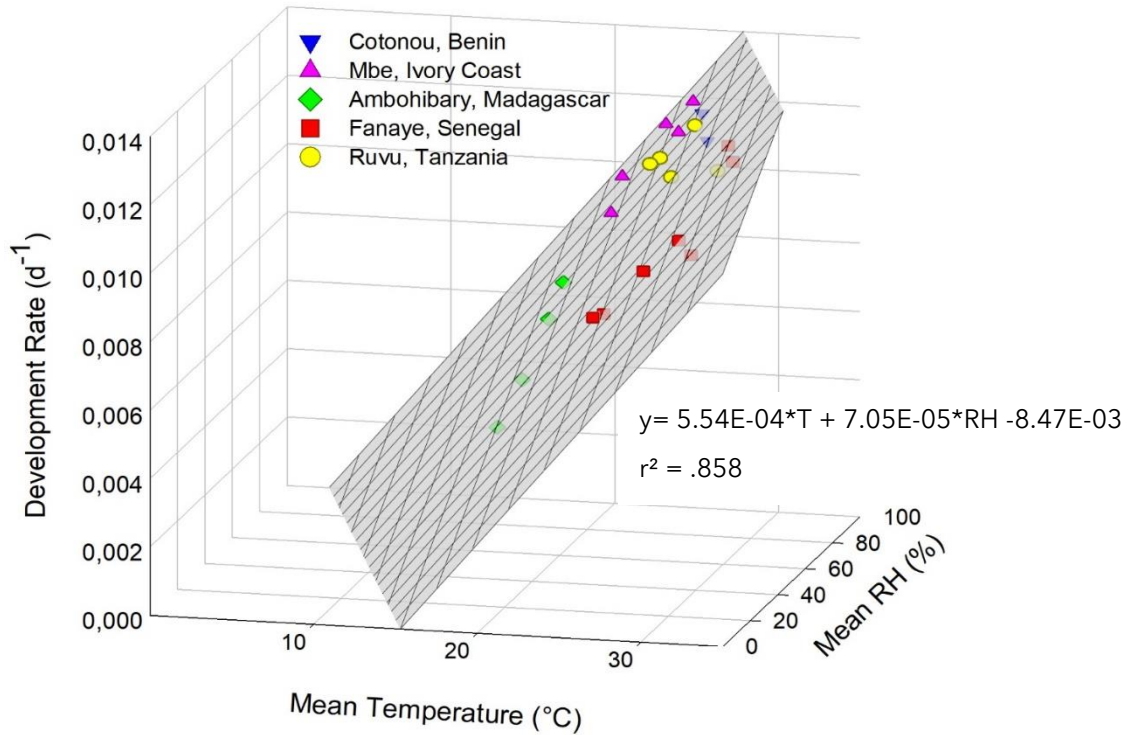


Figure 20: Multiple linear regression of DR of IR64 versus mean air temperature and mean RH from sowing to flowering in 24 environments (E9 missing) across 5 different sites.

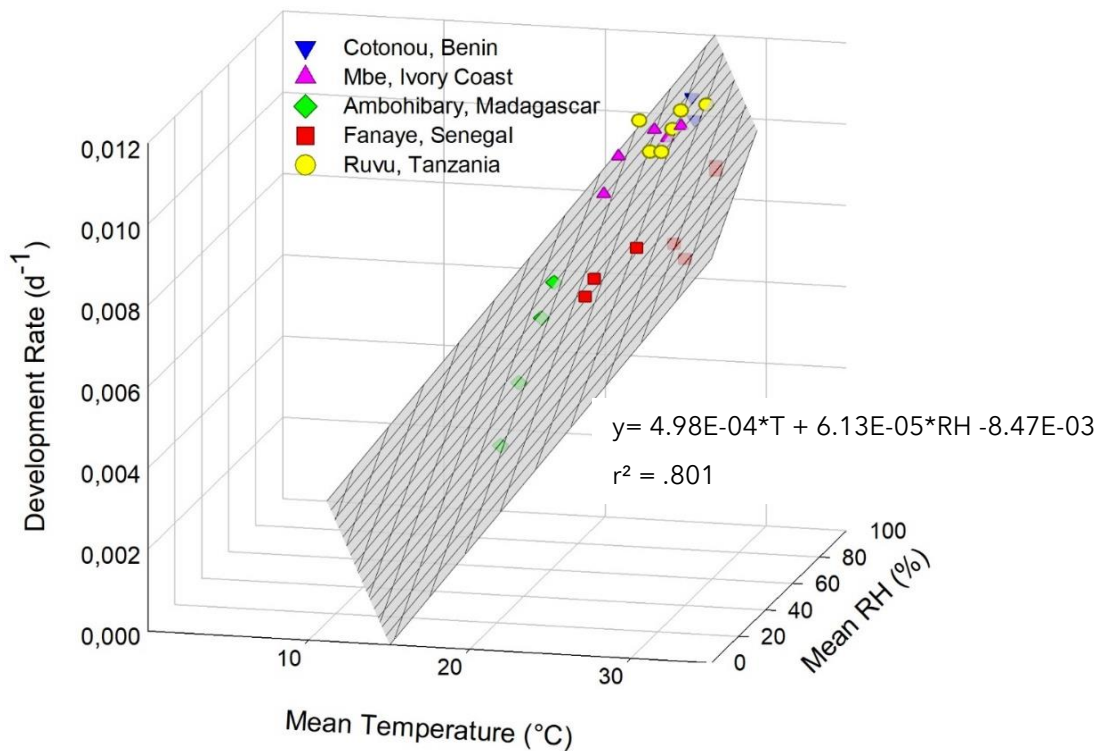


Figure 19: Multiple linear regression of DR of K5 versus mean air temperature and mean RH from sowing to flowering in 24 environments (E9 missing) across 5 different sites.

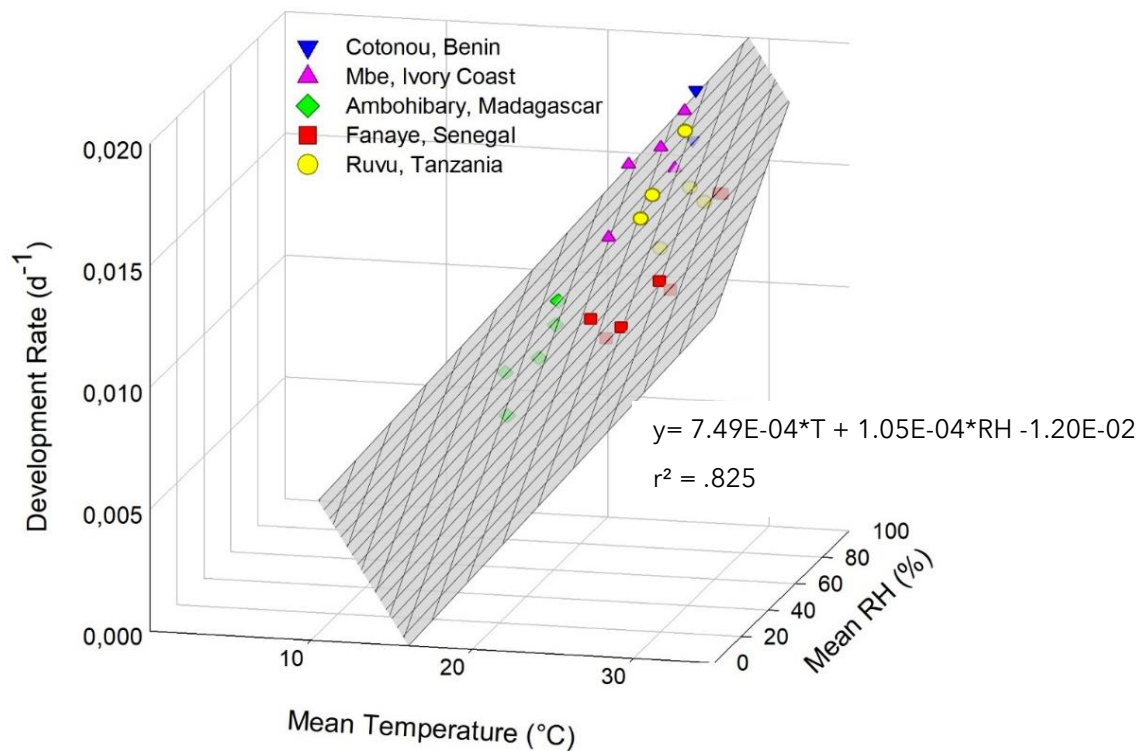


Figure 21: Multiple linear regression of DR of Chhomrong versus mean air temperature and mean RH from sowing to flowering in 25 environments across 5 different sites.

Stuerz' model is better at capturing f in Fanaye. However, it systematically overestimates DR at Ambohibary. This regression model has a better coefficient of determination than Summerfield and Dingkuhn with r^2 ranging from .679 (V16) to .923 (V7), with average $r^2 = .827$ across all genotypes, suggesting that adding the extra explanatory variable RH improves the regression model.

5.3.4 Asch-Groot Nibbelink

When regressing DR against mean temperature over the period from sowing to flowering following Summerfield's model, it became apparent that the data does not follow a linear pattern. Rather, DR stagnates as average temperatures increase. This indicates the existence of a T_{OPT} above which DR no longer increases. To capture this, a new simple phenology model was developed by Asch and Groot Nibbelink: the Asch-Groot Nibbelink (AGN) model. To find the cardinal temperatures, a second order regression was performed:

$$(14) \quad DR = a * \bar{T}^2 + b * \bar{T} + c$$

Based on this regression two tangents were taken, creating a broken-stick model where the intersect with the x-axis equals the base temperature and the breaking

point equals the optimum temperature. The first tangent is horizontal touching the vertex. The vertex x-coordinate (h) were calculated as

$$(15) \quad h = -\frac{b}{2a}$$

The vertex y-coordinate (k) was found by applying h into eqn 14:

$$(16) \quad k = a * h^2 + b * h + c.$$

The horizontal tangent is thus equal to $DR = k$. The second, sloped, tangent was taken where DR was halfway between 0 and the maximum DR. The tangency point's y-coordinate was

$$(17) \quad y_{tan} = 0.5 * k$$

Tangency point's x-coordinate was found by rewriting eqn 14 and substituting DR by y_{tan} :

$$(18) \quad x_{tan} = \frac{\sqrt{-b + (b^2 - (4a * (c - y_{tan})))}}{2a}.$$

The tangent line equation is:

$$(19) \quad DR = m * \bar{T} + c_{tan}$$

Where m is the slope of the tangent line, calculated as

$$(20) \quad m = 2a * x_{tan} + b.$$

c_{tan} is the constant of the sloped tangent:

$$(21) \quad c_{tan} = y_{tan} - (m * x_{tan})$$

The intersect of the sloped tangent with the x-axis is taken to be the base temperature:

$$(22) \quad T_{base} = -\frac{c_{tan}}{m}$$

The optimum temperature is the intersect of the two tangents:

$$(23) \quad T_{opt} = \frac{k - c_{tan}}{m}$$

T_{SUM} is the inverse of the slope of the sloped tangent:

$$(24) \quad T_{SUM} = \frac{1}{m}$$

The results of this model as applied to IR64, K5 and Chhomrong are visualised in figures 22-24, where the black line is the second order regression and the grey lines are the tangents forming the broken-stick model.

With coefficients of determination ranging from .591 (V28) to .907 (V44) and an average of $r^2 = .759$, this second order regression equation is a significant improvement compared to Summerfield and has similar fit to Dingkuhn, while Stuerz' regression still has a better fit to the data. The AGN-model captures Ambohibary's data better, although it overestimates DR for most sowing dates in Fanaye. T_{BASE} estimates are rather high, ranging between 10.74°C (V78) and 13.95°C (V39).

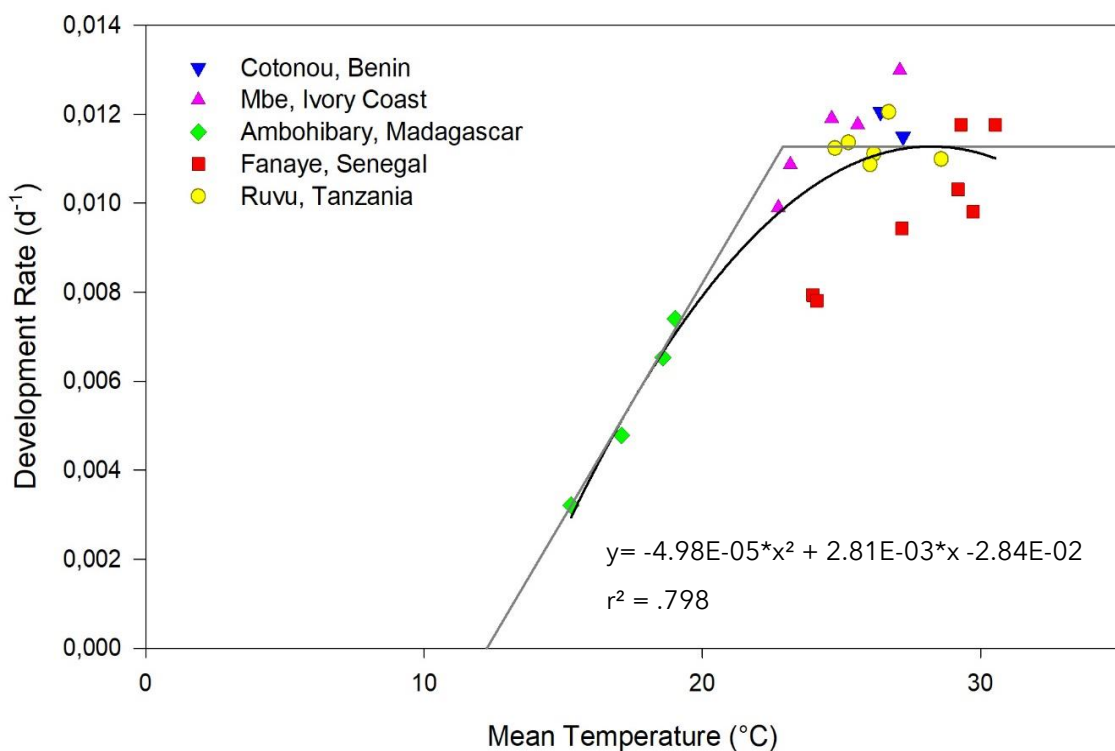


Figure 22: Development rate of IR64 versus mean air temperature from sowing to flowering in 24 environments (E9 missing)

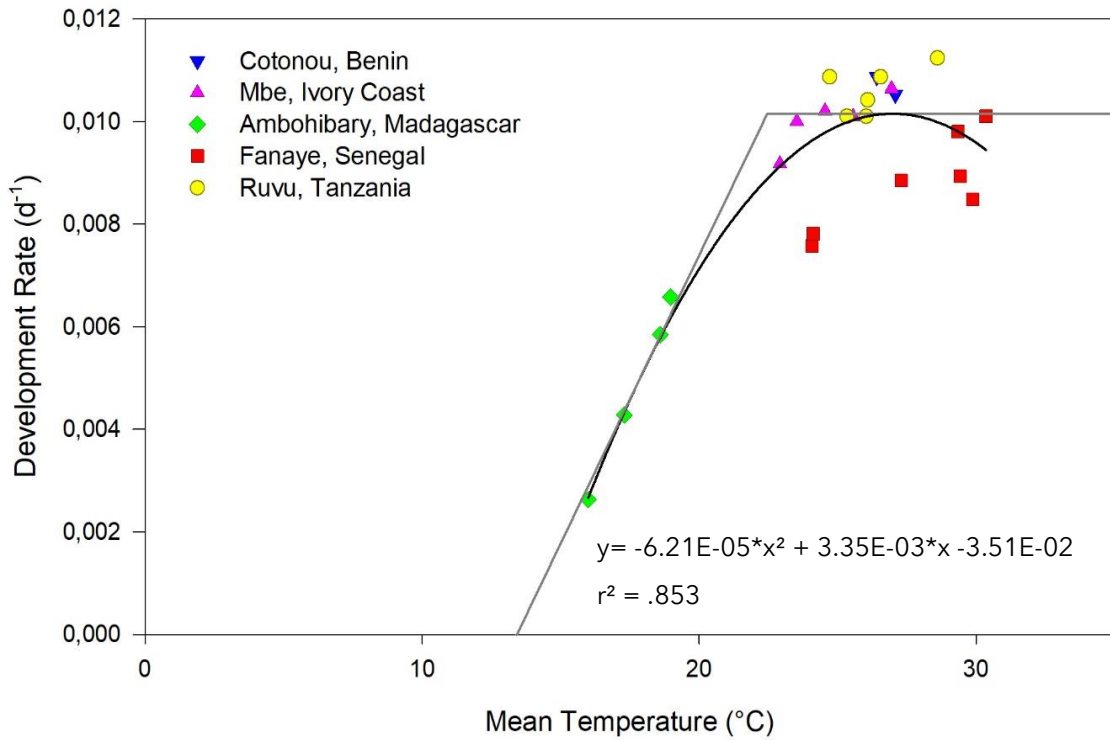


Figure 23: Development rate of K5 versus mean air temperature from sowing to flowering in 24 environments (E9 missing)

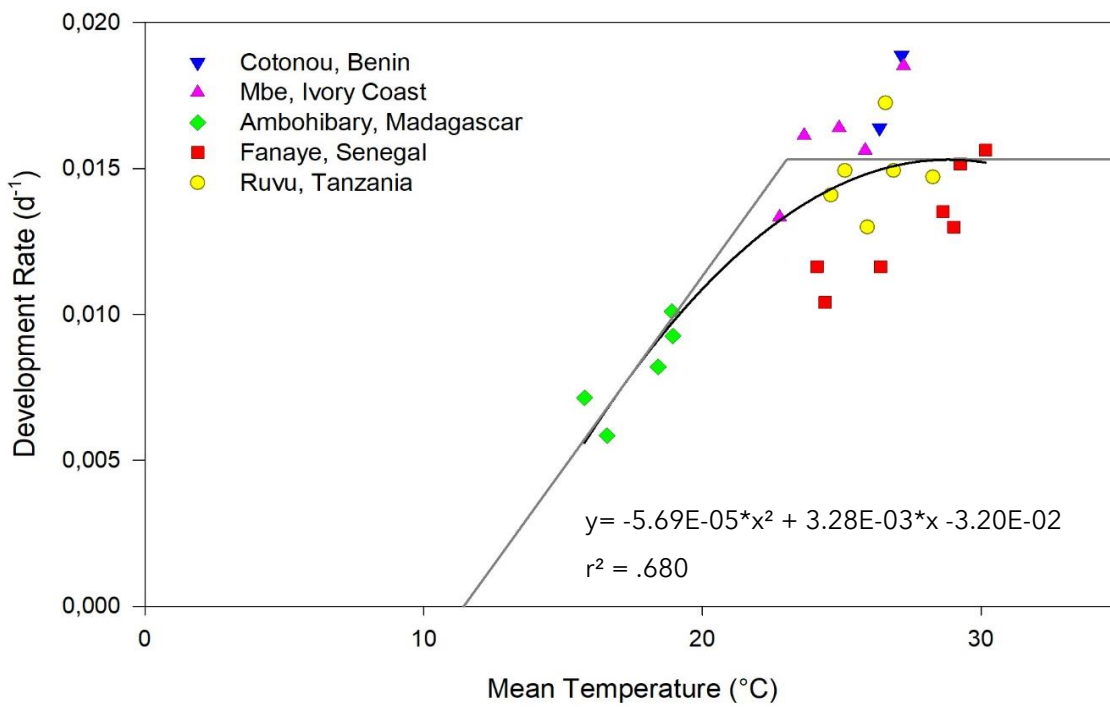


Figure 24: Development rate of Chhomrong versus mean air temperature from sowing to flowering in 25 environments

5.3.5 Cardinal Temperature Estimates

Cardinal temperature estimates for IR64, K5 and Chhomrong (table 2) differ between genotypes and phenology models applied. T_{SUM} estimates are highest under Summerfield, which goes hand in hand with this model resulting in lowest T_{BASE} estimates. If T_{BASE} is low, more degree-days are accumulated per day. Stuerz has high T_{SUM} estimates combined with high T_{BASE} estimates at $RH=0\%$. However, the rice plants always experience a lower T_{BASE} , as it reduces with RH and RH is never equal to 0% . Air humidity typically ranges between 50 to 100%, depending on the environment. Although in Fanaye, Senegal, during 41 days an average air humidity of less than 10% was recorded. Nevertheless, according to our findings of applying Stuerz' model, the rice plant will experience base temperatures ranging between $2^{\circ}C$ to $9^{\circ}C$ on the vast majority of days, depending on genotype and environment. Even the cool Madagascar environments average temperatures are well above $9^{\circ}C$ on most days. The introduction of T_{OPT} in the AGN-model limits the amount of degree-days a plant can collect per day. This is reflected by lower T_{SUM} estimates. Cardinal temperature estimates found by applying the Dingkuhn-model are moderate. They are not extremely high or low compared to the results of the other phenology models.

Table 2: Cardinal temperature estimates for IR64 (V2), K5 (V27) and Chhomrong (V30) using four different phenology models

Variety	Summerfield		Dingkuhn		Stuerz			AGN		
	T_{SUM}	T_{BASE}	T_{SUM}	T_{BASE}	T_{SUM}	T_{BASE_0}	RH_{ADJ}	T_{SUM}	T_{BASE}	T_{OPT}
IR64	1976	5.22	1439	10.62	1807	15.30	-0.127	944	12.26	22.90
K5	2219	5.01	1460	11.85	2007	15.04	-0.123	891	13.42	22.46
Chhomrong	1489	4.64	1108	9.84	1335	16.05	-0.140	758	11.44	23.03

The short duration variety Chhomrong always has the lowest T_{SUM} and for three out of four models the lowest T_{BASE} . Only in Stuerz' model Chhomrong has the highest T_{BASE} , but at the same time it has the highest RH -adjustment factor. Thus it is more sensitive to RH and in environments with a high RH it actually has a lower T_{BASE} than the other varieties. Chhomrong also has the highest T_{OPT} , thus it is able to collect more degree-days per day than any of the other varieties. The long duration variety K5 has the highest T_{SUM} for three out of four models. T_{SUM} found with AGN is highest

for IR64. However, since IR64 has lower T_{BASE} and higher T_{OPT} than K5, it can collect more degree-days per day and thus will be able to reach T_{SUM} and therefore flowering sooner.

5.4 Simulated Flowering Dates

Genotype-specific cardinal temperatures were used in combination with weather data to simulate flowering dates. This was done by calculating daily physiological temperature (T_{PHYS}), the degree-days a rice plant can use for development. T_{PHYS} was calculated as the daily average temperature (T_{AV}) above T_{BASE} and below T_{OPT} , with T_{BASE} adjusted for daily RH:

$$(25) \quad T_{phys} = \max(\min(T_{opt}, T_{av}) - (T_{base} + RH_{adj} * RH_{av}), 0)$$

For those models without T_{OPT} , T_{OPT} was set to 99°C. As this temperature is never reached in field conditions, it is effectively the same as applying no T_{OPT} . For models without RH-adjustment, this factor was set to 0, so no correction for RH was made to T_{BASE} . The *max*-term ensures that if $T_{av} < T_{base}$, T_{PHYS} cannot become negative and no degree-days are subtracted, since development does not reverse. Note that T_{AV} and RH_{av} are daily averages, while \bar{T} and \overline{RH} are averages of the observed time from sowing to flowering

Next, daily T_{PHYS} was summed from the sowing date until the date that T_{SUM} was reached. This date was returned as the simulated flowering date. This was done for each genotype x environment combination and for each phenological model. Simulated flowering dates were regressed versus observed flowering dates to analyse the accuracy of the phenology models (figures 26-37).

5.4.1 Summerfield

The Summerfield-model performs well when simulating f for Cotonou, but underestimates f in Fanaye and in Ambohibary (figure 25). The regression is far from a 1:1 line ($y=0.555+45.45x$), but yet a high correlation ($r^2=.831$), which suggests that

the Summerfield-model assumptions might be incorrect, or the limits within which this model works well have been transgressed.

Figure 26, presenting the individual sowing dates at Ambohibary, shows that this model is able to simulate E8, sown November 2015, quite well. However, for the other sowing dates, especially E10 (sown February 2016), Summerfield’s model cannot accurately simulate days to flowering. When looking at the individual sowing dates in Fanaye (figure 27), E14 (sown July 2014) and E18 (sown July 2015) are captured relatively well, but there is systematic underestimation of time to flowering at the other environments (E13, E15-E17, E19), resulting in a skewed overall regression line for this location.

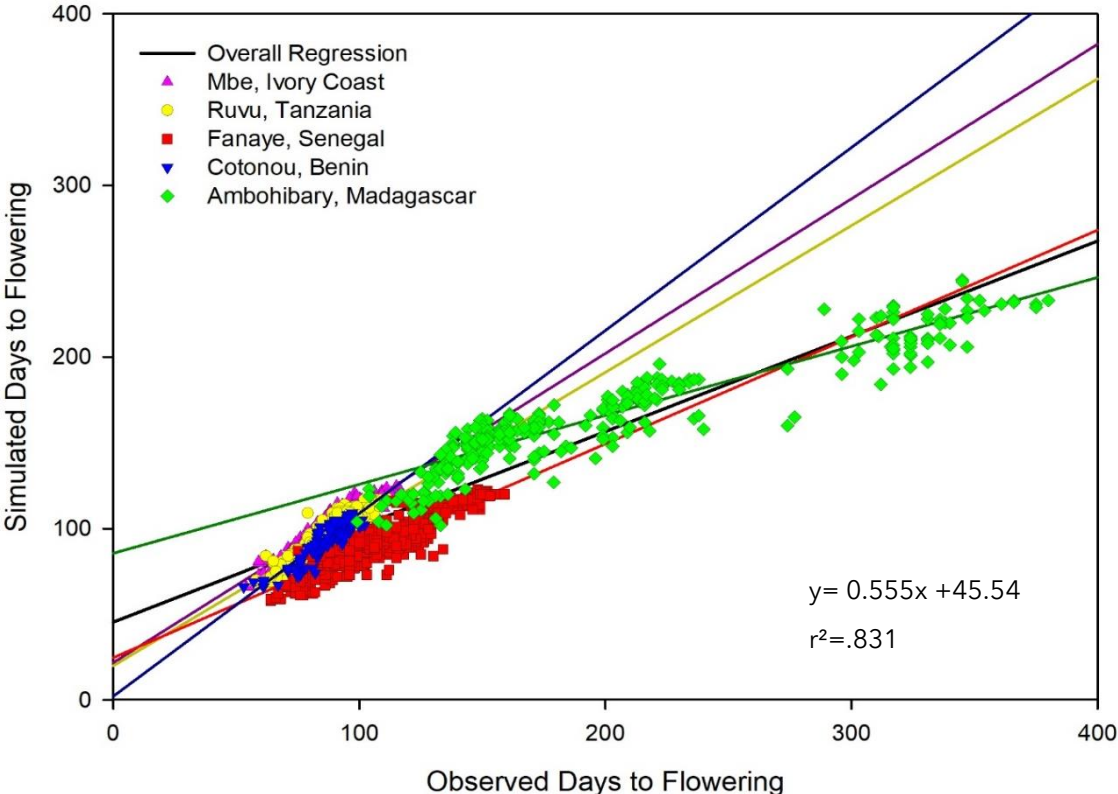


Figure 25: Observed versus simulated days to flowering following Summerfield-model across all environments and genotypes.

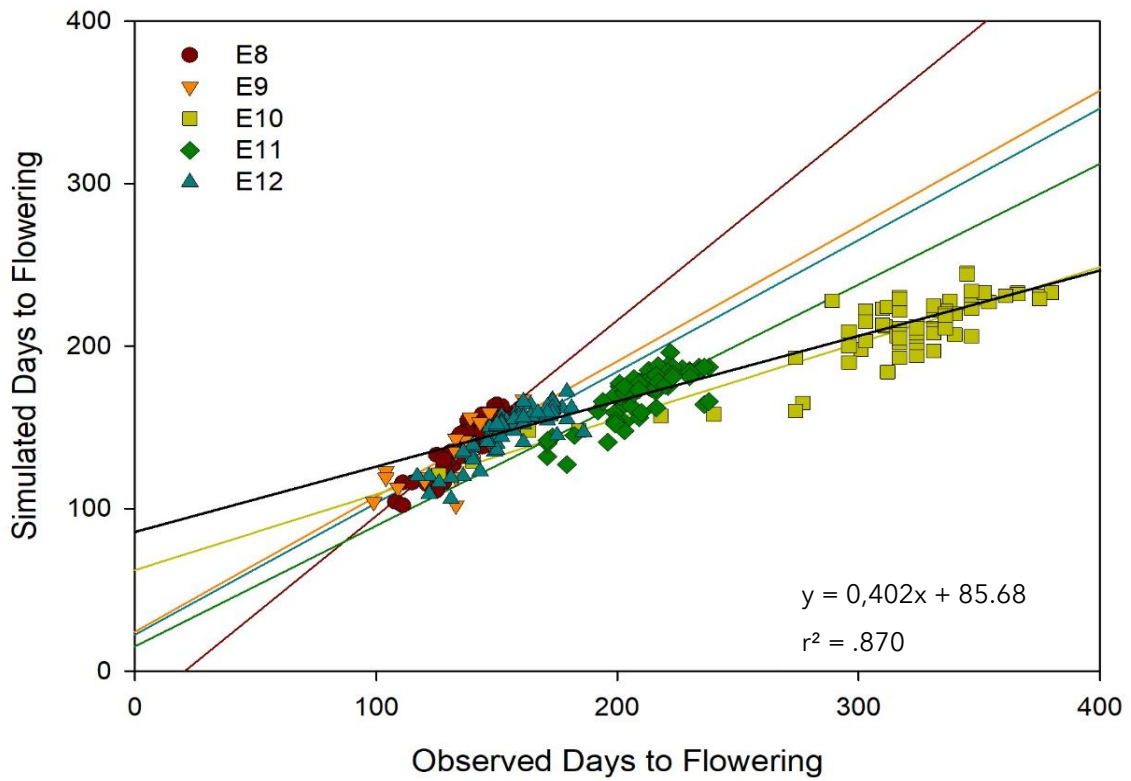


Figure 26: Observed versus simulated days to flowering following Summerfield-model for sowing dates in Ambohibary, Madagascar (E8-E12) across all genotypes.

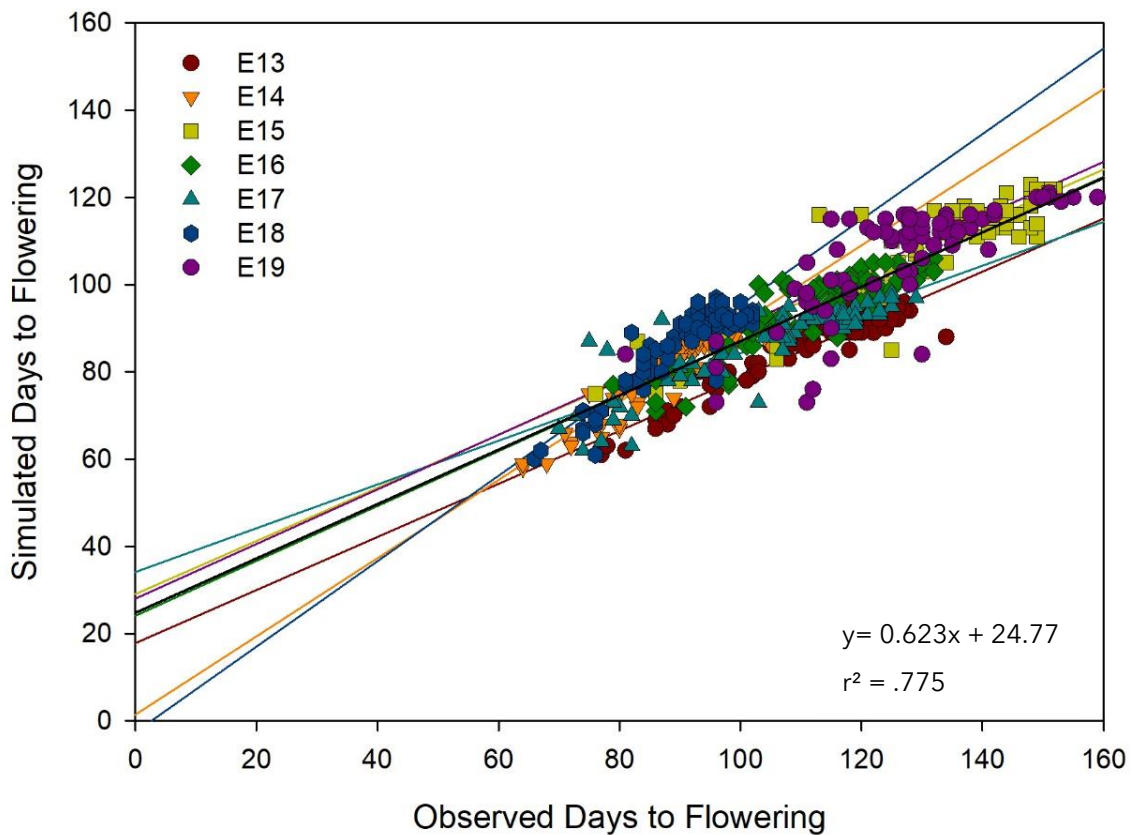


Figure 27: Observed versus simulated days to flowering following Summerfield-model for sowing dates in Fanaye, Senegal (E13-E19) across all genotypes.

5.4.2 Dingkuhn

The Dingkuhn-model results in quite accurate simulations of time to flowering in Cotonou, Mbe and Ruvu (figure 28). However, there is large variation in accuracy of crop duration simulation in Ambohibary and a systematic underestimation in Fanaye across all sowing dates (figure 30). Looking at the individual sowing dates at Ambohibary (figure 29) it can be observed that Dingkuhn is not able to accurately capture any of the individual sowing dates, with a particularly strong overestimation of f at E8 and a great scatter at E9. Interestingly, most flowering dates for E10 are close to the 1:1 line, but for some genotypes observed f was much shorter than the model predicts, which skews the complete regression.

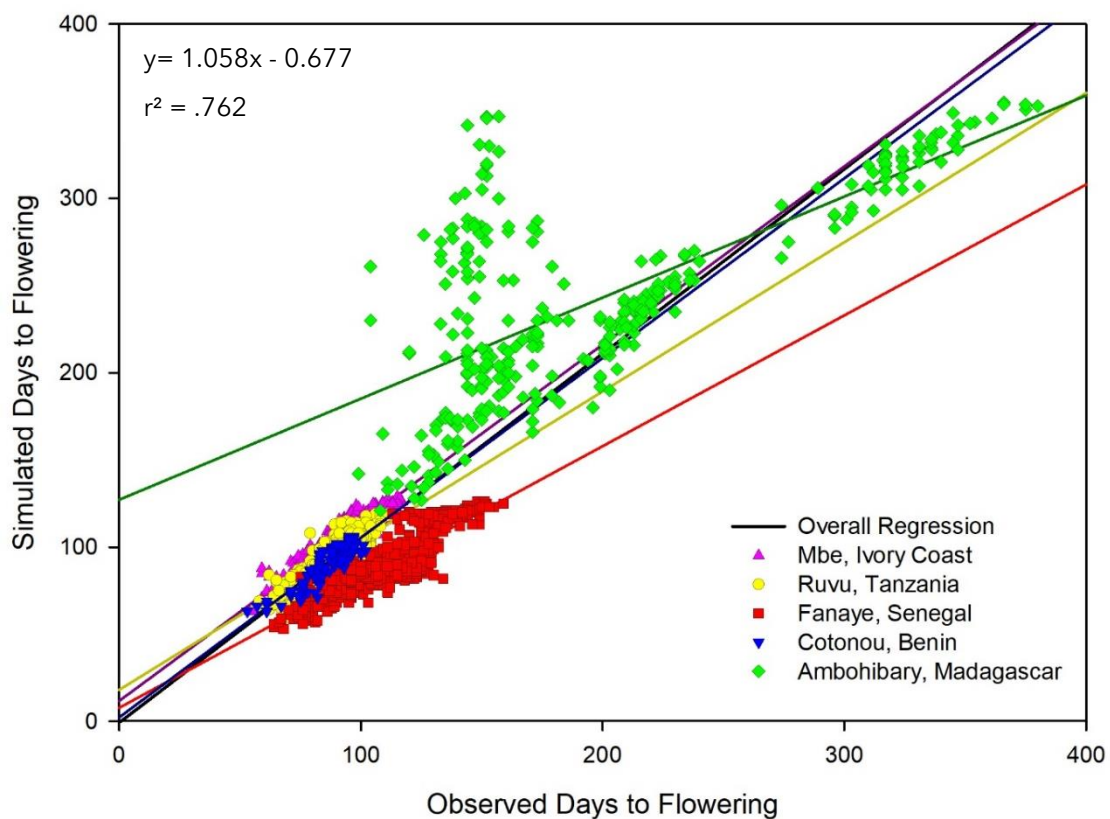


Figure 28: Observed versus simulated days to flowering following Dingkuhn-model across all environments and genotypes.

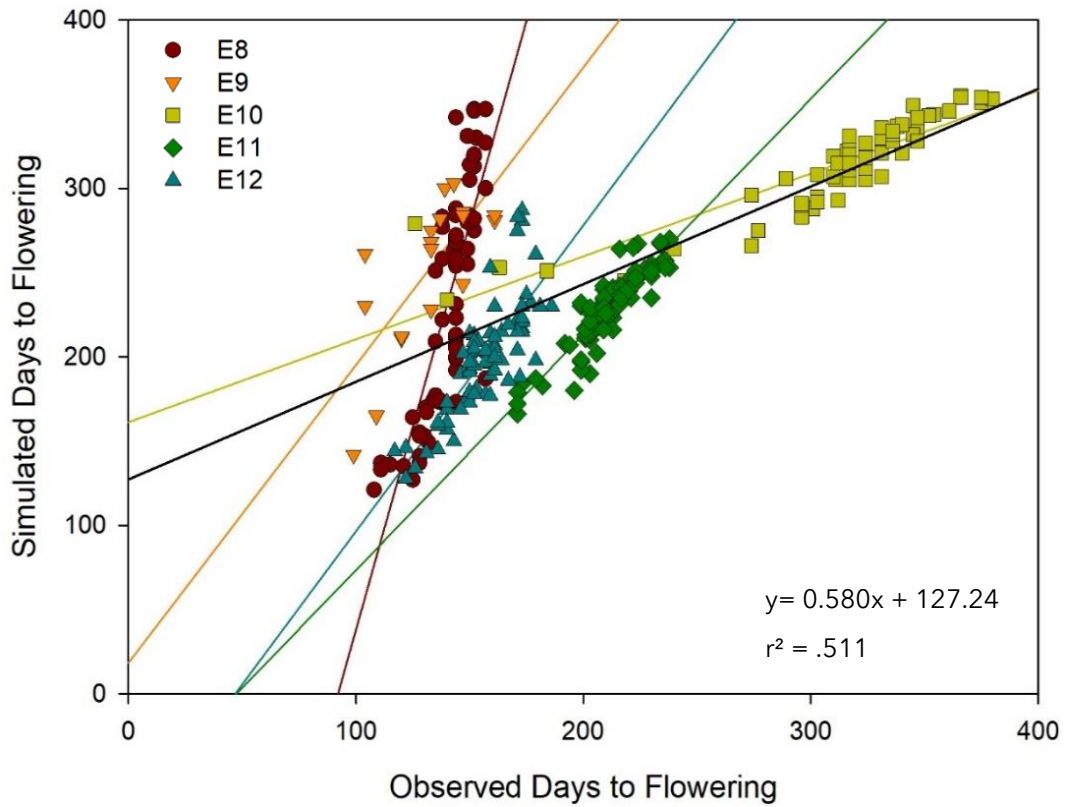


Figure 30: Observed vs simulated days to flowering following Dingkuhn for Ambohibary (E8-E12) across all genotypes

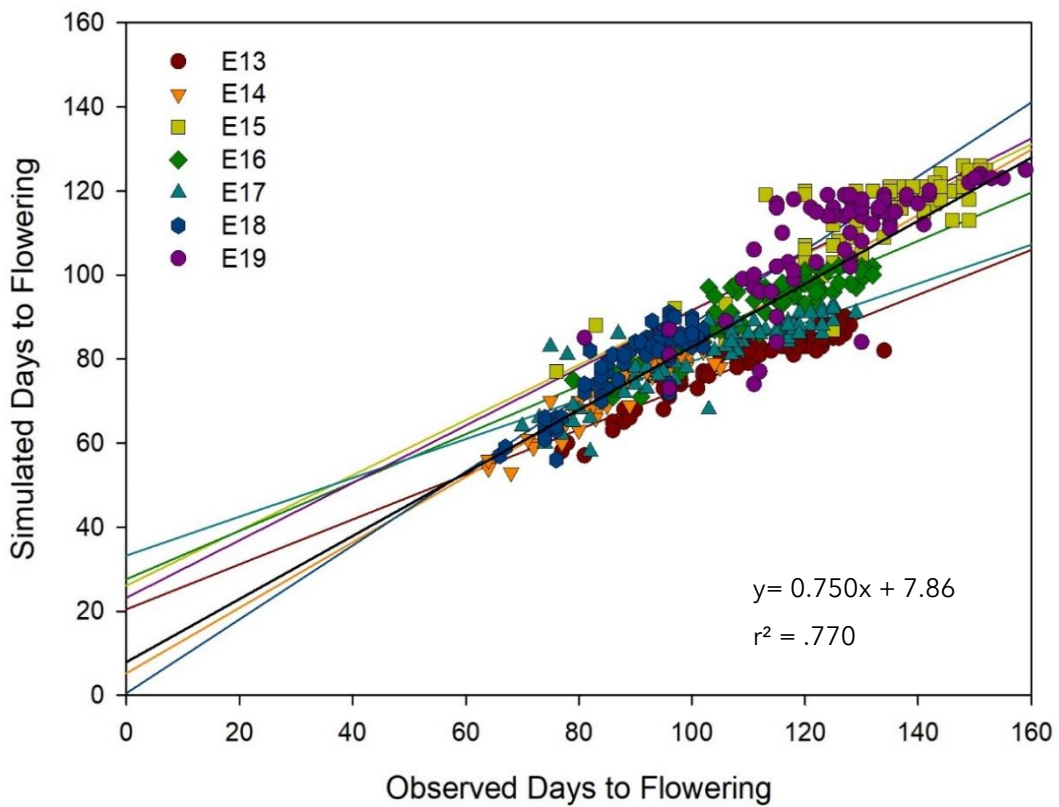


Figure 29: Observed versus simulated days to flowering following Dingkuhn for all sowing dates in Fanaye, Senegal (E13-E19) across all genotypes.

5.4.3 Stuerz

The Stuerz-model was better able to simulate f in Senegal than the other tested models (figure 31). However it struggles to capture the crop duration at some of Ambohibary's sowing dates, which skews the overall regression line downwards. When looking at the individual sowing dates in Ambohibary (figure 32), it can be seen that Stuerz' model is still able to capture E8, but overestimates f at the other sowing dates. Especially at E10 the simulated crop duration is too short, thus this environment again forms leverage points and suggests that Stuerz' model cannot capture this extreme environment. At Fanaye at all sowing dates, Stuerz' model simulates f better than Summerfield, Dingkuhn or AGN (figure 33).

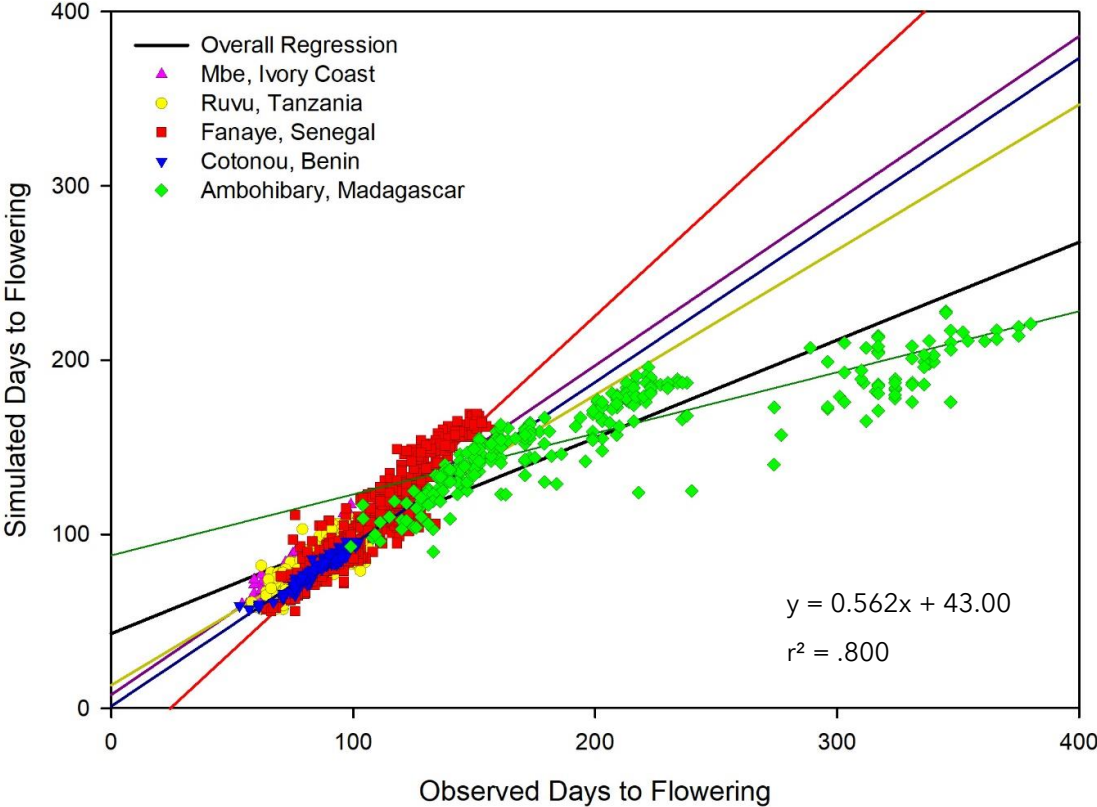


Figure 31: Observed versus simulated days to flowering following Stuerz-model across all environments and genotypes.

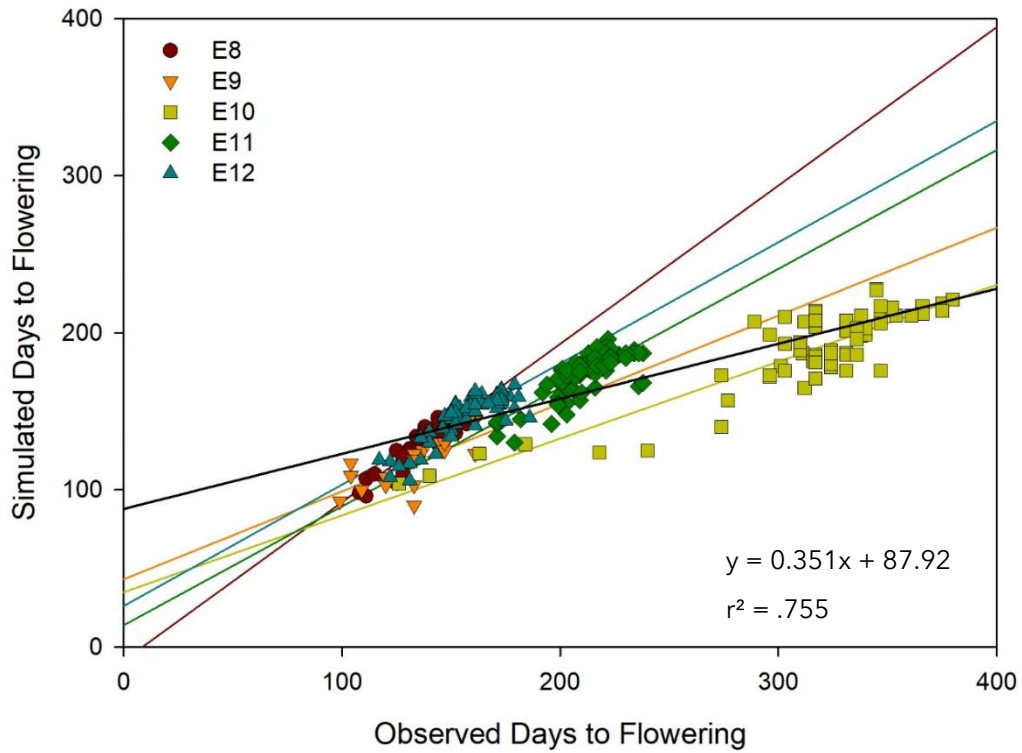


Figure 33: Observed versus simulated days to flowering following Stuerz-model for all sowing dates in Ambohibary, Madagascar (E8-E12) across all genotypes.

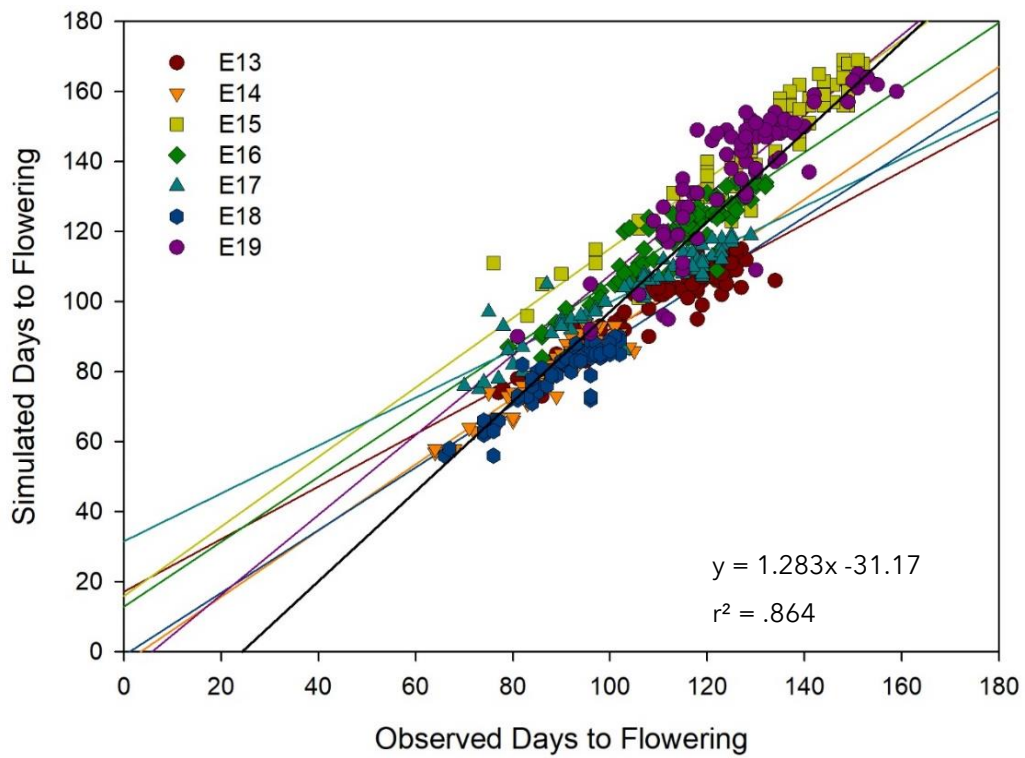


Figure 32: Observed versus simulated days to flowering following Stuerz-model for all sowing dates in Fanaye, Senegal (E13-E19) across all genotypes.

5.4.4 Asch-Groot Nibbelink

The simple AGN-model is a great improvement on the Summerfield-model with a slope that is 11.4% off and the highest r^2 at .900 of the tested phenology models (figure 34). This model is best at simulating crop duration in the cool environment of Ambohibary, however it was unable to capture some genotypes at E9 and E10 (figure 35). There is a severe systematic underestimation of crop duration in Fanaye (figure 36), with a slope of 0.345 and an r^2 of .473. It is able to simulate time to flowering for E14 and E18 very accurately actually, however, this model severely underestimates f for E13, E15-E17 and E19.

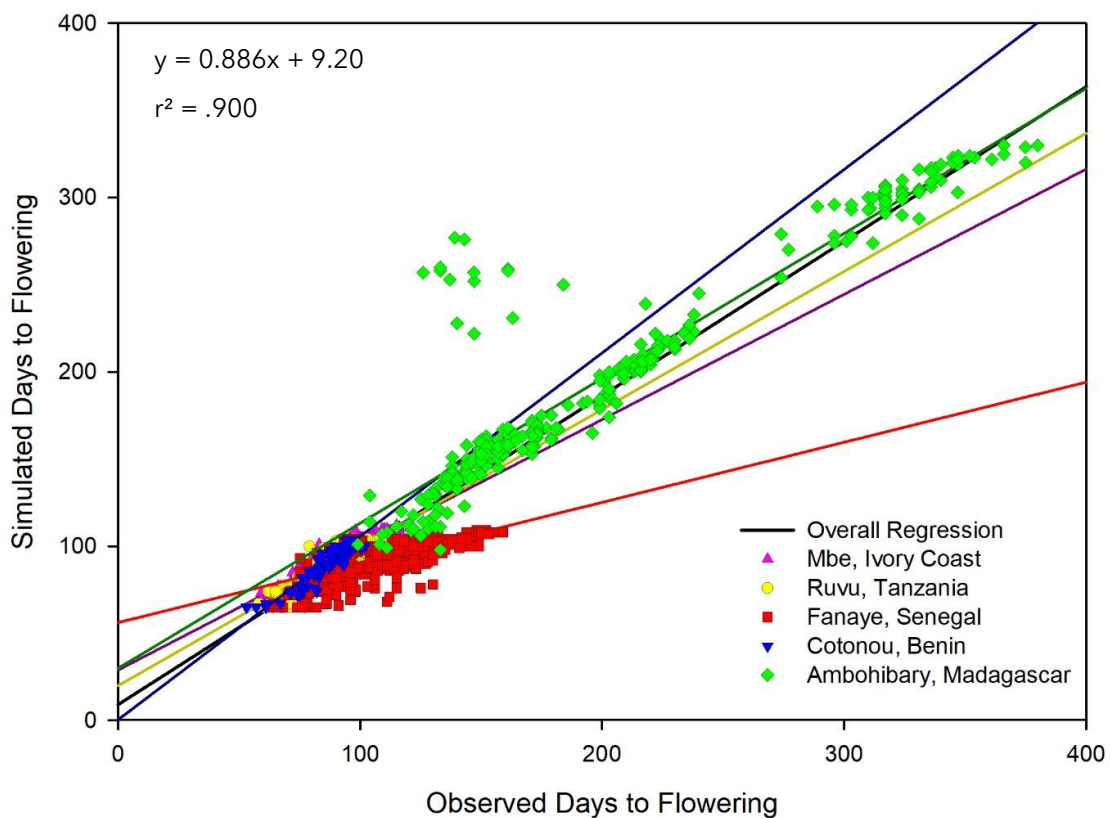


Figure 34: Observed versus simulated days to flowering following simple AGN-model across all environments and genotypes.

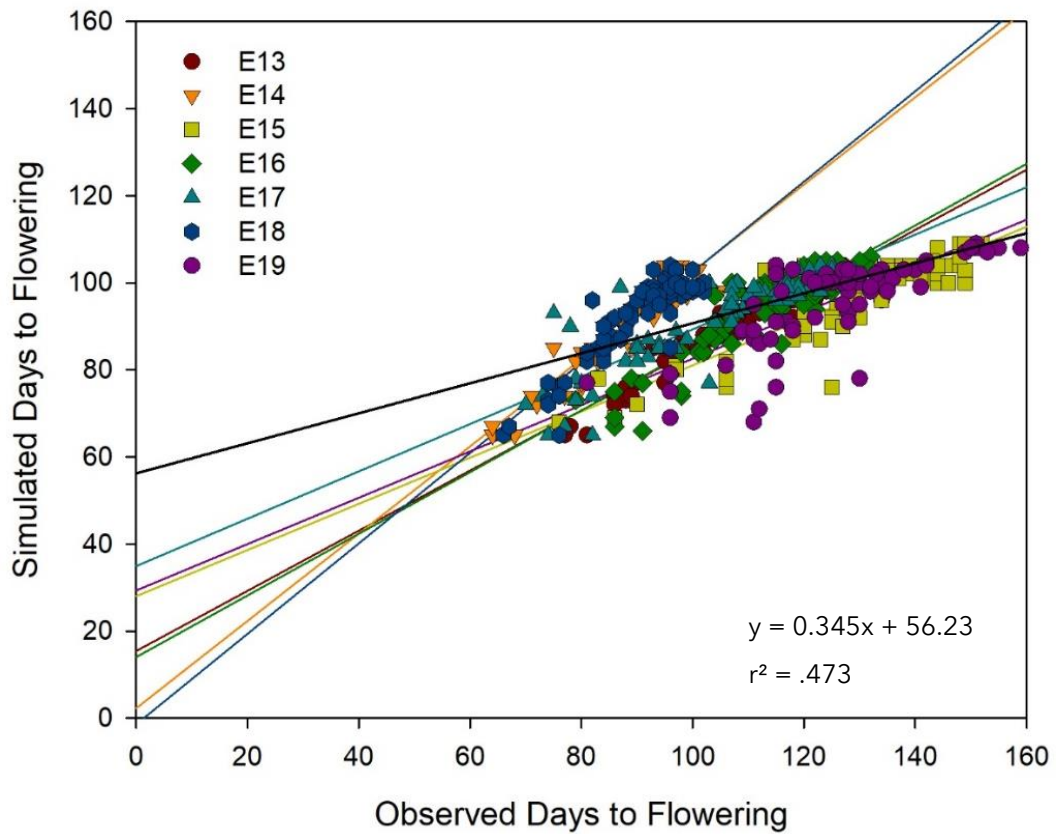


Figure 36: Observed versus simulated days to flowering following simple AGN-model for all sowing dates in Fanaye, Senegal (E13-E19) across all genotypes.

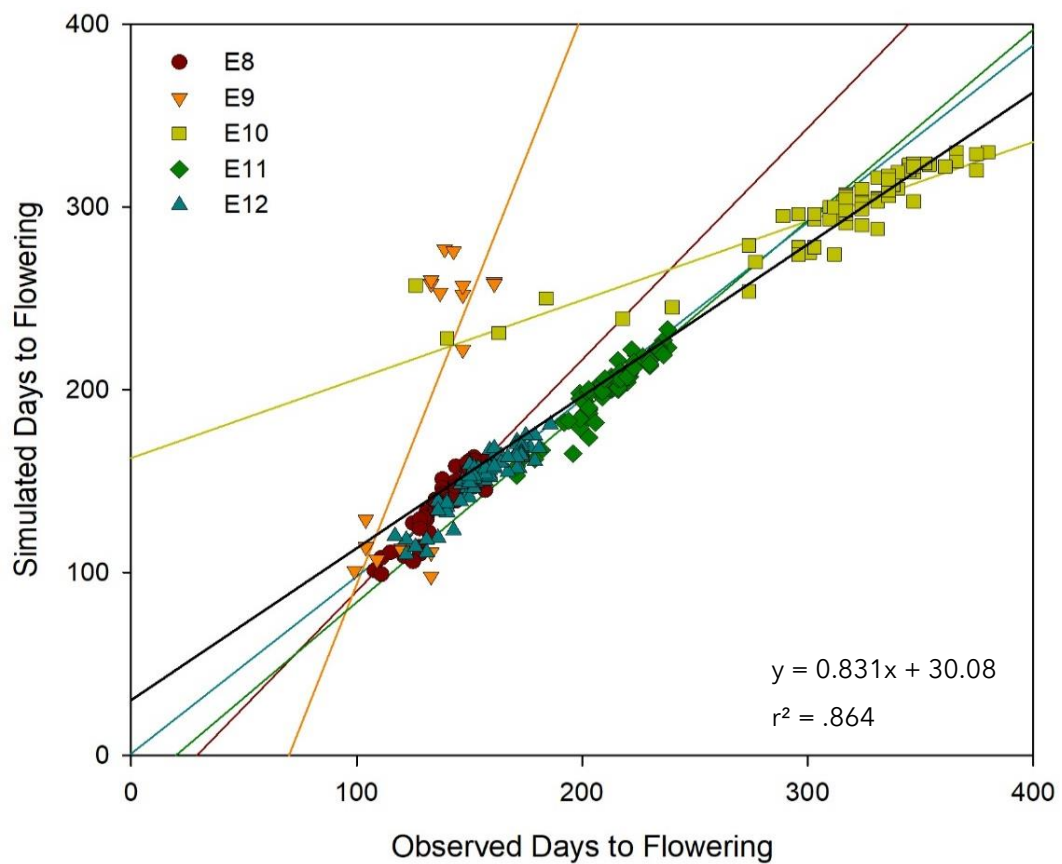


Figure 35: Observed versus simulated days to flowering following simple AGN-model for all sowing dates in Ambohibary, Madagascar (E8-E12) across all genotypes.

5.5 Comparing phenology models

The residuals (simulated f - observed f) of the four phenology models tested (figure 37), are all significantly different from each other and from 0. Dingkuhn is the only model with a positive residual least squares (LS) mean, which is furthest deviated from 0. Thus this model simulates on average a too long crop duration, while for the other models the time to flowering is on average underestimated. LS-mean for AGN was closest to 0.

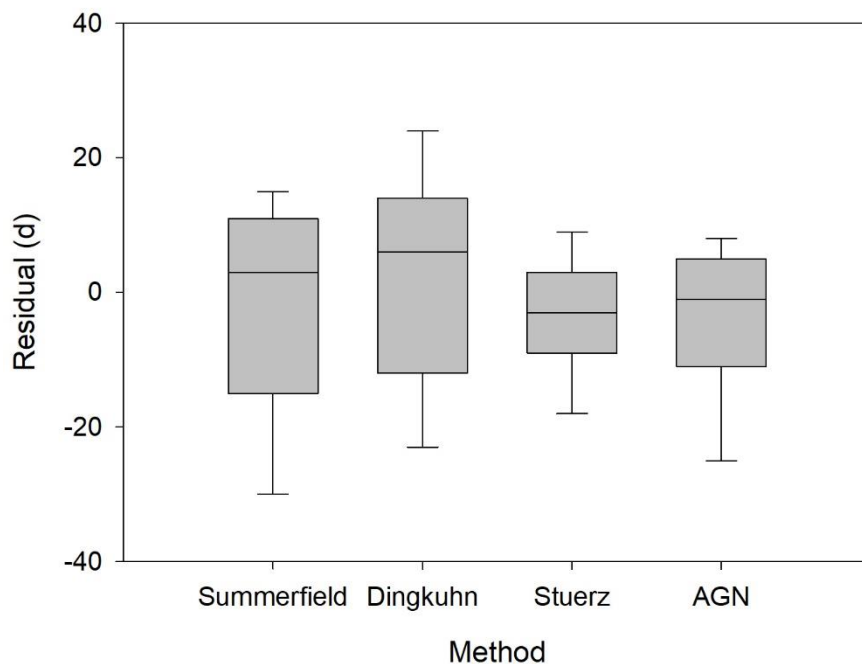


Figure 37: Boxplot of residuals (simulated f - observed f) for the four tested phenology models

Dingkuhn had had the highest RMSE (30.1 days), but the regression of simulated versus observed time to flowering was closest to a 1:1 line (only 5.8% off, intercept closest to 0). Lowest RMSE (12.7 days) was found in Summerfield, where the slope was furthest off with 44.5% (table 3). The coefficient of determination was highest for AGN, which also had the second-best slope (11.4% off) and intercept, while RMSE (15.0 days) was close to those of Summerfield and Stuerz.

Table 3: Results from regressing simulated versus observed time to flowering for Summerfield, Dingkuhn, Stuerz and AGN phenology models

<i>Method</i>	<i>Intercept</i>	<i>Slope</i>	<i>r²</i>	<i>RMSE</i>	<i>LS-mean Residual</i>
<i>Summerfield</i>	45.54	0.555	0.831	12.7	-5.6043 ^a
<i>Dingkuhn</i>	-0.68	1.058	0.762	30.1	6.0189 ^b
<i>Stuerz</i>	43.00	0.562	0.799	14.3	-7.4198 ^c
<i>AGN</i>	9.20	0.886	0.900	15.0	-3.9303 ^d

Each phenology model has their own strengths and weaknesses. Dingkuhn and Stuerz were best at simulating f for the arid Senegalese environments with a 25% underestimation and 28% overestimation respectively. However, Summerfield and AGN were best at capturing E14 and E18 with the sowing dates in July at the start of the rainy season in Fanaye. However, these phenology models fell short when trying to simulate f for the other sowing dates at Fanaye, when RH was much lower. Time to flowering in Ambohibary was best approached by the AGN-model. In general the inclusion of an optimum temperature had a greater effect on improving phenology modelling than the inclusion of RH. However, including both may improve phenology models even further.

5.6 Analysing residuals

A simple linear regression was performed of the individual environmental variables RH, VPD, cumulative radiation (rad), PP and PP including twilight (PP_{TWI}) against residuals to see which of these, besides temperature and, in case of Stuerz, RH, are correlated (table 4). If any of these environmental factor are correlated, including them in the phenology model might improve its predictive power.

Cumulative radiation explained 69.5% of the residuals from the Summerfield-model. This was the highest correlation found between residuals and an environmental factor of all four models. Radiation explained with 67.8% only a slightly lower percentage of the residuals of the Stuerz-model. Radiation is positively correlated with temperature: a high solar radiation goes together with high temperatures. In the AGN-model this effect has already been captured by the quadratic temperature term in the regression and the subsequent inclusion of an optimum temperature.

This explains the lower coefficient of determination ($r^2=0.091$) between radiation and residuals in the AGN-model.

Table 4: Results of simple linear regressions of the individual environmental variables (RH, VPD, Rad, PP and PP_{TWI}) against residuals (simulated f - observed f) for each phenology model.

	Summerfield			Dingkuhn			Stuerz			AGN		
	Int.	slope	r^2	Int.	slope	r^2	Int.	slope	r^2	Int.	slope	r^2
RH	-47.81	0.639	0.138	-56.37	0.95	0.223	10.65	-0.274	0.024	-47.62	0.662	0.384
VPD	3.29	-0.509	0.041	35.21	-1.67	0.327	-18.50	0.635	0.061	8.86	-0.732	0.221
Rad	35.92	-0.020	0.695	-2.513	0.0041	0.022	34.46	-0.020	0.678	5.41	-0.0045	0.091
PP	24.64	-2.509	0.002	-214.6	18.29	0.068	131.33	-11.513	0.035	-81.02	6.397	0.029
PP_{TWI}	46.16	-4.009	0.005	-233.0	18.51	0.072	148.29	-12.059	0.040	-74.15	5.438	0.022

The main factor explaining residuals in Dingkuhn is VPD with 32.7%. VPD is calculated based on both temperature and RH. RH in itself would explain 22.3% of the residuals. PP_{TWI} and radiation only explained 7.2% and 2.2% of the residuals respectively. In other models the correlation of daylength, with or without twilight, was even lower. This is likely due to the fact that PP was averaged over the complete period from sowing to flowering, while a rice plant is only sensitive to daylength during PSP. If PSP could be simulated and average PP during this period would be used for the regression, perhaps this would result in a higher correlation between PP and residuals.

Relative humidity is highly positively correlated with residuals in the AGN-model ($r^2=.384$). This correlation is higher than VPD. Probably this is because VPD is based on both temperature and RH and there is already an additional temperature term included in AGN. Interestingly, there is a low but still significant correlation between RH and the residuals of the Stuerz-model, despite this environmental factor already being included into the model.

Next, multiple linear regressions with forward selection of these environmental factors was carried out for each of the four phenology models (tables 5 - 8). Since PP with and without twilight are highly correlated by definition, including both factors would result in multicollinearity. Therefore, and because PP_{TWI} had a slightly

higher correlation with residuals in three out of four models, PP_{TWI} was included in the multiple linear regression and PP was excluded.

Table 5: Multiple linear regression with forward selection of environmental factors on residuals of Summerfield-model.

<i>Summerfield</i>							
<i>Step</i>	Variable	Number	Partial R²	Model R²	C(p)	F Value	Pr > F
Vars in							
1	Rad	1	0.6952	0.6952	2045.75	4347.85	<.0001
2	VPD	2	0.0938	0.7891	831.833	847.28	<.0001
3	PP_{TWI}	3	0.0532	0.8423	143.986	642.60	<.0001
4	RH	4	0.0109	0.8532	5.000	140.99	<.0001

Table 6: Multiple linear regression with forward selection of environmental factors on residuals of Dingkuhn-model.

<i>Dingkuhn</i>							
<i>Step</i>	Variable	Number	Partial R²	Model R²	C(p)	F Value	Pr > F
Vars in							
1	VPD	1	0.3268	0.3268	377.665	925.40	<.0001
2	PP_{TWI}	2	0.0498	0.3766	210.952	152.11	<.0001
3	RH	3	0.0359	0.4125	91.2057	116.41	<.0001
4	Rad	4	0.0260	0.4386	5.000	88.21	<.0001

Table 7: Multiple linear regression with forward selection of environmental factors on residuals of Stuerz-model.

<i>Stuerz</i>							
<i>Step</i>	Variable	Number	Partial R²	Model R²	C(p)	F Value	Pr > F
Vars in							
1	Rad	1	0.6777	0.6777	2205.88	4008.27	<.0001
2	RH	2	0.0540	0.7317	1519.76	383.10	<.0001
3	VPD	3	0.0425	0.7742	979.333	358.68	<.0001
4	PP_{TWI}	4	0.0766	0.8508	5.000	976.33	<.0001

Table 8: Multiple linear regression with forward selection of environmental factors on residuals of AGN-model.

AGN							
Step	Variable	Number	Partial R ²	Model R ²	C(p)	F Value	Pr > F
		Vars in					
1	RH	1	0.3842	0.3842	329.538	1189.1	<.0001
2	VPD	2	0.0639	0.4481	99.799	220.53	<.0001
3	Rad	3	0.0179	0.4660	36.8465	63.85	<.0001
4	PP _{TWI}	4	0.0093	0.4753	5.000	33.85	<.0001

All variables entered into the multiple linear regression were significant for all models, thus the forward selection resulted in all variables being included in the final regression models. Although all factors were found to be significant, some of them only slightly improve overall model R², e.g. inclusion of PP_{TWI} in the multiple linear regression for AGN only improved the model fit with 0.93%.

For Stuerz and Summerfield, the complete regression model explained >85% of the residuals, while in AGN the complete regression model explained 47.53% and in Dingkuhn it only explained 43.86%. This is partly because these models were already better at simulating flowering dates, thus the residuals are smaller, while in Summerfield and Stuerz, which have a larger discrepancy between simulated and observed flowering dates, a larger part of these residuals can be explained by these climatic factors.

It was found that RH explained 38.4% of the residuals of the AGN-model. While other environmental factors also significantly explained part of the residuals, they could only explain a rather small proportion. After fitting RH, VPD only explained an additional 6.4%. Including more factors into a phenology model complicates the model and requires higher data input. The general mantra in modelling is 'simple is beautiful'. Therefore it was decided to further develop the AGN-model to include the effect of RH, without considering the other environmental factors.

5.7 Improved Asch-Groot Nibbelink model

The original AGN-model was further developed to include the effect of RH to improve the simulation of time to flowering. This was done by applying a multiple regression including both the quadratic temperature term and RH:

$$(26) \quad DR = a * \bar{T}^2 + b * \bar{T} + c * \overline{RH} + d$$

The challenge was to translate this regression equation into estimations of cardinal temperatures including an RH-adjustment factor, so it can be used to simulate days to flowering. Five alternative versions were developed and tested to see which one was best at balancing simplicity and accuracy.

5.7.1 AGN Version 1

In the first version T_{BASE} and T_{SUM} were calculated as in the simple AGN-model, while T_{OPT} is adjusted to RH. As can be seen in figure 38, the sloped tangent remains constant, while the horizontal tangent changes position with changing RH. Tangents that change with RH are coloured red, while cardinal temperatures affected by RH are coloured dark red. Tangents and cardinal temperatures that remain unaffected by RH are black. Regression equation has only been given in figure 38, not in the figures of versions 2-5 as it is the same regression, just different tangents.

Horizontal tangent lines and corresponding optimum temperatures were calculated for $RH=0\%$ (T_{opt0}) and for $RH=100\%$ (T_{opt100}). The RH-adjustment factor for T_{OPT} is calculated as:

$$(27) \quad RH_{adj.opt} = \frac{T_{opt100} - T_{opt0}}{100}$$

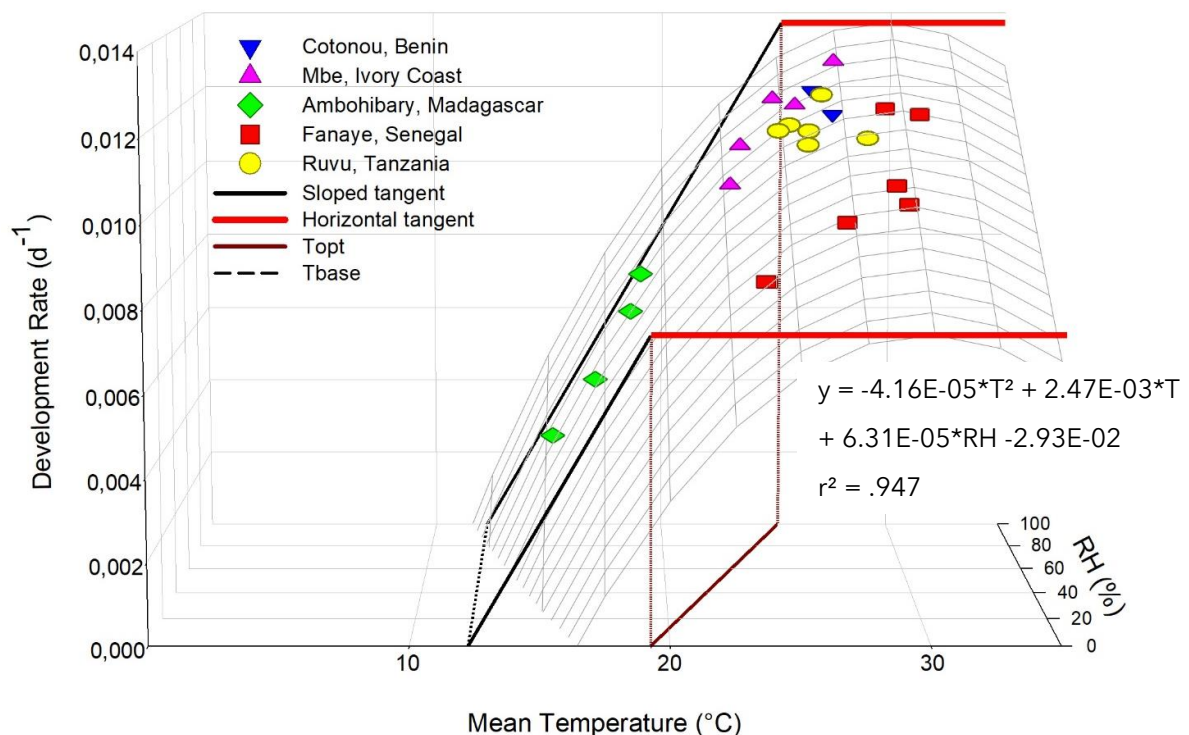


Figure 38: Multiple regression of development rate ($1/f$) of IR64 versus mean air temperature and mean relative air humidity (RH) in 24 environments (E9 missing) across 5 different sites. AGN version 1 where T_{OPT} increases with RH, while T_{BASE} and T_{SUM} remain constant.

5.7.2 AGN Version 2

In the second version, T_{SUM} and T_{OPT} remain constant and are calculated as in the original AGN-model, while T_{BASE} is adjusted for RH (figure 39). Thus both tangents change position, while only T_{BASE} decreases as RH increases.

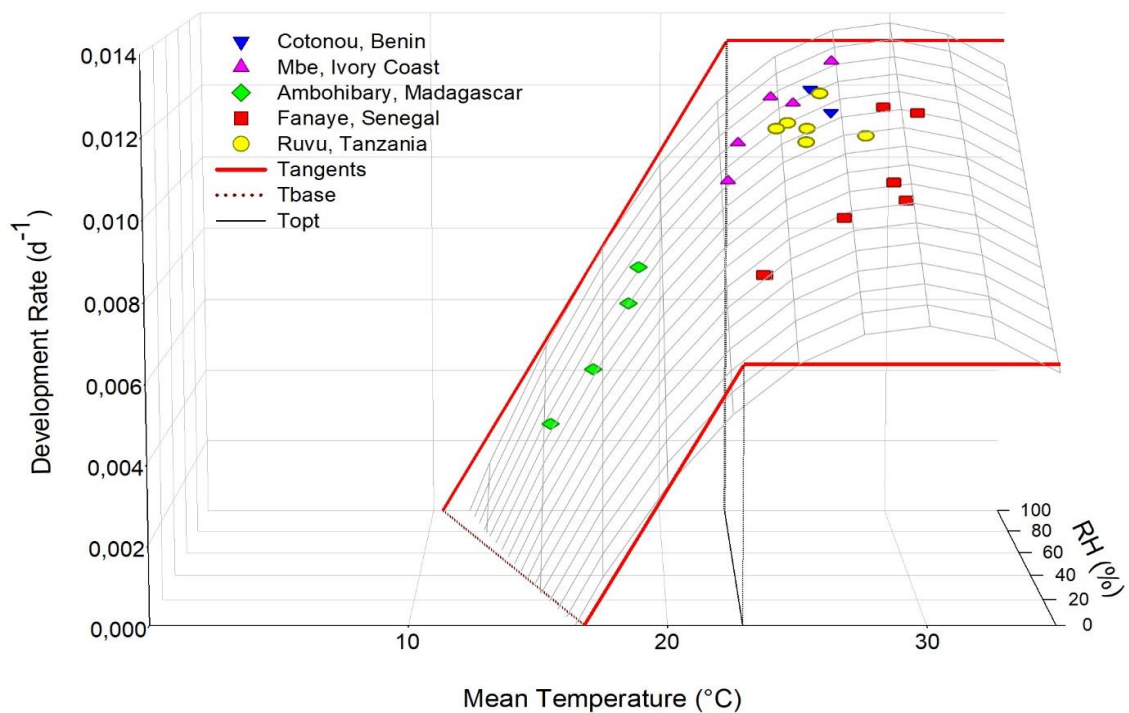


Figure 39: Multiple regression of DR of IR64 vs mean T and mean RH in 24 environments (E9 missing) across 5 different sites. AGN version 2 where T_{BASE} decreases with increasing RH , while T_{OPT} and T_{SUM} remain constant.

5.7.3 AGN Version 3

In the third version, the horizontal tangent remains unaffected by RH, while the sloped tangent changes with RH while its slope remains constant (figure 40). Thus, T_{BASE} and T_{OPT} change with RH but the same RH-adjustment factor applies to both T_{BASE} and T_{OPT} .

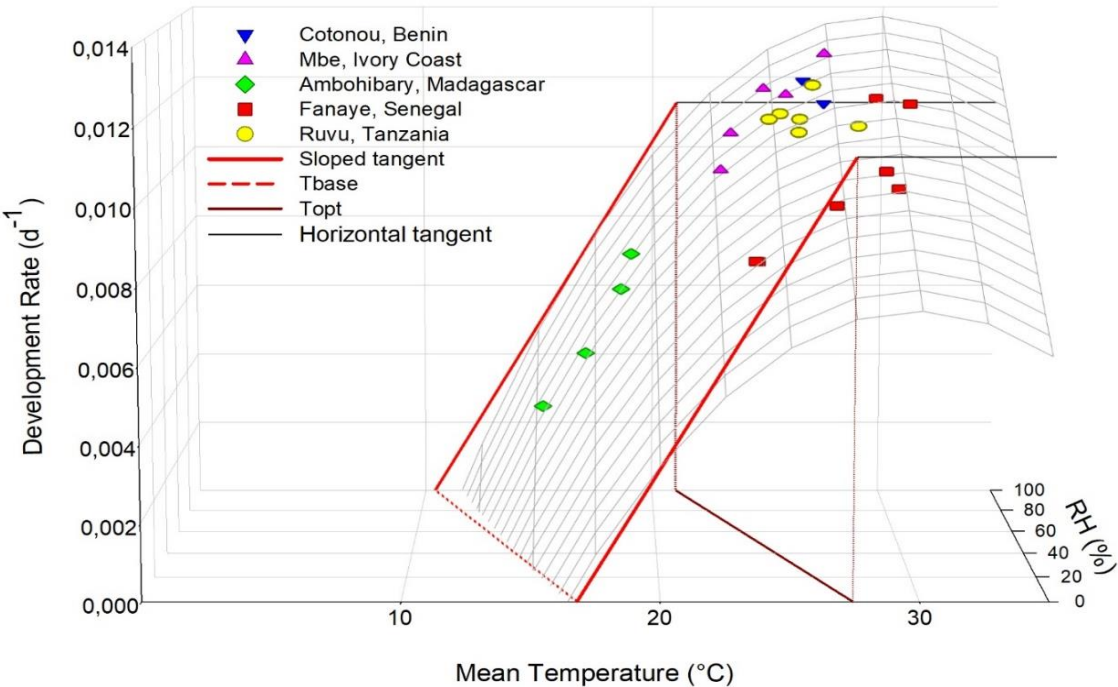


Figure 40: Multiple regression of DR of IR64 vs mean T and mean RH in 24 environments (E9 missing) across 5 different sites. AGN version 3 where sloped tangent moves with RH while horizontal tangent remains as in simple AGN; thus T_{BASE} and T_{OPT} vary with same RH_{ADJ} factor.

5.7.4 AGN Version 4

In this version both tangents move with RH, while the slope of the sloped tangent remains constant. This means that both T_{BASE} and T_{OPT} are adjusted to RH, although they are not equally sensitive. Figure 41 shows that T_{BASE} responds much stronger to humidity than T_{OPT} , where the change is barely noticeable.

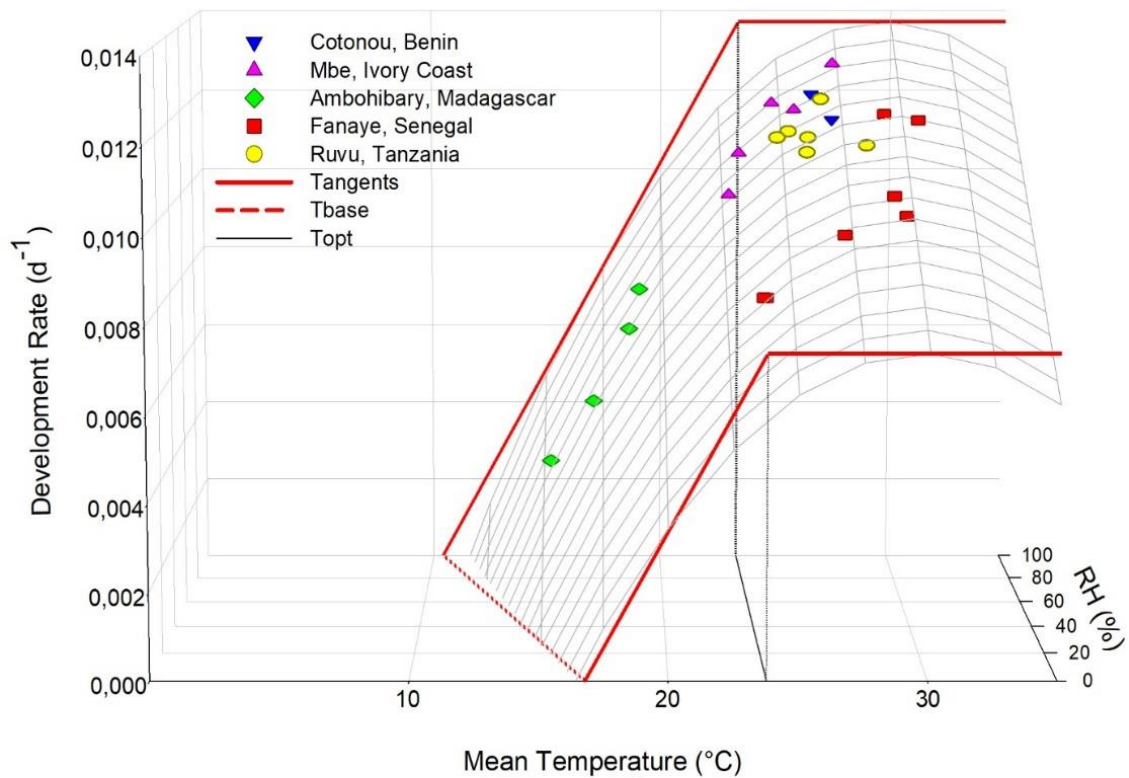


Figure 41: Multiple regression of development rate ($1/f$) of IR64 versus mean air temperature and mean relative air humidity (RH) in 24 environments (E9 missing) across 5 different sites. AGN version 4 where both tangents move with RH, thus both T_{BASE} and T_{OPT} are adjusted to RH while T_{SUM} remains constant.

5.7.5 AGN Version 5

In this last and most complex version all cardinal temperatures are adjusted to the effect of RH (figure 42). The sloped tangent changes in angle, causing T_{SUM} to change with RH. When simulating the flowering dates this is captured by multiplying T_{SUM} with an RH-adjustment factor. Thus in humid environments the slope of the tangent increases and T_{SUM} is reduced.

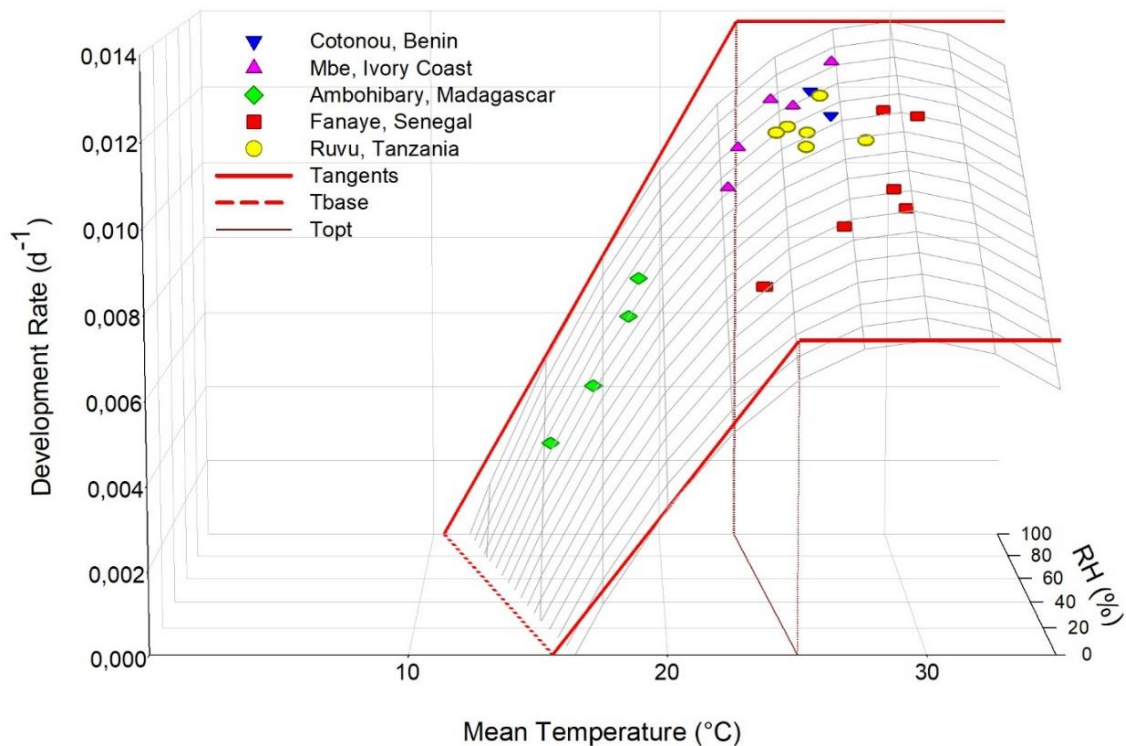


Figure 42: Multiple regression of development rate ($1/f$) of IR64 versus mean air temperature and mean relative air humidity (RH) in 24 environments (E9 missing) across 5 different sites. AGN version 5 where both tangents move with RH, and the slope changes with RH. Thus all cardinal temperatures have an individual RH-adjustment factor.

5.7.6 Comparing model versions

Table 9 shows the cardinal temperatures and RH-adjustment factors for IR64 as estimated with the five different versions of the improved AGN-model. This was done for each of the 80 genotypes.

Table 9: Cardinal temperature for IR64 as estimates based on the five versions of AGN-model

Method	T_{SUM}	T_{BASE}	T_{OPT}	$RH_{ADJ.SUM}$	$RH_{ADJ.BASE}$	$RH_{ADJ.OPT}$
--------	-----------	------------	-----------	----------------	-----------------	----------------

AGN v1	944	12.26	19.26	0	0	0.060
AGN v2	944	16.79	22.90	0	-0.064	0
AGN v3	944	16.79	27.44	0	-0.064	-0.064
AGN v4	944	16.79	23.79	0	-0.064	-0.004
AGN v5	1274	15.57	25.01	-3.38	-0.051	-0.017

Based on the genotype-specific cardinal temperatures and RH-adjustment factors, daily T_{PHYS} was calculated. For this, eqn 25 was adapted to include both an RH-adjustment factor for T_{BASE} and for T_{OPT} :

$$(28) \quad T_{\text{phys}} = \max \left(\min \left((T_{\text{opt}} + RH_{\text{adj.opt}} * RH_{\text{av}}), T_{\text{av}} \right) - (T_{\text{base}} + RH_{\text{adj.base}} * RH_{\text{av}}), 0 \right)$$

Note that the RH-adjustment factor for T_{BASE} was renamed to specify which cardinal temperature it adjusts. Whenever in a model version a cardinal temperature is not adjusted for RH, this factor is simply set to 0. For version 5, T_{SUM} was calculated as $T_{\text{SUM}} + RH * RH_{\text{ADJ.SUM}}$, and thus varied per day. T_{phys} was again summed until T_{SUM} was reached, returning a flowering date. The simulated days from sowing to flowering were regressed versus observed days from sowing to flowering (table 10 and figure 43) and subsequently residuals were calculated and analysed (figure 44).

Table 10: Results from regressing simulated vs. observed time to flowering for the five versions of AGN-model

Method	Intercept	Slope	r ²	RMSE	LS-mean Residual
AGN v1	1.65	0.937	0.938	12.3	-5.547 c
AGN v2	11.85	0.880	0.959	9.3	-1.907 a
AGN v3	13.78	0.849	0.956	9.2	-3.597 b
AGN v4	5.45	0.899	0.969	8.2	-6.192 c
AGN v5	9.19	0.904	0.954	10.1	-1.880 a

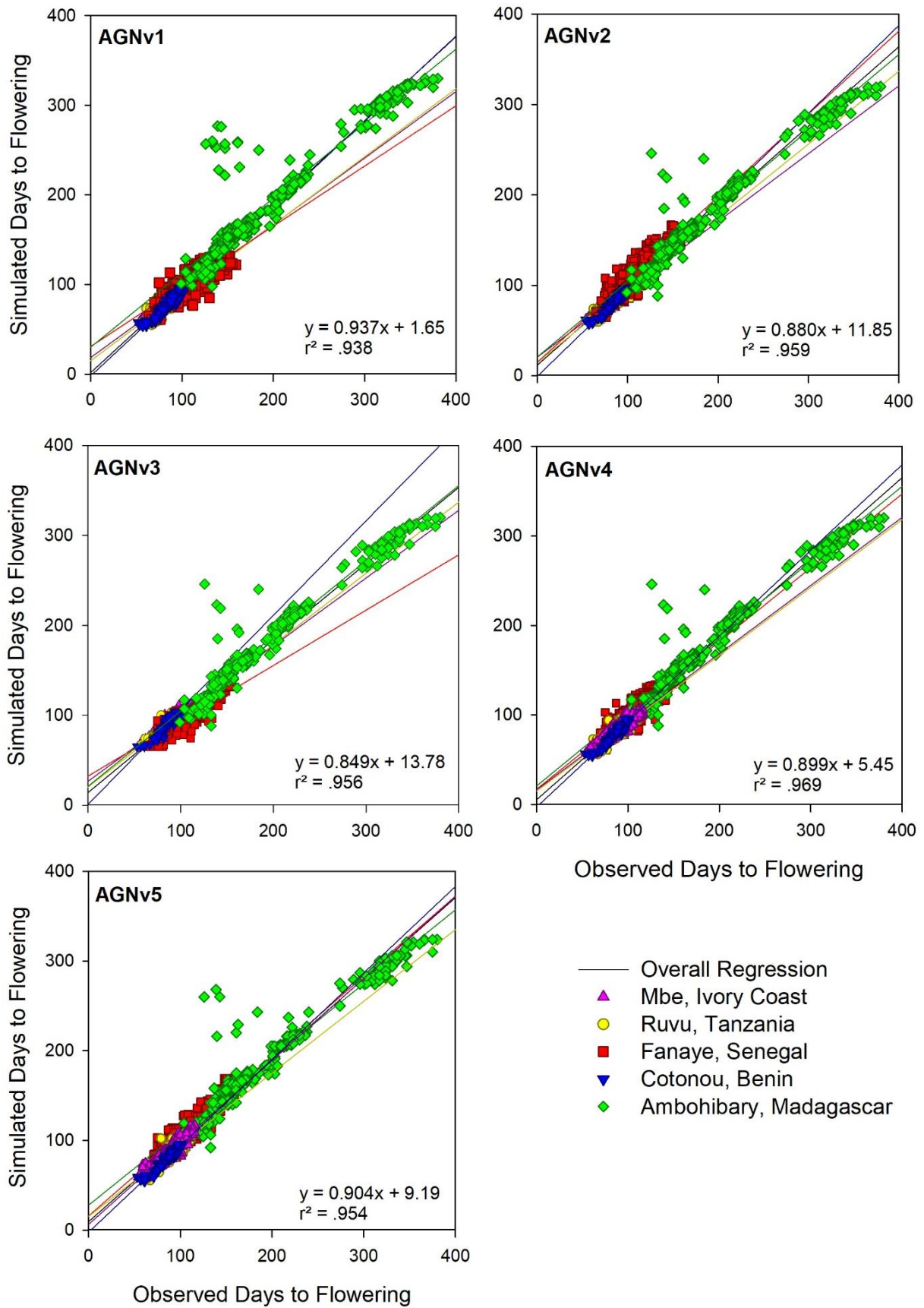


Figure 43: Simulated versus observed days to flowering for all five versions of the improved AGN-model

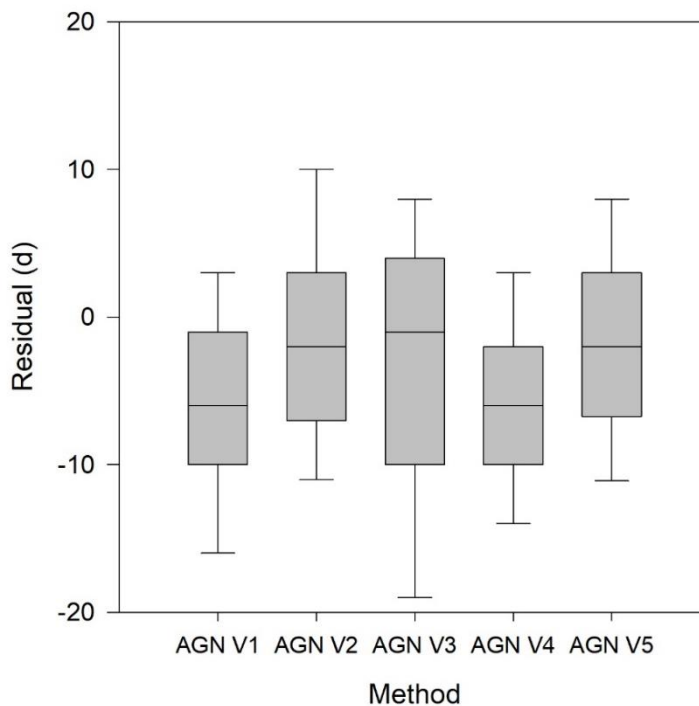


Figure 44: Boxplot of residuals of the five AGN versions

Mean residuals of version 2 and 5 were not significantly different ($p=.941$). It is surprising how close the residuals of these two versions are, considering how different the cardinal temperatures are estimated. Mean residuals of versions 1 and 4 were also found to be not significantly different from each other at $p=.0796$.

Since version 5 is the most complex version with a variable T_{SUM} , and it is not significantly better at simulating crop duration than any of the other versions, this version was discarded. Version 1 and 4 have mean residuals furthest deviating from 0. Version 4 has the lowest RMSE (8.2 days). Version 1 has the best results of the regression from simulated versus observed days to flowering with an intercept of 1.65 and a slope of .937 it was only 6.3% off. Despite this version having a higher RMSE (12.3 days) and a slightly lower r^2 (.938), these values are still a great improvement compared to the phenology models of Summerfield, Dingkuhn and Stuerz. The increased complexity from versions 2-5 did not show a clear added value, i.e. they did not provide major improvements in phenology modelling. Therefore version 1 is selected to be the final version of the AGN-model.

6 Discussion

6.1 Timing of Panicle Initiation

According to Vergara (1991) and IRRI (n.d.), RP lasts approximately 35 days. Dingkuhn et al. (1995) estimate PI to occur 30 days before flowering, while GRiSP (2013) describe PI to occur about 25 days before heading. In contrast to literature, according to the data from this project duration from PI to flowering is not fixed in number of days. The results show a large variation in time from PI to flowering, suggesting a considerable environmental influence on duration of RP. In the cool environments of Ambohibary the average time from PI to flowering was much longer than at other locations. It was more than twice as long as the average duration in the warm environments of Ruvu.

Our findings are to some level in accordance with Vergara (1991), who already reported that the length of RP might take twice as long in temperate and high-altitude regions. Ambohibary with its elevation of 1634 m above sea level is a typical high-altitude environment. However, Vergara, (1991) also wrote that length of RP is fixed in tropical environments, while this study found considerable differences in duration between tropical environments. E.g duration from PI to flowering for rice sown in August 2014 in Cotonou was on average 21 days, while for rice sown in November 2015 in Mbe duration of RP was on average 41 days, while both are low-altitude tropical environments.

In RIDEV2 TSUM during RP is set to 400°Cd (Dingkuhn et al., 2017). However, our data showed an average TSUM during RP of 772°Cd, however this was purely the sum of air temperatures, without subtracting a daily Tbase. Nevertheless, our data showed considerable variation in RP measured in dd between locations and within locations. Although assuming a constant TSUM during RP is better than assuming a constant number of days, it can still not capture the variation observed in reality.

The variation in duration from PI to flowering can be partially explained by the influence of environment, partially by measurement error (different observers at different locations could observe PI slightly differently) and possibly the genotype

plays a role as well, e.g. in sensitivity to temperature during RP (Dingkuhn et al., 2017).

In the phenology subroutine of ORYZA2000, phenology is ranked on a numerical scale, from emergence (DS=0) to end of BVP i.e. start of PSP (DS=0.4), PI (DS=0.65), flowering (DS=1) and maturity (DS=2), where DS is the integral of DR (Bouman et al., 2001; van Oort et al., 2011). In this model, there is a fixed ratio rather than fixed number of days between PI and flowering date. Duration of VP can be estimated as $0.65 \cdot f$ and duration of RP can be estimated as $0.35 \cdot f$. Here PI date is not fixed in number of days, but instead depends on crop duration, which in turn is influenced by the environment. However, applying this approach to estimate PI to our dataset did not give better results (regression of estimated vs observed days from sowing to PI: $y = .773x + 11.34$; $r^2 = .931$) than simply estimating PI as 30 days before flowering date ($y = 1.162x - 13.92$; $r^2 = .921$). Neither estimating PI as a fixed number of days before flowering nor as a ratio gave satisfactory results.

There is potential to develop a model to simulate PI date based on the data from this research project. However, this was not the focus of my thesis research. If PI date could be simulated accurately, the models by Summerfield (eqn 3) and Dingkuhn (eqn 10) including the effect of PP could be tested and compared to the AGN-model.

The exact PI date is difficult to measure and prone to human error, as was shown for the erroneous PI data recorded at E13 and E15 in Fanaye, Senegal. The stem has to be dissected to observe the start of the panicle, which is barely visible with the bare eye at about 1mm in length (GRiSP, 2013). The AGN-model circumvents this problem by simulating flowering date without accounting for daylength during PSP, thus there is no need to know PI date. Instead it simulates flowering dates based on cardinal temperatures, air temperature and relative air humidity over the period from sowing to flowering.

6.2 Model Limits

Every model works well within certain limits. Rice phenology models are limited to certain environmental conditions. Outside the environmental range they have been

designed and calibrated for, their predictive power is limited. In this subchapter the model limits for the tested and newly developed phenology models are discussed.

6.2.1 Summerfield

Summerfield et al. (1992) have clearly defined model limits regarding temperature, namely that the *"coldest values of T experienced by plants are not below the base temperature at which $1/f = 0$ "* and *"that the warmest temperatures experienced are not above the optimum temperature at which $1/f$ is a maximal value"*. Only when these conditions are met the relationship between DR and \bar{T} is linear.

RGT experiments for this project were conducted at a wide range of environments. At some environments temperatures dropped below base temperatures, particularly at Ambohibary (E8-E12), while at other environments the rice plants experienced temperatures beyond T_{OPT} , particularly at Fanaye (E13-E19) with maximum daily temperatures beyond 40°C. At other environments maximum temperatures peaked beyond T_{OPT} as well, e.g. at Ruvu (E20-E25), where daily maximum temperatures were well above 30°C at most days, which is reflected in DR no longer increasing with increasing \bar{T} for some genotypes e.g. IR64. Thus, at a number of environments Summerfield's model limits were transgressed, resulting in unrealistically low T_{BASE} estimations: for three genotypes T_{BASE} was estimated below freezing point at the highest T_{BASE} found with Summerfield was 7.92°C, which is still lower than the default base temperatures in most crop models.

Summerfield et al. (1992) already observed that DR stagnates beyond T_{OPT} and propose a broken-stick model with constant or slightly decreasing DR beyond T_{OPT} . T_{OPT} was estimated at approximately 25°C (Summerfield et al 1992). However, this seems to be simply based on visual interpretations of the data and they do not offer a method for estimating T_{OPT} .

6.2.2 Dingkuhn

The simplest Dingkuhn-model as applied in this thesis is limited in that it does not account for the effects of photoperiodism and transplanting shock, something the more complex model (eqn 9) does (Dingkuhn et al., 1995). They state that *"prediction errors in exclusively thermal simulation of f partly are due to*

photoperiodism". They also found a systematic overestimation of T_{BASE} , ranging from 14.5 to 19.5°C, which is significantly higher than T_{BASE} estimates found when applied to our dataset (ranging from 8.9 to 11.0°C). They identified a need for including an optimum temperature and using water temperature instead of air temperature to improve the model accuracy.

Dingkuhn's model was developed based on data collected in the Sahel. Interestingly, this model resulted, similar to Summerfield, in a systematic underestimation of crop duration at the hot-arid Fanaye environments. Thus, suggesting that Dingkuhn's model is limited in simulating crop duration in dry environments as well, when genotype-specific parameters are calibrated over a wide range of environments. Overall, this model was better at predicting crop duration than the Summerfield- and Stuerz-model, mainly due to accurate simulations of f at Cotonou, Mbe and Ruvu, and due to an overestimation of f in Ambohibary, which partly compensates for the underestimation of crop durations at Fanaye. Dingkuhn's model was able to simulate flowering dates at E10 quite well for most genotypes, yet it gave poor results at other cool environments, especially E8 and E9. This is odd, as E10 was the most extreme environment regarding low temperatures and short days, while E8 and E9 had longer days and cool but not quite as cold temperatures.

Dingkuhn et al. (1995) identified that using water temperatures (T_{WATER}) instead of air temperatures when estimating cardinal temperatures improves accuracy, because, as they argue, the temperature at the shoot apex i.e. growing point, is the physiologically relevant temperature and until booting the apex is below the water surface. T_{WATER} is influenced by air temperature, wind speed, RH, solar radiation, water source (e.g. irrigation water heated in a basin or directly from a glacier-fed river) and crop cover (expressed in leaf area index; LAI). Water temperature was found to be usually cooler than air temperature at low RH and high LAI. After booting, the shoot apex rises above the water surface and a rice plant experiences canopy temperatures from then on, which may significantly differ from air temperatures outside the canopy i.e. at a meteorological station. During this project, T_{WATER} was measured at MC plots, however it was complete for only two

environments (E16 and E17). RIDEV2 offers the possibility to simulate T_{WATER} based on LAI (Dingkuhn et al., 2017). However, LAI data collected during this project was insufficient to simulate T_{WATER} . Therefore air temperature was used instead. Perhaps estimating cardinal temperatures based on T_{WATER} would have resulted in better predictions of f , but the need for additional data on T_{WATER} and/or LAI is a limitation as this data is often lacking or incomplete.

6.2.3 Stuerz

Stuerz' model is similar to Summerfield and therefore by definition subject to the same temperature limitations. Therefore this model ran into the same problems when simulating flowering dates for Ambohibary as Summerfield's model. It is, like Summerfield, still able to simulate flowering dates for E8, but not for any of the other cool Ambohibary environments. On the other hand the inclusion of RH makes this model applicable to a wider range of environments with regard to differences in RH. This is shown by the significant improvements simulation of crop duration for the arid Fanaye environments.

6.2.4 Asch-Groot Nibbelink

The inclusion of T_{OPT} in AGN improves the simulation of flowering dates at environments with temperatures near and beyond T_{OPT} . This model is applicable to a wider range of environments, especially to hotter environments, than both Summerfield and Stuerz. The inclusion of an RH-adjustment factor widens the applicability of this model to more arid environments.

AGN may have an upper temperature limit. When a rice plant experiences temperatures significantly beyond T_{OPT} , DR may reduce, which is reflected by some rice crop models (e.g. ORYZA-family) by including a maximum temperature (T_{MAX}) at which DR=0. However, recent studies found that models without a T_{MAX} actually gave more accurate crop duration simulations (van Oort et al., 2011; Zhang et al., 2016). No decline in DR at temperatures $> T_{\text{OPT}}$ was observed in this dataset.

There is potential to include a T_{MAX} in the AGN-model as it is based on a second order regression and a third tangent could potentially be included, mirroring the first sloped tangent. The intersect of this tangent with the x-axis would be T_{MAX} .

However, additional data on rice grown in extremely hot environments, especially hot-humid environments, is required to see first of all if DR declines at mean temperatures beyond T_{OPT} , and if yes, to quantify this decline and estimate T_{MAX} .

6.3 Influence of relative humidity on phenology

It has been shown that RH is positively correlated with DR. Thus the time from sowing to flowering of rice is shorter in humid environments than in dry environments with the same mean temperature. This relationship between air humidity and phenology in rice has been reported by Stuerz et al. (2020). That leads to the question: How does RH influence phenology?

One explanation could be that low RH conditions lead to higher VPD, thereby increasing transpiration. This causes the plant to lose more water to the air and stomatal closure in response to dry conditions to reduce water losses. Stomatal closure limits gas exchange and all processes depending thereon, including photosynthesis and development rate. However, rice was grown in a lowland irrigated production system, thus the plant never experienced drought stress during the experiments. Thus reduced development rate due to drought-induced stomatal closure cannot be the answer as to how RH influences phenology in paddy rice.

A more likely explanation is that low RH leads to higher transpiration cooling of the plant and thus cools down the canopy temperature. This process of transpiration cooling affecting rice has also been described by Julia & Dingkuhn (2013), who found that *“warm-humid conditions cause more heat stress than hot-arid conditions”*. Transpiration cooling avoids heat stress in rice by reducing panicle temperatures (Julia & Dingkuhn, 2013), but if this leads to temperatures below T_{OPT} it will reduce DR.

6.4 Improving rice crop models

Including an optimum temperature for simulating phenology, as proposed with the AGN-model, is not new. Many rice crop models already include optimum and maximum temperatures in their phenology subroutine. Commonly used temperature response functions are 1) Blackman, where DR increases linearly from

T_{BASE} (DR=0) until max. DR at T_{OPT} , thereafter at temperatures $> T_{OPT}$ DR remains at max. value (employed in Ceres-rice); 2) Bilinear, where DR increases from T_{BASE} to max. DR at T_{OPT} and at temperatures beyond T_{OPT} DR declines linearly to DR=0 at T_{MAX} (employed in ORYZA2000); 3) Beta, similar to the bilinear function, but with a bell-shape, thereby modelling a slower change in DR at temperatures near the cardinal temperatures (van Oort et al., 2011). The AGN phenology model uses the *Blackman* temperature response function, or can be seen as a special case of the bilinear function where T_{MAX} has been set to infinity.

Cardinal temperatures are often assumed at default values (Ceres-rice T_{BASE} 9°C, T_{OPT} 33°C, no T_{MAX} ; Oryza T_{BASE} 8°C, T_{OPT} 30°C, T_{MAX} 42°C), making it easier to calibrate the remaining phenology parameter i.e. T_{SUM} (van Oort et al., 2011). However, as van Oort et al. (2011) show, using default cardinal temperatures often leads to highly flawed results. Van Oort et al. (2011) propose a new ORYZA2000-compatible calibration tool that is able to estimate all phenological input parameters simultaneously: Pheno_opt_rice. This approach is purely statistical, without incorporating the effects of individual environmental factors. Stuerz et al. (2020) applied Pheno_opt_rice and found that it was better at simulating f at individual sites, however it fell short of Stuerz' method when predicting crop duration across a wider range of environments, which shows that this purely statistical approach lacks a certain level of robustness as it does not account for the influence of individual climatic determinants i.e. environmental factors, while Stuerz-model does with the inclusion of RH.

What is new with the AGN-model is the way T_{BASE} , T_{OPT} and T_{SUM} and an RH-adjustment factor for T_{OPT} are calibrated simultaneously based on time from sowing to flowering, mean air temperature and mean RH over the same period. Adjusting phenological parameters to RH significantly improves robustness of phenology modelling over a wide range of environments. It should be quite easy to incorporate an RH-adjustment factor for cardinal temperatures into the phenology subroutine of existing rice crop models as the formulas are relatively easy and do not require much calculation time.

6.5 Future research

The data collected for this project by AfricaRice is a magnificent data source. It holds much more information than what has been analysed and presented in this thesis. There is e.g. data on grain and straw yield and yield separation data (ratio and amount of partially and completely filled grains), which a next researcher could use to try to understand the interactions between genotype, environment and yield. There is also data on spikelet sterility, which could be used to improve models of cold and heat induced spikelet sterility. The data offers the potential to develop a method to improve PI date estimation and therefore duration of the reproductive phase. Once PI date is known or estimated, photoperiod-sensitivity during PSP can be included in phenology modelling.

Continuing the path started by this thesis, it is recommended to conduct more RGTs at environments similar to Ambohibary with regard to temperature. The cardinal temperatures estimated in this study are highly influenced by four to five data points -per genotype- from Madagascar. The reliability of the cardinal temperature estimates would increase if more data from 'cooler' environments could be incorporated.

Moreover, it would be interesting to dissect the data for E10, where there was clear G x E interaction affecting some short-duration varieties. What could be the reason that these genotypes cannot be captured by the AGN-model? Furthermore, it would be interesting to run existing rice crop models with the cardinal temperatures found in this study and to see how accurately they can simulate flowering dates. Also, it would make sense to look at the grain yield and SST data, and to combine those results with the improved phenology model, to create cropping calendars and location-specific advice on optimum sowing dates in order to avoid environmental risks and increase rice yields.

7 Conclusion

Genotype by environment interactions affect crop duration of rice. Temperature and relative humidity are the two main environmental factors influencing this trait, while daylength was found to be less important than previously stated in literature. Furthermore it was found that duration from PI to flowering is not fixed in number of days nor in number of degree-days. PI date appears to be influenced by G x E interactions as well. Genotype-specific cardinal temperatures of the 80 rice varieties tested during this project were estimated by applying three readily available simple phenology models from literature, as developed by Summerfield et al. (1992), Dingkuhn et al. (1995) and Stuerz et al. (2020). Besides these three models, a new phenology model was developed by Asch and Groot Nibbelink: The AGN-model. This model is based on a multiple linear regression including both a quadratic temperature term and relative humidity: $DR = a * \bar{T}^2 + b * \bar{T} + c * \overline{RH} + d$. Cardinal temperatures are estimated by taking the tangents and including a genotype-specific RH-adjustment factor resulting in T_{OPT} increasing with increasing RH. Simulations of crop duration are made based on these cardinal temperatures in combination with daily weather data. With a slope of 0.937, an r^2 of 0.938 and RMSE of 12.3 days when regressing observed versus simulated crop duration, the AGN-model was found to be better at simulating f than the three tested phenology models. Therefore it is suggested to include an RH-adjustment factor for optimum temperature into the phenology subroutines of existing rice growth models. This should be easily possible for crop modellers proficient in the respective code languages.

This thesis is a step towards improving rice crop models. It helps creating a better understanding of the environmental factors affecting phenology and how to incorporate these to create a better phenology subroutine in rice crop models. This in turn can be used to improve yield modelling under climate change scenarios, to create better locally-adapted cropping calendars and to improve decision-support-tools, such as RiceAdvice, which can provide location-specific advice to farmers and extension workers on optimum sowing date and suitable varieties, so yields may be increased without a need for additional external inputs.

References

- AfricaRice (Africa Rice Center). (2018). *Continental Investment Plan for accelerating Rice Self-Sufficiency in Africa (CIPRiSSA)*.
- Aguilar, A. (2019). *Machine learning and big data techniques for satellite-based rice phenology monitoring*. <https://doi.org/10.13140/RG.2.2.27404.26245>
- Bernardo, R. (2010). *Breeding for quantitative traits in plants* (2nd ed.). Stemma Press.
- Bouman, B. A. M., Kropff, M. J., Tuong, T. P., Wopereis, M. C. S., ten Berge, H. F. M., & van Laar, H. H. (2001). *ORYZA2000: modelling lowland rice*. IRRI. http://books.irri.org/9712201716_content.pdf
- Dingkuhn, M. (1995). Climatic determinants of irrigated rice performance in the Sahel - III. Characterizing environments by simulating crop phenology. *Agricultural Systems*, 48(4). [https://doi.org/10.1016/0308-521X\(94\)00029-K](https://doi.org/10.1016/0308-521X(94)00029-K)
- Dingkuhn, M., Pasco, R., Julia, C., & Souli, J. C. (2014). *RIDEV V2, Rice Model of Phenology and Thermal Sterility of Spikelets*.
- Dingkuhn, M., Pasco, R., Pasuquin, J. M., Damo, J., Soulié, J. C., Raboin, L. M., Dusserre, J., Sow, A., Manneh, B., Shrestha, S., Balde, A., & Kretschmar, T. (2017). Crop-model assisted phenomics and genome-wide association study for climate adaptation of indica rice. 1. Phenology. *Journal of Experimental Botany*, 68(15). <https://doi.org/10.1093/jxb/erx249>
- Dingkuhn, M., Sow, A., Samb, A., Diack, S., & Asch, F. (1995). Climatic determinants of irrigated rice performance in the Sahel - I. Photothermal and micro-climatic responses of flowering. *Agricultural Systems*, 48(4). [https://doi.org/10.1016/0308-521X\(94\)00027-I](https://doi.org/10.1016/0308-521X(94)00027-I)
- FAO (Food and Agricultural Organisation). (2020, February 17). *FAO Database*. Retrieved July 30, 2022, from <http://www.fao.org/faostat/en/#data/QC>

- GRiSP (Global Rice Science Partnership). (2013). *Rice almanac: source book for one of the most economic activities on Earth* (4th ed.). International Rice Research Institute.
- IRRI. (n.d.). *Crop calendar - IRRI Rice Knowledge Bank*. Retrieved July 30, 2022, from <http://www.knowledgebank.irri.org/step-by-step-production/pre-planting/crop-calendar>
- Jagadish, S. V. K., Craufurd, P. Q., & Wheeler, T. R. (2007). High temperature stress and spikelet fertility in rice (*Oryza sativa* L.). *Journal of Experimental Botany*, 58(7). <https://doi.org/10.1093/jxb/erm003>
- Julia, C., & Dingkuhn, M. (2013). Predicting temperature induced sterility of rice spikelets requires simulation of crop-generated microclimate. *European Journal of Agronomy*, 49. <https://doi.org/10.1016/j.eja.2013.03.006>
- Kropff, M. J., van Laar, H. H., & Matthews, R. B. (1994). *ORYZA1: An ecophysiological model for irrigated rice production*. SARP Research Proceedings.
- Penning de Vries, F. W. T., Jansen, D. M., ten Berge, H. F. M., & Bakema, A. (1989). *Simulation of ecophysiological processes of growth in several annual crops*. Pudoc.
- Rao, A. N., Wani, S. P., Ramesha, M. S., & Ladha, J. K. (2017). Rice production systems. In *Rice Production Worldwide*. https://doi.org/10.1007/978-3-319-47516-5_8
- Reynolds, M., Kropff, M., Crossa, J., Koo, J., Kruseman, G., Molero Milan, A., Rutkoski, J., Schulthess, U., Singh, B., Sonder, K., Tonnang, H., & Vadez, V. (2018). Role of modelling in international crop research: Overview and some case studies. *Agronomy*, 8(12). <https://doi.org/10.3390/agronomy8120291>
- RiceAdvice. (2022). *RiceAdvice - Tools for improving rice value chains in Africa*. Retrieved July 30, 2022, from <https://www.riceadvice.info/en/riceadvice/>
- Romagosa, I., Fox, P. N., García del Moral, L. F., Ramos, J. M., García del Moral, B., Roca de Togores, F., & Molina-Cano, J. L. (1993). Integration of statistical and

- physiological analyses of adaptation of near-isogenic barley lines. *Theoretical and Applied Genetics*, 86(7). <https://doi.org/10.1007/BF00212607>
- Saito, K., Vandamme, E., Johnson, J. M., Tanaka, A., Senthilkumar, K., Dieng, I., Akakpo, C., Gbaguidi, F., Segda, Z., Bassoro, I., Lamare, D., Gbakatchetche, H., Abera, B. B., Jaiteh, F., Bam, R. K., Dogbe, W., Sékou, K., Rabeson, R., Kamissoko, N., ... Wopereis, M. C. S. (2019). Yield-limiting macronutrients for rice in sub-Saharan Africa. *Geoderma*, 338. <https://doi.org/10.1016/j.geoderma.2018.11.036>
- Shrestha, S., Asch, F., Brueck, H., Giese, M., Dusserre, J., & Ramanantsoanirina, A. (2013). Phenological responses of upland rice grown along an altitudinal gradient. *Environmental and Experimental Botany*, 89. <https://doi.org/10.1016/j.envexpbot.2012.12.007>
- Stuerz, S., Shrestha, S. P., Schmierer, M., Vu, D. H., Hartmann, J., Sow, A., Razafindrazaka, A., Abera, B. B., Chuma, B. A., & Asch, F. (2020). Climatic determinants of lowland rice development. *Journal of Agronomy and Crop Science*, 206(4). <https://doi.org/10.1111/jac.12419>
- Summerfield, R. J., Collinson, S. T., Ellis, R. H., Roberts, E. H., & de Vries, F. W. T. P. (1992). Photothermal responses of flowering in rice (*Oryza sativa*). *Annals of Botany*, 69(2). <https://doi.org/10.1093/oxfordjournals.aob.a088314>
- United Nations, DESA Population Division (2022). *World Population Prospects 2022*. Retrieved July 30, 2022, from <https://population.un.org/wpp/Graphs/DemographicProfiles/Line/1834>
- van Oort, P. A. J., de Vries, M. E., Yoshida, H., & Saito, K. (2015). Improved climate risk simulations for rice in arid environments. *PLoS ONE*, 10(3). <https://doi.org/10.1371/journal.pone.0118114>
- van Oort, P. A. J., & Dingkuhn, M. (2021). Feet in the water and hands on the keyboard: A critical retrospective of crop modelling at AfricaRice. *Field Crops Research*, 263. <https://doi.org/10.1016/j.fcr.2021.108074>

- van Oort, P. A. J., Zhang, T., de Vries, M. E., Heinemann, A. B., & Meinke, H. (2011). Correlation between temperature and phenology prediction error in rice (*Oryza sativa* L.). *Agricultural and Forest Meteorology*, 151(12).
<https://doi.org/10.1016/j.agrformet.2011.06.012>
- Vergara, B. S. (1991). Rice Plant Growth and Development. In *Rice*.
https://doi.org/10.1007/978-1-4899-3754-4_2
- Zhang, T., Li, T., Yang, X., & Simelton, E. (2016). Model biases in rice phenology under warmer climates. *Scientific Reports*, 6.
<https://doi.org/10.1038/srep27355>